SINGLE-CELL MICRORNA SEQUENCING OF CIRCULATING TUMOUR CELLS: A NEW TOOL FOR MONITORING PROSTATE CANCER

by

Kevin Richard Jepson

BSc, McGill University, 2013

A THESIS SUBMITTED IN PARTIAL FULFILLMENT OF

THE REQUIREMENTS FOR THE DEGREE OF

MASTER OF SCIENCE

in

THE FACULTY OF GRADUATE AND POSTDOCTORAL STUDIES

(Genome Science and Technology)

THE UNIVERSITY OF BRITISH COLUMBIA

(Vancouver)

April, 2018

The following individuals certify that they have read, and recommend to the Faculty of Graduate and Postdoctoral Studies for acceptance, a thesis/dissertation entitled:

Single-cell microRNA sequencing: a new tool for monitoring prostate cancer

submitted by Kevin Jepson in partial fulfillment of the requirements for

the degree of Master of Science

in Genome Science and Technology

Examining Committee:

Dr. Carl Hansen
Supervisor

Dr. Marco Marra
Supervisory Committee Member

Dr. Alexander Wyatt
Supervisory Committee Member

Dr. Joerg Gsponer
Additional Examiner

Additional Supervisory Committee Members:

Supervisory Committee Member

Supervisory Committee Member

Abstract

A major challenge in monitoring and managing metastatic cancer is the frequent inability to use invasive biopsies as a means of obtaining information regarding tumour progression. Circulating tumour cell (CTC) liquid biopsies—that is, collecting and analyzing CTCs from a blood sample—represent an opportunity for non-invasive cancer monitoring. The challenges of obtaining rare CTCs and sequencing single cell-amounts of miRNA have thus far made it impossible to accurately assess miRNA from CTCs. Here we present an integrated method combining negative-selection, high-throughput microscopy, micromanipulation, and microfluidics to measure the genome-wide expression of microRNAs (miRNAs) in single CTCs. Using our method, we generated single-cell miRNA expression profiles for 258 CTCs from 14 late-stage metastatic prostate cancer patients (mean 18 per patient). The total miRNA reads per cell was 27,423—accounting for 39% of aligned reads—while the mean detected miRNA species per cell was 155. Individual CTCs displayed significant interpatient heterogeneity, while intrapatient heterogeneity was comparatively low. Retrospective analysis of CTCs from castration-resistant prostate cancer patients provides preliminary evidence that miR-200b and miR-200a expression is negatively correlated with more aggressive tumour phenotypes; this demonstrates the potential of this method for monitoring and predicting disease progression in prostate cancer. This study establishes a method for obtaining single-cell miRNA profiles of CTCs, thereby enabling the ability to assess the important roles miRNAs play in cancer development, progression and response to treatment.

Lay Summary

Cancer cells are constantly evolving, and thus, clinicians must obtain information regarding current tumour state in order to treat cancer patients effectively; this is often infeasible due to the invasive nature of metastatic biopsies. To solve this problem, researchers have begun investigating circulating tumour cells (CTCs) as a non-invasive tumour monitoring method. However, there is currently a lack of single-cell analysis methods compatible with CTC research. The goal of this work is to add to the measurement capabilities by developing a method for enriching, isolating, and performing single-cell miRNA sequencing on CTCs from metastatic cancer patients. To demonstrate the functionality of the method, I generated single-cell miRNA sequencing profiles of 258 CTCs from 14 late-stage metastatic prostate cancer patients. Analysis of the resulting data set provided preliminary evidence that miRNA expression patterns can retrospectively classify aggressive tumour phenotypes; these results demonstrate potential applications for CTC miRNA sequencing in the clinic.

Preface

Dr. Carl Hansen, Dr. Marijn van Loenhout and I identified the topic for my Master's thesis. The negative selection, high-throughput imaging, micromanipulation, library prep, quality control, size-selection, and sequencing was performed by me, with supervision from Dr. van Loenhout and Michael VanInsberghe, a PhD student in the Hansen Lab. The PReMiSe platform, which was used for high-throughput imaging, micromanipulation, and reagent dispensing had been previously designed by Dr. van Loenhout. The single-cell miRNA library prep protocol was based on a protocol that had been previously established by Michael VanInsberghe. The gel-based size-selection method was based on a protocol that had been previously established by Canada's Michael Smith Genome Sciences Centre, and modified/optimized by Michael VanInsberghe. The bioinformatics alignment, annotation, quality control, and expression quantification pipeline was based off of that developed by Chu *et al.* to profile microRNAs for The Cancer Genome Atlas. Michael VanInsberghe performed the analysis of the raw sequencing data. Patient samples were collected by Nikita Ivanov and organized by Lejla Gavranovic, who both work at the Prostate Research Centre at Vancouver General Hospital. I developed and applied the data analysis pipeline.

My committee members Dr. Hansen, Dr. Marra, and Dr. Wyatt, as well as Dr. Kim Chi, Dr. Lucia Nappi, and other members of the Hansen lab provided me with advice throughout my project. The entirety of this thesis was written by me, with proofreading done by Michael VanInsberghe and Dr. Carl Hansen prior to submission to my committee for approval. Figure 3.8 was based on a figure previously drawn by Michael VanInsberghe.

Table of Contents

List of Tables

List of Figures

List of Abbreviations

ADT…….Androgen Deprivation Therapy

AR……...Androgen Receptor

CAM……Collagen Adhesion Matrix

CAR…….....Chimeric Antigen Receptor

cDNA……..Complimentary Deoxyribonucleic Acid

cfNA…….Cell-Free Nucleic Acid

cfRNA……Cell-Free Ribonucleic Acid

CK……...Cytokeratin

CNV……Copy Number Variation

CRPC……...Castration Resistant Prostate Cancer

ctNA…….Circulating Tumour Nucleic Acid

CTC……Circulating Tumour Cell

DEA……...Differential Expression Analysis

DEP……Dielectrophoresis

DNA…….Deoxyribonucleic Acid

DOP-PCR……Degenerate Oligonucleotide Primed Polymerase Chain Reaction

DPBS……Dulbecco's Phosphate Buffered Saline

ECM……..Extracellular Matrix

EGFR…….Epidermal Growth Factor Receptor

EMT……..Epithelial-to-Mesenchymal Transition

EpCAM……..Epithelial Cell-Adhesion Molecule

EPISPOT……...Epithelial Immunospot

FAST……...Fiber-Optic Scanning Technology

FBS……Fetal Bovine Serum

FDA……..Food and Drug Administration

FDR…….False-Discovery Rate

FISH……Fluorescence *in situ* Hybridization

GO…….Gene Ontology

ISET……Isolation by Size of Epithelial Tumour Cells

LNA…….Locked Nucleic Acid

MALBAC……...Multiple Annealing and Looping-Based Amplification Cycles

MAST……...Model-based Analysis of Single-cell Transcriptomics

MDA……..Multiple Displacement Amplification

MET……..Mesenchymal-to-Epithelial Transition

miRNA…….……microRNA

M-MLV……Moloney Murine Leukemia Virus

NGS…….....Next-Generation Sequencing

PAGE……...Polyacrylamide Gel Electrophoresis

PBMC……...Peripheral Blood Mononuclear Cell

PBS……..Phosphate Buffered Saline

PCR……Polymerase Chain Reaction

PD-1…….Programmed Cell Death Receptor-1

PDMS……..Polydimethylsiloxane

PReMiSe…….Pipette Recovery and Microscopy for Sequencing

PSA……...Prostate-Specific Antigen

PSMA…….Prostate-Specific Membrane Antigen

qPCR……Quantitative Polymerase Chain Reaction

RBC……...Red Blood Cell

RNA……...Ribonucleic Acid

RNA-seq……RNA Sequencing

RT……...Reverse Transcriptase

RT-PCR……Reverse-Transcription Polymerase Chain Reaction

scRNA-seq……...single-cell RNA Sequencing

snoRNA……..Small Nucleolar RNA

SSNV…….Somatic Single Nucleotide Variant

TNFR……...Tumour Necrosis Factor Receptor

t-SNE……t-Distributed Stochastic Neighbor Embedding

TSO…….Template-Switching Oligonucleotide

WES……Whole-Exome Sequencing

WGA…….Whole-Genome Amplification

WGS…….Whole-Genome Sequencing

Acknowledgements

I would like to thank my supervisor Dr. Hansen for his guidance, support, and motivation over the course of my Master's thesis. Whenever I was confronted with a tricky research problem or was unsure how to proceed with the project, he was always available to help me determine the best path forward.

I am grateful for the time and effort Dr. Marijn van Loenhout put into helping me on a day-to-day basis. His guidance was imperative to the success of the research. I am thankful to Michael VanInsberghe for providing advice regarding protocol development and data analysis. His depth of knowledge and willingness to share that knowledge was an invaluable resource for me. Lastly, I am thankful to Carmen de Hoog, Hans Zahn, Matthew Bundala, and all the other members of the Hansen Lab for their input over the course of my Master's degree.

Chapter 1: Introduction

Cancer often arises due to the accumulation of genetic mutations that lead to the dysregulation of several key biological mechanisms, including cell signalling, survival, growth, proliferation, and differentiation (1). The underlying mutational signatures are highly variable between patients, and for this reason, the development of a universal treatment for any specific cancer has proven to be extremely elusive and is likely to remain so (2,3).

In recent years the enhancement of patient anti-cancer immune responses has emerged as a new cancer treatment paradigm that can be applied across many patients and even tumour types (4). Rather than targeting cancer cells, as is done using chemotherapy or previous antibody-based strategies, this approach works by enhancing the patient's own anti-cancer immune surveillance through a variety of mechanisms including blockade of immune checkpoints, agonism of immunostimulatory pathways, vaccination, or targeting engagement of T cells (4). The most successful of this has been blockage of the programmed cell-death protein-1 (PD-1) axis using monoclonal antibodies, a strategy that has been successful in generating complete and durable responses in a variety of tumours including lung, skin, and gastric cancers (5,6). Despite the dramatic success in many indications, such complete remissions are only observed in a minority of patients, and there is little understanding of why patient responses are varied. Another recent breakthrough in the treatment of leukemia is by engineering T-cells and arming them with chimeric antigen receptors (CARs) targeting various tumour-specific antigens (9–14). Recent trials using CARs targeting CD19, including trials by Juno Therapeutics, Kite Therapeutics, and Novartis, have demonstrated over 60% response rates and long-term remission in patients that otherwise had no options. Both of these strategies highlight the power of using the immune

system to attack cancer, and highlight that cancer is in part a failure of immune-surveillance. Of note, these approaches are not exclusive of existing chemotherapy and small molecule drug treatments, and there are hundreds of clinical trials in progress to investigate combination strategies. This, coupled with the incomplete response in patients, as well as very low responses in many cancer types, motivates improved methods of stratifying patient populations using clinical biomarkers.

As an alternative to generalized treatments, clinicians have also attempted to develop personalized treatment strategies. To do so, researchers have investigated the possibility of implementing treatment regimens based on insights into tumour weaknesses obtained through modern genomic and transcriptomic analysis techniques (15). However, due to high levels of intra-tumour heterogeneity and clonal diversity, initial lines of treatment inevitably trigger "Darwinian" selection for the most fit tumour subpopulations; therapy-resistant cells can then continue to proliferate unimpeded until subsequent therapies have been administered (2,3,16). In this sense, a major challenge of personalized medicine is that oncologists are not only fighting the tumour cells themselves, but also one of the most powerful natural phenomena on Earth—evolution (17). For this reason, methods that allow for the monitoring of tumours before, during, and after administration of therapies may be useful for directing treatment options for cancer patients; as a tumour evolves, so too must therapeutic strategies (18). Unfortunately, acquiring up-to-date information regarding the state of tumour progression poses a serious technical challenge (19,20). Metastatic biopsies, which are sometimes the only option for obtaining relevant tumourigenic information, can require extremely invasive procedures that are not feasible in the clinical setting. This is especially true in prostate cancer, where metastases target the bone in roughly 90% of patients (21). Therefore, in order for personalized medicine to

continue to grow and exert its full potential in the management of cancer, methods for non-invasive monitoring of tumour progression must be developed.

To help advance the field of personalized medicine, researchers have begun to investigate the clinical potential of circulating tumour cells (CTCs) (22). CTCs are cells that have been shed from a tumour into the circulation (23), and are therefore a minimally invasive source of tumour material that can be used to diagnose (24,25), inform the treatment of (26–30), and monitor disease (22,31–33). Current lines of research in this field are aimed at developing methods to enrich for, detect, isolate, and measure these extremely rare cells, and identifying different biomolecules with diagnostic and prognostic potential.

The goal of my thesis project was to develop the first integrated method for sequencing microRNAs (miRNAs) in single CTCs. Towards this goal, I successfully established and benchmarked a sensitive and specific CTC purification strategy by combining existing pre-enrichment steps with high-throughput microscopy. Next, a single-cell miRNA sequencing method was adapted and optimized to be compatible with this purification platform. Finally, genome-wide miRNA expression profiles were obtained from 258 CTCs isolated from 14 patients with metastatic prostate cancer, generating initial observations of miRNA expression changes during disease progression and, perhaps more importantly, establishing the feasibility of CTC miRNA profiling. This chapter will provide background information regarding the latest CTC research, while focusing on enrichment, detection, and analysis strategies that have been used for prostate cancer. Chapter 2 details the development of our CTC purification strategy and its comparison against the current leading methods, and Chapter 3 describes the miRNA sequencing method and results. Finally, Chapter 4 provides a summary and future recommendations.

1.1 Overview of Liquid Biopsy Methods

A non-invasive tumour monitoring method that has gained traction in recent years is the "liquid biopsy"— that is, using biomarkers circulating through the bloodstream to inform diagnosis, prognosis, and/or treatment outcomes in cancer patients (15,18). The goal of liquid biopsy research is to gain enough knowledge regarding circulating biomarkers to replace invasive biopsies with a standard blood test. In doing so, this assay has the potential to enable the development of routine diagnostic cancer tests in the general population, which could help clinicians save lives by detecting cancer sooner and initiating therapies or surgical procedures earlier in tumour progression (25). Liquid biopsies also represent a promising approach for tracking prognosis, residual disease, and post-treatment relapse by enabling a non-invasive method for serial tumourigenesis monitoring (26–28,31,32). By providing more accessible and complete molecular analysis of tumours, circulating biomarkers have the potential to arm clinicians with knowledge regarding vulnerabilities that could help dictate personalized treatment options (30). Furthermore, performing liquid biopsies over the course of a therapy would help clinicians monitor tumour burden, thereby improving estimates of therapeutic success and preventing under-/overtreatment of patients (20,22,26). For these reasons, liquid biopsy research has become very popular over the past few decades, and the two major biomarkers of interest are circulating tumour nucleic acids (ctNAs) and circulating tumour cells (CTCs).

1.1.1 Cell-Free Nucleic Acids

Cell-free nucleic acids (cfNAs) were first discovered in 1948 by Mandel and Metais (34). In the 1970's, it was reported that cfNA levels were significantly elevated in the blood of cancer patients, and subsequent findings showed that these sequences partially originated from the

tumour cells themselves (35,36). A separate group confirmed these findings and pushed the field further by successfully detecting the presence of circulating mutant *KRAS* sequences identical to mutations found in the primary tumour of a pancreatic cancer patient (37). This finding demonstrated the potential of ctNA liquid biopsies as a tool for monitoring the mutational landscape of tumours without the need for invasive biopsies, and spurred interest in the field. Since this landmark paper, researchers have pursued clinically relevant correlations between ctNAs and diagnosis, prognosis, treatment response, and tumour burden estimates in cancer; in doing so, many useful ctNA biomarkers have been discovered (18). For example, it has been shown that specific genomic alterations of clinically actionable genes—such as *AR*, *BRCA2*, *ATM*, *PTEN*, *PIK3CA*, *PIK3R1*, *TP53*, and *RB1*—can be detected in metastatic castration-resistant prostate cancer (CRPC) patients via ctNA liquid biopsies; these observations were concordant with results from metastatic biopsy analyses from the same patient (38). Cell-free RNA (cfRNA)-based liquid biopsies have also shown promise, with several miRNAs arising as potentially clinically relevant prostate cancer biomarkers (39–43).

However, there are inherent limitations of cfNA analysis. The signal-to-noise ratio for ctNA analyses is low, since wild-type nucleic acids from non-tumourigenic hematopoietic cells represent the vast majority of cfNA; this background noise is further increased during chemotherapy (44). Therefore, the majority of cfNA analyses are limited to monitoring tumour-specific gene mutations, where *a priori* information regarding a target-of-interest is required (15). Untargeted approaches are also possible, however such analysis methods are expensive and tend to suffer from low limits of detection (45–48). Additionally, aside from miRNAs, it has proven difficult to obtain relevant gene expression or transcriptomic data from cfNAs (49,50).

For these reasons, researchers have found it necessary to investigate additional blood-bound cancer biomarkers to overcome these deficiencies.

1.1.2 Circulating Tumour Cells

As an alternative to ctNA analyses, liquid biopsy researchers have become increasingly interested in CTCs. CTCs were first observed in 1869 by an Australian physician, Thomas Ashworth, when he noted the presence of "cells identical with those of the cancer itself" in the blood stream (51). These cells were naturally of interest to researchers. However, due to their rarity—they constitute 1 out of a ~10^7 white blood cells per millilitre of blood (52)—further studies to determine the origin and importance of CTCs were severely hindered until technical capabilities improved over a century after Ashworth's discovery.

Now, it is widely believed that CTCs play an important role in the spread of epithelial-derived carcinomas throughout the body via a cyclic mechanism (23). First, cancer cell subpopulations within the primary tumour begin to exhibit a loss of adhesion to their neighbouring cells and basement membrane, through a process known as the epithelial-to-mesenchymal transition (EMT) (53,54). Subsets of these cells are then able to migrate into the blood stream—intravasation—and survive in circulation as CTCs during the so-called leukaemic phase (23). Eventually, it is believed that specific clusters of CTC clones begin to form in the capillary beds of distant regions of the body, where some gain the ability to invade nearby organs through extravasation (55). Upon extravasation, a subset of tumour cells regain their epithelial phenotype through mesenchymal-to-epithelial transition (MET), begin to proliferate as a solid metastatic tumour, and the cycle continues (23,56). Therefore, CTCs represent a potentially

crucial cancer biomarker, as they are metastatic tumour cells flowing through the bloodstream that can act as a window for clinicians to investigate current tumour states.

When done correctly, CTC analysis is not plagued by the same signal-to-noise ratio difficulties as cfNA analysis, as it eliminates the overwhelming presence of wild-type molecules. Furthermore, by analyzing the cells themselves, CTC research allows for a wider variety of analyses—such as differential gene expression, protein expression, protein localization, and cell-surface antigen expression (22,52). In this way, CTC analysis can function as an alternative method for monitoring current tumourigenic molecular signatures with potential for use in personalized medicine. In recent years, modern technological advances have helped researchers develop ways of detecting, isolating, and analyzing CTCs, while demonstrating the potential applications for CTCs in the clinical setting.

1.2 Enrichment and Detection of Circulating Tumour Cells

The main technical challenge for CTC researchers arises due to the rarity of these cells, as there is only ~1 CTC per 10^7 peripheral blood mononuclear cells (PBMCs) in the blood (52). For this reason, enrichment—that is, obtaining a concentrated sample of CTCs from whole blood— and detection—determining which cells from the enriched sample are indeed CTCs—are perhaps the most crucial steps in CTC research. In order to successfully enrich for CTCs, scientists rely upon specific differences between tumour cells and the surrounding hematopoietic cells; these include biological variations, such as cell-surface markers or functional characteristics, as well as physical differences, such as cell density, size, charge or symmetry. Over the years, researchers have developed a wide variety of innovative techniques that leverage these unique cellular characteristics in order to successfully enrich and detect CTCs.

1.2.1 Biological Characteristic-Based Enrichment/Detection Strategies

The most popular CTC enrichment methods take advantage of biological variations in cell-surface antigens and follow two distinct strategies: positive or negative selection. Positive selection uses antibodies targeting CTC-specific cell-surface markers to select CTCs for removal from whole blood, whereas negative selection relies upon antibodies targeting PBMC-specific surface markers in order to select and remove unwanted cells from a sample. For prostate cancer, the most commonly targeted CTC-specific cell-surface marker is epithelial cell adhesion molecule (EpCAM)—a transmembrane glycoprotein involved in cell-adhesion, signalling, cell migration, proliferation, and differentiation that is highly expressed in epithelial-derived tumour cells and not expressed in PBMCs (57,58). Despite the wide-spread use of EpCAM as a prostate CTC marker, it has been shown that EMT in CTCs leads to decreased expression of EpCAM; this presents an important limitation of EpCAM-based positive selection, as it is only capable of enriching for epithelial-like CTC subpopulations (59). One way to address this issue is to perform positive selection using antibodies targeting a wider variety of cell-surface markers. For example, mixing anti-EpCAM antibodies with antibodies targeting mesenchymal markers such as cadherin-11 can help enrich for a broader range of CTC subpopulations (60). Another way in which researchers have combatted this issue is by developing more generic enrichment methods, the main example of which is negative selection. Rather than targeting the CTCs directly, negative selection often targets the PBMC-specific cell-surface marker CD45 and removes all $CD45^+$ cells from a sample. The remaining cells will therefore be enriched for a wider variety of CTCs, independent of epithelial cell-surface marker expression (22). In recent years, researchers have developed many CTC enrichment techniques that leverage differences in cell-surface markers through positive or negative selection.

1.2.1.1 Positive Selection

The only CTC enrichment method to be approved for clinical use in prostate cancer by the FDA, CellSearch® (Veridex, USA), uses positive selection. The CellSearch® protocol uses anti-EpCAM antibody-coated ferromagnetic beads to bind epithelial-derived cells in a 7.5 mL blood sample. Once EpCAM-positive cells are bound, the CellSearch® platform employs a magnetic field to isolate these cells into a CTC-enriched solution. Next, there is an immunofluorescence-based detection step where enriched cells are fixed and stained with epithelial cell-specific cytokeratin (CK) antibodies and PBMC-specific CD45 antibodies; CTCs are detected as cells with CK+/CD45- signatures (61). In order to address the problem of enriching CTCs that have undergone EMT, an adjustment to the platform can be made using a cadherin-11-based capture approach to enrich for mesenchymal tumour cells (60). These enrichment/detection approaches allow CellSearch® to successfully enumerate carcinoma tumour cells, and for this reason, it is often used in the clinic as a prognostic measurement for metastatic prostate cancer patients (62).

The CellSearch® platform, however, leaves a lot to be desired. The positive selection-based enrichment method results in rather impure samples and the detection/enumeration steps can easily be affected by technician biases, leading to highly variable count measurements (63). Another major limitation of CellSearch® is that it is not well-suited for in-depth downstream analyses due to both the low-purity of CTCs within the enriched sample and the fixation/processing steps required for detection. In recent years, adjustments to the CellSearch® platform have been made to address these issues (60,64,65); however, due to these original concerns, several other interesting techniques have been explored for enriching/detecting CTCs.

Following the success of the CellSearch® assay, similar positive selection CTC enrichment approaches were developed. Building upon this strategy, Todenhöfer *et al.* developed the Adnatest, which selects CTCs by targeting epithelial and tumour-associated markers with antibodies conjugated to magnetic beads. Following extraction using a magnetic particle concentrator (AdnaMag-L and AdnaMag-S), cells are lysed in bulk and RNA from the lysates is purified for downstream RT-PCR analyses. This RT-PCR step uses primers for known tumour-specific transcripts in order to detect the presence of CTCs; in prostate cancer, these targets often include prostate-specific antigen (*PSA*), prostate-specific membrane antigen (*PSMA*), and epidermal growth factor receptor (*EGFR*). As proof of concept, Todenhöfer *et al.* used the AdnaTest to perform serial CTC detection experiments on castration-resistant prostate cancer (CRPC) patients of the course of a treatment regimen (66).

While this experiment demonstrated the AdnaTest's potential, there were evident limitations. Again, this positive selection technique likely resulted in low-purity samples exhibiting overrepresentation of specific CTC subpopulations. The subsequent batch lysis step eliminated the ability to analyze heterogeneity from the sample, as RNA transcripts from different CTCs are indistinguishable; this also prevented the AdnaTest from generating accurate CTC count estimates, which have been shown to infer prognosis (67). A potential solution to this limitation would be to combine the AdnaTest with a downstream micromanipulation step in order to isolate individual cells prior to lysis.

Taking a slightly different positive selection approach, a group at Stanford University created the MagSweeper, which uses anti-EpCAM Dynabeads (CELLection Epithelial Enrich; Invitrogen, and Dynal) to target epithelial-derived cells and a magnetic rod to attract bead-bound cells. Once cells are attached to the rod, the sheer force generated by gently mixing it through a

wash buffer removes contaminants and non-specifically bound cells. To gain additional purity, the manufacturers recommend performing several rounds of wash-release-capture; in doing so, they report near 100% purity and ~60% capture efficiency in cell-line experiments. While the MagSweeper is still subject to the standard limitations of positive selection, this technique has the added benefit of enriching viable CTCs that can be used for a variety of downstream molecular analyses (31,68). In fact, subsequent RNA sequencing (RNA-seq) studies have shown that the MagSweeper can successfully isolate CTCs with only modest perturbations to the cell (69).

Positive selection has also been adapted for *in vivo* CTC enrichment by a German company, GILUPI. This group developed the CellCollector®—a structured medical Seldinger guidewire coated with anti-EpCAM antibodies—to allow collection of CTCs directly from the veins of metastatic cancer patients (70). This *in vivo* design means the CellCollector® has the potential to select CTCs from very large volumes of blood as it circulates past the wire; additionally, it is compatible with downstream molecular analyses (71). While each of these positive selection-based CTC enrichment strategies are uniquely promising, they rely upon the assumption that all available CTCs within a sample collide with, and become bound by, functionalized antibodies; since this is most definitely not the case, capture efficiencies suffer.

In order to address the capture efficiency concerns of the aforementioned methods, more sophisticated CTC enrichment approaches have been designed by combining positive selection with microfluidics. In 2007, Nagrath *et al.* published a paper describing the CTC-Chip—a microfluidic device consisting of an array of 78,000 anti-EpCAM antibody-coated microposts within a 970 mm^2 surface. Samples are passed through the chip at 1-2 mL/h and, as cells collide with the microposts, $EpCAM^+$ cells are bound and immobilized while untargeted cells are

discarded. CTCs are detected from the resulting $EpCAM^+$ enriched sample using on-chip immunofluorescence and monitoring for $CK^+/CD45^-/DAPI^+$ signatures. Using this device, Nagrath *et al.* reported being able to successfully identify CTCs in 99% of metastatic prostate cancer patients, with an average purity of 49% (72).

In 2012, Kirby *et al.* published a paper describing a similar microfluidic chip, called the GEDI device, which employs an array of offset anti-PSMA antibody-coated microposts to disrupt streamlines and maximize cell-post collisions in a size-specific manner. Due to the alignment and geometry of the micropost array, increased cell size correlates with increased collisions, thereby promoting CTC-micropost interactions. Following immobilization of cells, prostate CTCs were detected as PSMA+/CD45- cells. Using the GEDI device for CTC enumeration on CRPC patients, research groups have reported a 2-400 fold increase in sensitivity when compared to the CellSearch platform, as well as 90% capture efficiency and 62% purity values (73,74). A subsequent iteration of the CTC-Chip eliminated the need for complex micropost design by integrating surface ridges and herringbones throughout the microfluidic chip's channels to disrupt streamlines and maximize cell collisions with anti-EpCAM antibody-coated walls; CTCs were once again detected by $CK^+/CD45^-/DAPI^+$ signatures. Using this microfluidic device, the authors were able to capture CTCs in 93% of prostate cancer patients, with a mean purity of 14%. The declines in capture efficiency and mean purity values compared with the previous iteration of the CTC-Chip are likely due to the potentially large effect of technician bias during detection. This device also proved to be compatible with basic downstream analyses, as this group successfully performed on-chip RT-PCR to identify the *TMPRSS2-ERG* chimeric transcript in a patient whose primary tumour also contained this translocation event (75).

Another microfluidic device that uses a similar positive selection approach was published in 2013 by Lu *et al*. Rather than using antibody-coated microposts or walls, this group designed what they called NanoVelcro—anti-EpCAM antibody-coated silicon nanowires (SiNW) to select and immobilize CTCs (76,77). This microfluidic device combined a NanoVelcro base with an "overlaid polydimethylsiloxane (PDMS) chaotic mixer", which was designed to increase cell collisions with the underlying NanoVelcro. This design had the added benefit that all enriched CTCs are bound on an equal plane, thereby rendering subsequent immunofluorescence detection steps easier, without the requirement of analyzing at multiple focal planes. Using this system, Lu *et al.* were able to demonstrate potential clinical utility by performing serial CTC enumerations in prostate cancer patients undergoing chemotherapy (78).

While all of these microfluidic devices have been shown to perform quite well on CTC enumeration experiments, they result in immobilized CTCs, thereby severely hindering their downstream analysis capabilities. To overcome this issue, yet another version of the CTC-Chip was designed, called the CTC-iChip. This device integrates three sequential microfluidic methodologies into a single platform. First, blood is treated with ferromagnetic anti-EpCAM antibodies and passed through an array of offset microposts, separating red blood cells (RBCs) from larger nucleated cells based on size. Next, the nucleated cells pass through a winding channel to stimulate inertial focusing and cause the cells to align nicely. Finally, the aligned nucleated cells pass through a magnetic field causing magnetically tagged cells to deflect into a collection channel while untagged cells continue into a waste channel. Through this three-step approach, the CTC-iChip is able to enrich for mobilized, viable CTCs suitable for downstream analyses (79).

While this iteration of the CTC-Chip is widely considered the state-of-the-art example of a positive selection platform, it still suffers from the standard issues associated with this enrichment method. To overcome the issue of CTC surface-marker heterogeneity inherent in positive selection, each of these microfluidic devices can be modified with different capture antibodies specifically tailored to cell-surface markers of target cells—for example, anti-cadherin-11 antibodies for CTCs that have undergone EMT, or anti-PSMA antibodies for prostate CTCs. However, until a well-defined antibody cocktail is developed which can efficiently target a broad range of CTC subpopulations, positive selection will remain an enrichment method that suffers from high selection bias.

1.2.1.2 Negative Selection

As mentioned above, another approach for CTC enrichment is negative selection, where unwanted cells are targeted and removed from a blood sample. Negative selection has the added benefit of being tumour antigen-independent, thereby avoiding the issue of targeting specific CTC populations (22,52). There are several examples of relatively basic, widely available negative selection-based CTC enrichment kits.

One popular example is the RosetteSep kit from STEMCELL™ Technologies, which uses tetrameric antibody complexes to crosslink hematopoietic cells together, thereby increasing the density of unwanted cells (80). Following antibody treatment, the sample is centrifuged through a density gradient, causing crosslinked cells to pellet out of solution; the cells remaining on top of the density gradient are thus enriched with CTCs.

There are also slight alterations that can be made to change more complex enrichment methods from positive selection to negative selection. For example, by simply pretreating blood

samples with ferromagnetic anti-CD45 antibodies, rather than anti-EpCAM antibodies, the CTC-iChip can function as a negative selection-based enrichment mechanism. In this case, PBMCs and other unwanted nucleated blood cells are magnetically deflected and the $CD45^-$ CTCs flow undisturbed into a collection channel. Using this negative selection version of the CTC-iChip, Ozkumur *et al.* reported being capable of capturing CTCs in 90% of CRPC patients and were successful in performing relevant downstream analyses on these viable cells. However, they also reported an average purity of only 7.8%, likely owing to the fact that negative selection causes high levels of contamination from PBMCs exhibiting low CD45 expression (79).

Low purity samples cause technical challenges for performing downstream analyses following negative selection, however, this is a reasonable trade-off to obtain a diverse population of CTCs. The resulting diverse CTC populations present another major technical hurdle during subsequent steps, as they are likely to exhibit highly heterogeneous antigen expression patterns, thereby resulting in difficulties during immunofluorescence-based detection. Ignoring this problem would result in lower enumeration counts and prevent the analyses of novel and potentially interesting CTC subpopulations. Therefore, more work needs to be done to be able to provide accurate detection and enumeration of CTCs obtained via negative selection.

1.2.1.3 High-Throughput Imaging

Another enrichment strategy relying heavily on immunofluorescence-based CTC detection that has become increasingly popular in recent years is high-throughput imaging. This approach combines high-throughput imaging with complex segmentation and classification algorithms to detect fluorescently labelled CTCs from a background of millions of PBMCs.

One example of this type of methodology is the Epic Platform, which was designed for the detection and molecular analysis of CTCs without the need for complex enrichment, depletion, or micromanipulation procedures. This platform's workflow begins with red blood cell lysis to remove the vast majority of potential contaminants from a blood sample. Next, nucleated cells are isolated via centrifugation and plated on three separate glass slides for immunofluorescence analyses. One of these slides is set aside for future analyses, while the other two are treated with DAPI and a cocktail of CK- and CD45-targeting antibodies, and scanned using fiber-optic array scanning technology (FAST). Once the scan is complete, Epic Sciences' proprietary algorithms distinguish CTCs from PBMCs and provide enumeration values (81,82). The Epic Platform has been shown to detect >5 CTCs in 80% of metastatic prostate cancer patients, and was reported to detect ≥2 CTCs in nearly three times more metastatic cancer patients than the CellSearch® platform (83).

A similar platform that has the added benefit of being commercially distributed is Rarecyte's (Seattle, WA, USA) AccuCyte CyteFinder®. This method uses a density-based enrichment method, called AccuCyte®, to enrich for nucleated cells prior to high-throughput imaging (84). Importantly, this enrichment is performed without any washing steps in order to minimize CTC loss. Following enrichment, the sample is loaded onto the CyteFinder® for semi-automated high-throughput image analysis similar to that of the Epic Platform (85). An additional functionality of the AccuCyte CyteFinder®, however, is the CytePicker®—a micromanipulation instrument that can be used for individual CTC isolation, thereby enabling a wide variety of potential downstream analyses (86,87).

These commercially available high-throughput imaging techniques have exciting potential to revolutionize CTC enrichment and downstream analyses in the lab. Unfortunately,

they are not immune to the complications inherent in detecting a wide variety of CTC subpopulations, but as cocktails of CTC detection antibodies become more complete, high-throughput imaging-based enrichment/detection techniques have the potential to become the gold standard in the field.

1.2.1.4 Functional Enrichment/Detection

Aside from cell-surface marker-based enrichment/detection, other techniques have been developed to take advantage of different biological characteristics of CTCs. One example of a unique biological characteristic-based detection assay is the epithelial immunospot (EPISOT) assay. This assay requires a pre-enriched sample and performs *in vitro* short-term culturing of CTCs on a nitrocellulose plate coated with antibodies for specific protein markers of interest. Therefore, based on the choice of antibodies, the EPISOT assay is capable of determining whether an enriched sample of CTCs contains viable, clinically relevant cells via secretion protein analysis (88,89). While this assay does not have enrichment capabilities, it presents a unique method for detecting viable CTCs.

Another functional assay based on biological CTC characteristics is the Vita-Assay™, which cultures enriched samples on a collagen adhesion matrix (CAM)-coated plate overnight; CTCs are further enriched based on their high affinity to CAM scaffolds. This methodology allows the Vita-Assay to detect CTCs with invasive phenotypes by measuring their ability to ingest fluorescently labeled CAM. Paris *et al.* tested this technique by performing invasive prostate cancer cell line spike-in experiments, and reported a recovery efficiency of 50% (90). Although functional assays lack the efficiency of other enrichment/detection techniques, they

have the ability to provide unique and potentially clinically valuable phenotypic information describing a patient's CTCs.

1.2.2 Physical Characteristic-Based Enrichment/Detection Strategies

As an alternative to biological characteristic-based CTC enrichment strategies, other methods have been designed which rely on the unique physical characteristics of cancer cells.

1.2.2.1 Filtration

Early examples of physical characteristic-based enrichment relied on observations that tumour cells generally had significantly larger cell diameters than hematopoietic blood cells (91). This led to the creation of several microfabricated filtration systems, including the ISET (isolation by size of epithelial tumour cells) assay (RARECELLS, France). This assay simply filters blood through a polycarbonate membrane consisting of an array of 8 μm pores with the goal of capturing CTCs on the filter as smaller blood cells pass through. This design was tested using spike-in experiments, which found that the ISET assay was consistently able to recover low numbers of spiked-in cell line cells. Since the ISET assay results in viable cells, immunofluorescence and/or RT-PCR can be used for CTC detection/enumeration (91).

A similar filtration approach was taken by Lin *et al.* in 2010, and they reported higher CTC counts from a higher number of patients when compared to the CellSearch® platform (92). These results are relatively unsurprising, as antigen-independent filtration methods allow for the capture of a wider variety of CTC subpopulations.

However, the promise of filtration methods has been significantly diminished by subsequent research showing that CTC sizes are much more variable than previously assumed—

the average diameter of CTCs captured by CellSearch® has been measured as being approximately half the size of cultured cancer cells and, in fact, very similar to PBMCs (73,93). Therefore, spike-in experiments cannot be used as an accurate representation of functionality for any size-based enrichment technique. In an attempt to address these concerns, Lee *et al.* proposed pretreating samples with detachable beads targeting tumour cells; however, this alteration would render any size-filtration protocol antigen-dependent, thereby defeating the purpose of this method (94). Due to concerns over the variability of CTC size, the basis of filtration for CTC enrichment has been called into question, leading to research investigating alternate physical characteristic-based CTC enrichment strategies.

1.2.2.2 Dielectrophoresis

A more promising method of physical characteristic-based CTC enrichment takes advantage of their unique dielectric properties, also known as polarizability. The polarizability of a cell is dependent upon diameter, membrane area, density, conductivity, and volume (95,96). In 2009, Gascoyne *et al.* designed a microfluidic device capable of separating cultured cancer cells from peripheral blood cells through dielectrophoresis (DEP). They did so by passing a mixed batch of cells into a chamber containing a microelectrode array producing a 60 Hz electric field—the so-called “DEP cross-over frequency”. This frequency is special in that it simultaneously attracts cancer cells and repels blood cells due to their unique dielectric properties that arise from morphological and electrical conductivity differences (95,97). Therefore, once the mixture of cells enter the microfluidic chamber, cancer cells are attracted to the microelectrode array and PBMCs can be passed through the chamber and discarded. The rate at which PBMCs are discarded is measured by a laser counter-sizer, and when this value falls to

a negligible level the DEP frequency is dropped to 15 kHz. At this lower frequency, cancer cells begin to experience negative forces from the microelectrodes and can be passed through the microfluidic device into a collection tube. To prove functionality, Gascoyne *et al.* performed spike-in experiments to demonstrate the ability to collect viable cancer cells from a mixture of PBMCs (98). However, this initial design was rather limited by its low-throughput one-batch-at-a-time methodology; to address this issue, Gupta *et al.* created the continuous flow ApoStream™. This device continuously passes cells through a microfluidic chamber containing an array of microelectrodes emitting the DEP cross-over frequency. As a mixture of cells pass through the device, PBMCs are deflected away from the microelectrodes towards a waste channel and CTCs are pulled towards a separate CTC collection channel. This results in an ameliorated high-throughput design, since the ApoStream™ does not require batches of cells to be processed independently (99). Furthermore, this device's antibody-independent mechanism has allowed researchers to use the device for the enrichment of CTCs from metastatic sarcoma patients, which was previously unattainable using EpCAM-based systems (100).

These pilot studies have demonstrated the considerable potential of DEP-based CTC enrichment as an antigen-independent strategy, but further research must be done in order to determine the heterogeneity of CTC populations that can be effectively captured using this system. It is conceivable that this method only captures specific CTC subpopulations based on their dielectric properties and this would result in selection bias problems similar to those that arise with positive selection.

1.2.3 Summary

As described above, the difficulty of enriching and detecting CTCs from whole blood has led to a wide variety of technical strategies to solve this problem. What becomes clear when comparing and contrasting these different techniques—whether it be biological or physical characteristic-based, positive or negative selection, filtration or DEP—is that we need to establish standardized methodology to understand and control for the implicit biases associated with each method. Furthermore, additional research must be made in the field of CTC antigen expression patterns in order to determine a consensus immunofluorescence cocktail for CTC detection. Such a cocktail would allow labs to confidently provide enumeration values and perform downstream analyses on a wider variety of CTC subpopulations. Additionally, the standardization of detection cocktails would lead to greater reproducibility of experiments, thereby helping CTC liquid biopsies become approved for further clinical uses. CTC enrichment and detection technologies have progressed rapidly in the past two decades, but significant improvements must be made before CTC liquid biopsies can exert their full potential in the clinical setting.

1.3 Circulating Tumour Cell Analysis

As the technical capabilities for enriching/detecting CTCs continue to grow, so too have the methods for analyzing CTCs. Detecting CTCs represents only a fraction of their potential clinical utility, and a wide variety of CTC analysis techniques have been developed in order to investigate diagnosis, prognosis, and treatment outcome biomarkers. Due to the rarity of CTCs, such analyses must be functional with low input levels of cells, proteins, and/or nucleic acids (101). CTC analyses range from relatively basic correlative studies, such as enumeration, to

increasingly complicated molecular analyses, such as fluorescence *in situ* hybridization (FISH), reverse-transcription polymerase chain reaction (RT-PCR), protein-based immunofluorescence studies, and even next-generation sequencing (NGS) (22,52,101). Some of these methods have shown significant clinical potential in monitoring and treating carcinoma patients (15). Of the most common carcinomas, prostate cancer represents one of the diseases that could be largely impacted by the development of a liquid biopsy, since prostate cancer metastases target bone in roughly 90% of patients (21). Therefore, by developing CTC analysis techniques that can monitor prostate cancer prognosis, tumour burden, and treatment outcome biomarkers, researchers are hoping to find exciting new ways to implement liquid biopsies into the clinic.

1.3.1 Enumeration

A basic analysis technique that has exhibited clinical utility in the management of cancer is CTC enumeration. Through the use of appropriate CTC enumeration methods, liquid biopsies can monitor patients' CTC counts at various stages of tumour progression and provide important, clinically relevant information. Since CTCs are not detected in healthy individuals, enumeration has the potential to act as a method of achieving early diagnosis of metastasis in pre-symptomatic patients. Although additional tests would be required to determine tumour origin and severity, enumeration could help bolster clinicians' early detection capabilities, thereby helping them initiate first-line treatments or surgical procedures earlier. Furthermore, elevated CTC counts often correspond to more aggressive, late-stage tumours (67,102); therefore, interpreting enumeration data following diagnosis has the potential to provide clinicians with a tool for increasingly accurate assessments of prognosis.

The most commonly used, and only FDA-approved, enumeration device is the CellSearch® system. The clinical trial that led to CellSearch®'s clearance for use in metastatic prostate cancer—the IMMC38 trial—consisted of 276 patients who had liquid biopsies taken prior to commencement of a new chemotherapy and monthly thereafter. Based on CellSearch® enumeration counts, patients were separated into favorable or unfavorable groups, corresponding to <5 and ≥5 CTCs/7.5mL of blood, respectively. The results of this trial showed that unfavorable pretreatment and posttreament CTC counts correlated with shorter overall survival. Perhaps more importantly, this trial also showed that CTC counts predicted overall survival better than traditional prostate cancer biomarkers—such as PSA—at each time point (67). Furthermore, by analyzing time as a continuous variable, it was shown that changes in CTC counts 4 weeks, 8 weeks, and 12 weeks after treatment were much more strongly associated with an increased risk of death ($p = 0.0001$; <0.0001; <0.0001 respectively) than changes in PSA levels ($p = 0.07622$; 0.0893; 0.0424 respectively) (102). These findings provide evidence that CTC counts are superior to traditional biomarkers, and monitoring them can ameliorate prognosis assessments for metastatic prostate cancer patients. In the years since the FDA-approval of CellSearch®, CTC enumeration has become commonplace in the clinic for evaluating prostate cancer prognosis, however, significant research must be done in order to investigate additional potential uses of this analysis technique.

1.3.2 Basic Molecular Analysis

While enumeration has been cleared for prognosis assessments, researchers have hoped to find additional clinical value of CTCs through a variety of molecular analysis techniques. Methods for monitoring the status of clinically relevant cancer pathways represent an enormous

opportunity for liquid biopsies in personalized medicine, as many chemotherapeutic agents actively target these pathways (15,18). There are several clinically implicated tumourigenic prostate cancer pathways, perhaps the most important of which is the androgen receptor (AR) signalling pathway (103). Following androgen deprivation therapy (ADT), prostate cancer will often eventually progress in an androgen-independent state—known as castration-resistant prostate cancer (CRPC)—through the acquisition of numerous key genomic alterations (104,105). Common examples of such alterations include copy number variations (CNVs) and mutations of the *AR* gene, splice-variants of the *AR* transcript, and mutations in genes that regulate peripheral aspects of the AR signalling pathway (104,105). Many of these mutations have previously exhibited correlations with prognosis and treatment outcomes, and thus, CTC analysis techniques designed to monitor these biomarkers represents a potentially important clinical role for CTCs in prostate cancer management.

1.3.2.1 Fluorescence *in situ* Hybridization

An example of a relatively simple CTC analysis method is fluorescence *in situ* hybridization (FISH). FISH uses fluorescently tagged nucleic acid probes designed to have high complementarity with a gene or transcript of interest. Upon capture of CTCs, cells are fixed, permeabilized, and incubated with a set of probes (106). Through subsequent microscopic analyses, researchers can use FISH on CTCs to determine the presence of mutant oncogenes, copy number variations (CNV), tumour suppressor gene deletions, relevant chimeric transcripts, and much more. In recent years, microscopic capabilities have improved to the point where single-molecule FISH is now achievable, thereby improving the resolution of this analysis technique and creating new potential applications (107,108). This information has the potential

to help clinicians obtain up-to-date insight into important tumourigenic mutations without the need for invasive metastatic biopsies or complex, expensive analyses. However, a major shortcoming of FISH is that it produces mainly qualitative data, as fluorescence measurements often simply detect the presence or absence of a given target; this leads to low sensitivities and limits the applicability of results. Furthermore, due to the *a priori* knowledge requirement of probe design, CTC FISH analyses are not well suited for novel biomarker discovery. Although the limitations of CTC FISH analysis have prevented it from being associated with any major breakthroughs in the field of liquid biopsy research, it represents a relatively simple method of non-invasive CTC biomarker monitoring.

Due to its ability to detect genomic alterations, many FISH experiments have been performed in prostate CTCs as a way to monitor various aspects of the AR signalling pathway. Using fluorescent probes designed to target the *AR* gene, several groups have reported amplified copy numbers in the CTCs of approximately 60% of CRPC patients, with relatively high inter-/intrapatient heterogeneity (109–111). A similar experiment showed that a variety of mutant *AR* genotypes are detectable in the CTCs of CRPC patients, some which have cited associations with resistance to therapies targeting the androgen axis (112). Since various isoforms of the androgen receptor can be targeted by specific therapies, experiments such as this, which monitor *AR*-gene status, demonstrate how CTC liquid biopsies could help dictate treatment options.

FISH experiments have also been used to detect copy number amplifications of the *MYC* oncogene and deletions of the *PTEN* tumour suppressor gene in the CTCs of CRPC patients. These results were concordant with those of primary tumour tissue, once again demonstrating the relevance of information obtained by this non-invasive biopsy method (110,111,113,114).

Aside from monitoring CNVs, mutations, and deletions, researchers have also used CTC FISH analysis to monitor CRPC patients for the presence of the *TMPRSS2-ERG* translocation genotype— a fusion event between the androgen-responsive *TMPRSS2* promoter and the *ETS* family oncogene which occurs in 30-70% of treatment naïve prostate cancer tumours (111). Taken together, these experiments demonstrate the promise of CTC FISH analysis as a simplistic, cost-effective method for non-invasive monitoring of relevant genomic prostate cancer biomarkers.

1.3.2.2 Protein Immunofluorescence

Similar to FISH, protein-based immunofluorescence experiments represent another avenue for relatively simple, yet potentially illuminating, CTC analysis. Many of these experiments use fluorescently labeled antibodies to target proteins that play significant roles in oncogenic processes. In doing so, researchers are able to gain insight into the expression and localization of proteins of interest within CTCs. Again, such analyses are hindered by *a priori* knowledge requirements, as antibodies must be selected for potentially relevant proteins, but they are able to efficiently monitor current phenotypes of tumourigenic pathways within CTCs. Furthermore, protein-based immunofluorescence experiments consist of relatively simple and affordable procedures that can be combined with immunofluorescence-based CTC detection steps commonly used for many enrichment devices. Therefore, protein-based CTC analyses exhibit high potential due to their simplicity, affordability, and applicability with a wide variety of enrichment/detection techniques.

Regardless of simplicity, protein-based immunofluorescence analyses of CTCs have revealed several exciting, and potentially clinically useful findings. In 2012, Miyamoto *et al.*

collected prostate cancer CTCs using the herringbone CTC-Chip, and performed on-chip immunofluorescence using monoclonal antibodies targeting PSA and PSMA (27). The genes of these two proteins are positively and negatively regulated by the androgen-receptor, respectively, and thus, were used as a means to monitor AR activation in response to traditional prostate cancer therapies (115,116). The results showed that prior to androgen deprivation therapy (ADT), nearly all patients' CTCs showed the "AR-on" phenotype (ie. PSA+/PSMA-), whereas following 1 month of ADT these patients' CTCs transformed almost entirely to the "AR-off" phenotype (PSA-/PSMA+). The same experiment in CRPC patients found significant intrapatient and interpatient heterogeneity in AR activation, with approximately 52% of patients showing the "AR-off" phenotype. Additional results showed that increased proportions of "AR-off" and "AR-mixed" (ie. PSA+/PSMA+) CTCs was predictive of lower survival following treatment with the androgen synthesis inhibitor abiraterone (27). These results show the potential for androgen-receptor-targeted CTC immunofluorescence as a means of monitoring prognosis in prostate cancer patients.

Another interesting protein-based CTC analysis was performed by Darshan *et al.*, who used anti-androgen-receptor monoclonal antibodies to monitor the cellular location of the androgen-receptor in response to taxane treatment (30). Taxanes—a family of drugs commonly used as a chemotherapeutic agent for prostate cancer—bind β-tubulin and stabilize microtubules, causing proliferative cells to undergo apoptosis (117). Through their immunofluorescence experiments, Darshan *et al.* were able to show a significant correlation between cytoplasmic sequestration of androgen receptor and clinical response to taxane therapy (30). Taken together, these results indicate the potential use for protein-based CTC immunofluorescence assays as a means for prognosis and treatment response predictions in prostate cancer.

1.3.2.3 Reverse-Transcription Polymerase Chain Reaction

Although immunofluorescence-based experiments can be useful for certain analyses, RNA-based analyses such as RT-PCR can enable heightened detection sensitivity and precision of known CTC biomarkers. Similar to immunofluorescence-based analyses, RT-PCR requires *a priori* knowledge of a transcript of interest, as oligonucleotide primers are needed to target a specific transcript for analysis. Upon conversion of RNA transcripts into complementary DNA (cDNA) by a reverse transcriptase enzyme, cDNA is amplified to observable levels through PCR. In doing so, RT-PCR is capable of detecting the presence of a transcript of interest even if it is undetectable by FISH-based analysis techniques. As mentioned above, many CTC enrichment devices result in relatively impure samples of CTCs, so the increased sensitivity of RT-PCR can help researchers detect the expression of tumour-specific transcripts regardless of sample purity. To do so, researchers can simply perform bulk lysis of an enriched CTC sample followed by RT-PCR, rendering this technique a useful downstream analysis for a wide variety of enrichment devices (66). Furthermore, this improved sensitivity means RT-PCR is compatible with enrichment strategies that result in fixed cells, as single-cell isolation of CTCs is not required for these analyses. For these reasons, RT-PCR has shown significant promise as a downstream molecular analysis technique for CTCs and has resulted in some exciting and potentially clinically relevant findings.

Due to the increased sensitivity and reliability of RT-PCR, many FISH-based CTC transcriptome analyses have been repeated using this technique. For example, liquid biopsy researchers have used RT-PCR on metastatic prostate cancer CTCs to detect the presence of the *TMPRSS2-ERG* chimeric transcript, and to test its potential as a therapeutic biomarker (118,119).

While these experiments present an additional technique by which to monitor known CTC biomarkers, they have not yet shown very high clinical utility.

More promisingly, RT-PCR-based CTC analyses investigating the *AR-V7* splice variant— a variant of the *AR* transcript that lacks the ligand binding domain, resulting in a constitutively active androgen-receptor—have led to some very exciting results (120,121). Since the androgen-receptor isoform encoded by the *AR-V7* splice variant is constitutively active in the absence of androgen, it has been postulated that the detection of *AR-V7* in CTCs would be associated with resistance to androgen-axis-targeted therapies, such as enzalutamide and abiraterone. To test this hypothesis, a group used the AdnaTest for CTC enrichment combined with bulk quantitative RT-PCR to analyze *AR-V7* status in the CTCs of 62 CRPC patients initiating enzalutamide or abiraterone treatment. Their results showed that *AR-V7* positive patients treated with enzalutamide or abiraterone had shorter PSA progression-free survival, shorter clinical or radiographic progression-free survival, and shorter overall survival (28).

Another paper from the same group, authored by Steinestel *et al.*, built upon this idea by detecting the presence of *AR-V7* as well as *AR* gene mutations in CTCs of PSA-progressed prostate cancer patients. This experiment analyzed 47 prostate cancer patients—51% of which had CTCs harboring *AR*-modifications—and estimated a positive predictive value of CTC *AR*-status for therapeutic response of nearly 94%. They postulated an effect size of 33% based on their selection of patients for their clinical trial. Most recently, this group expanded upon their work and analyzed 202 patients with CRPC commencing abiraterone/enzalutamide treatment and monitored the prognostic values of CTC detection combined with *AR-V7* detection. They found that outcomes were best for CTC-negative patients, intermediate for CTC-positive/*AR-V7*-negative patients, and worst for CTC-positive/*AR-V7*-positive patients (29). Therefore, analyzing

CTCs using RT-PCR appears to have the ability to determine which patients will respond to androgen-axis-directed therapies prior to administration of treatment; these findings represent one of the primary examples of the potential for CTC analysis in personalized medicine.

1.3.3 Single-Cell Sequencing

Although immunofluorescence and RT-PCR experiments have shown significant promise as tools for liquid biopsy analysis, the next frontier for CTC analysis is clearly next-generation sequencing (NGS). Unlike these other methods, NGS does not require *a priori* knowledge of potentially relevant genes/pathways and therefore has the ability to discover truly novel biomarkers. Due to the rarity of these cells, performing NGS methods on CTCs was infeasible until recently, when technological advances allowed for better isolation of pure samples (101,122). These isolation techniques include micromanipulation, microfluidics, and laser capture microdissection, and generally involve expensive, highly specific instruments that are not widely available in labs (101,122). As prices continue to fall for commercial CTC enrichment/detection/isolation platforms such as the AccuCyte CyteFinder, this should allow more labs to perform these analyses (84,85,87). Another issue arising from the rarity of CTCs, which previously added to the infeasibility of NGS analyses, is the miniscule amount of starting genomic/transcriptomic material. Since there are often <10 CTCs per 7.5 mL of metastatic cancer patient blood, traditional bulk NGS library preparation methods, which sometimes require ~1 μg of starting material, are not applicable for CTC analysis (101,122). For this reason, single-cell sequencing methods are required in order to deal with picogram input levels. Single-cell sequencing also allows researchers to analyze CTC heterogeneity and clonal evolution, thereby exhibiting extraordinary potential as an analysis method for cancer research (101). To date,

several different single-cell sequencing methods have been used on CTCs that have led to further classification of these unique cells and potentially clinically relevant discoveries.

1.3.3.1 Single-Cell Whole-Genome Sequencing

One of the primary single-cell sequencing methodologies that has been used on CTCs is whole-genome sequencing (WGS). The goal of WGS is to accurately sequence the entire length of the genome, thereby allowing for untargeted mutational analyses of CTCs. As mentioned above, the main challenge when attempting to perform single-cell genomics is dealing with picrogram input levels of genomic material. In order to address this issue, the majority of single-cell sequencing strategies require an initial whole-genome amplification (WGA) step.

One of the first WGA techniques—degenerate oligonucleotide primed PCR (DOP-PCR)—uses degenerate primers capable of annealing randomly throughout the genome via degenerate base pairing. Following primer annealing, the genome is amplified by several rounds of PCR using thermostable polymerases (123,124). This methodology causes DOP-PCR to have several limitations. Degenerate priming naturally results in selection biases towards specific loci due to variable primer annealing and PCR efficiencies; this results in poor coverage and allelic dropout in amplified genomes. Furthermore, the thermostable polymerases used in DOP-PCR are relatively error prone and result in high mutational rates during exponential amplification (125).

Isothermal amplification was developed to improve amplification bias problems arising from PCR, and the most common of these techniques is multiple displacement amplification (MDA). This WGA method consists of an isothermal primer annealing step using random hexamer primers followed by extension via the high-fidelity Φ29 polymerase; this enzyme results in much lower error rates than traditional thermostable polymerases. During extension,

this polymerase performs strand-displacement to allow primers to re-anneal and continue amplification (126,127). However, this method of WGA suffers from the issue that loci that are amplified first become overrepresented; this generally results in low uniformity of amplified genomes.

To overcome the deficiencies of DOP-PCR and MDA, hybrid methods have been devised to harness the benefits of each WGA technique. An example of such a method is displacement DOP-PCR—more commonly referred to as PicoPlex—which uses degenerate primers to anneal throughout the genome while adding a common sequence. This sequence can then be targeted by primers during subsequent PCR cycles, thereby theoretically standardizing amplification efficiencies (128).

Similarly, multiple annealing and looping-based amplification cycles (MALBAC) uses random primers that add a common sequence, followed by extension to create semiamplicons of variable length. Next, a melting step takes place where the semiamplicons are removed from the template by heating to 94 °C. After further pre-amplification, the semiamplicons obtain complementary ends and form loops as the temperature is lowered to 58 °C, thereby preventing any additional amplification. Following five rounds of pre-amplification, exponential amplification via PCR takes place in order to generate an appropriate amount of genomic material for sequencing. Once again, this methodology helps standardize PCR efficiencies and limit pre-amplification biases (129).

As of now, the most commonly used WGA methods are isothermal and hybrid amplification, and they exhibit increased functionality for separate genomic experiments. For example, MALBAC has been shown to be more adept at detecting CNVs, while MDA has been shown to exhibit higher somatic single-nucleotide variant (SSNV) detection rates (126,130).

These WGA techniques have allowed researchers to perform single-cell WGS in CTCs, which has led to exciting findings in the field of liquid biopsy research. As single-cell genome sequencing has entered the field of CTC research, some exciting discoveries have been made. One of the major examples of single-cell genome sequencing on CTCs was published by Lohr *et al.* in 2014. The authors used the Illumina MagSweeper to enrich for epithelial-derived cells from the whole blood of 36 CRPC patients, and then isolated individual EpCAM+/CD45- CTCs through robotic micromanipulation. WGA was performed via MDA in order to obtain sufficient genomic material for sequencing. Upon construction of single-cell sequencing libraries, the authors first performed low pass WGS as a quality control step; this ensured that the protocol was cost efficient by preventing poor quality libraries from being sequenced deeply in subsequent analyses. Next, whole-exome sequencing (WES) was performed by enriching for exomic sequences in libraries that had surpassed a specific quality threshold. In order to overcome poor coverage and high allelic drop out rates, the authors pooled individual CTC libraries from the same patient together and were able to accurately detect SSNVs that occurred in multiple cells. Using this method, the authors showed that 70% of CTC mutations (51/73) were also present in primary tumour tissue from the same patient, thereby establishing the potential for CTC single-cell genomics in the clinic (31).

In a similar manner, another group used single-cell WGS to compare SSNV signatures from a CRPC patient's CTCs with signatures from the same patient's primary and metastatic tumour tissue. This group enriched for CTCs using the NanoVelcro Chip, isolated CTCs using laser capture microdissection, and performed WGA via MDA. Using this protocol, the authors showed that 86% of clonal mutations identified in the CTCs were present in either the primary or metastatic tumours (32).

Together, these findings suggest that genomic analyses of CTCs allow accurate representations of current tumour genotypes and clonal subpopulations; this solidifies the basis of CTC analysis as a non-invasive biopsy method in the clinical setting. In order to further advance the field, additional serial analyses must be done over the course of treatment administration to investigate novel correlations between genotype and treatment outcome.

1.3.3.2 Single-Cell RNA-Sequencing

Another commonly used NGS-based CTC analysis methodology is single-cell RNA sequencing (scRNA-seq). Similar to WGS, early iterations of bulk RNA-seq protocols require millions of cells and approximately 1 μg of total RNA, and therefore were incompatible with CTC research (131). However, in recent years many protocols have been developed to overcome the issue of low transcriptomic input, thereby allowing the rapid growth of scRNA-seq analyses. The first step in all scRNA-seq protocols is first-strand cDNA synthesis via reverse transcription, where mRNA transcripts are often targeted by poly-dT RT primers containing PCR primer sequences and unique barcodes for downstream multiplexing. Several mechanisms have been devised to achieve subsequent second-strand synthesis. One such method, poly-A tailing, adds poly-A tails to the 3' ends of first-strand cDNAs and performs second-strand synthesis by adding another poly-dT primer containing the PCR primer sequence; this prepares the cDNA for amplification (132). Another common second-strand synthesis method, template-switching, relies on the unique terminal transferase functionality of the Moloney murine leukemia (M-MLV) reverse transcriptase, which adds 2-5 untemplated nucleotides to the 3' end of the cDNA when it reaches the 5' end of the template RNA. These terminal nucleotides can then act as an anchor point for a template switching oligonucleotide (TSO)—an oligo containing a

complimentary sequence to the untemplated nucleotides connected to a PCR primer. The M-MLV enzyme then completes cDNA synthesis to the 5' end of the TSO, thereby creating a new template which can be amplified through PCR (133–136). Template switching is now considered a superior method because it allows for complete transcript coverage by eliminating incomplete reverse transcription that causes 3' coverage biases. In the final step of most scRNA-seq library preparation protocols, cDNA is run through limited numbers of PCR cycles in order to amplify the sample to detectable levels; this step can lead to amplification bias which prevents accurate quantitative analyses. In order to overcome this deficiency, Islam *et al.* devised a way to use unique molecular identifiers (UMIs) to tag transcripts prior to amplification, thereby allowing for the measurement of absolute values of transcripts rather than reads per million (137). Therefore, advancements in scRNA-seq protocols have allowed researchers to accurately analyze transcriptomes of rare cells, and for this reason, has become an important area of CTC research.

Modern scRNA-seq methodologies have opened up another way in which to analyze CTCs and search for additional clinical utilities of liquid biopsies. While limited scRNA-seq research has been done in prostate CTCs, the studies that have been done have provided exciting results. For example, Ting *et al.* performed scRNA-seq on prostate CTCs that had been captured using the CTC-iChip and showed that they highly express extracellular matrix (ECM) genes. These results were corroborated in pancreatic and breast CTCs, and are consistent with the fact that ECM genes have been implicated in priming tumour cells for metastatic sites (138,139).

More interestingly, Miyamoto *et al.* performed scRNA-seq on prostate CTCs and investigated methods of drug resistance. The authors collected CTCs from 18 metastatic prostate cancer patients using the CTC-iChip and performed single-cell RNA-seq. In doing so, the group showed that there is significant intrapatient/interpatient CTC expression profile heterogeneity;

this was apparent when monitoring for *AR* mutation and splice-variant signatures. Furthermore, data from a group of patients that had been treated with, and become resistant to, enzalutamide was compared with data from enzalutamide-naïve patients. This analysis showed that the noncanonical Wnt signalling pathway was significantly enriched in enzalutamide-resistant patients, thereby implicating this pathway in antiandrogen resistance; results were confirmed *in vitro* (140). These findings were consistent with a separate study which used scRNA-seq on pancreatic CTCs and implicated the WNT signalling pathway in metastasis (33).

In all, these findings suggests a possible role for CTC scRNA-seq in the clinic, by potentially allowing doctors to prognosticate the metastatic potential of a tumour or even predict treatment outcomes before commencement of a therapy. In order for this to come to fruition, further scRNA-seq analyses must be done on CTCs to find new biomarkers and correlate them to prognosis and treatment outcomes.

1.3.3.3 Single-Cell miRNA Sequencing

An example of a next-generation sequencing method that has not yet been applied to CTC research is single-cell miRNA sequencing. miRNAs were first discovered in *C. elegans* mutagenesis screens that showed the presence of a short, non-coding RNA, lin-4, which was capable of regulating the translation of key developmental proteins (141–143). Since this landmark discovery, there has been significant interest into the biological and clinical significance of miRNAs. Until recently, the main methods of analyzing miRNA expression was via FISH and RT-PCR and, using such experiments, several miRNAs have been shown to play oncogenic or tumour suppressor roles in prostate cancer. For example, miR-21 has been shown to regulate vascular proliferation and tumour invasiveness in prostate cancer, and its expression

is correlated with biochemical recurrence, castration resistance and metastatic phenotypes (144,145). miR-125b—a miRNA species highly expressed in prostate cancer (146,147)—has been shown to negatively regulate tumour suppressor genes, leading to increased proliferation and inhibition of apoptosis (146,148,149). Conversely, miR-145 and miR-224 have been shown to be downregulated in prostate cancer, as they normally function as tumour suppressor miRNAs inhibiting cell invasion and migration (150–153). Therefore, miRNAs have been shown to play key roles in tumour progression and, for this reason, exhibit exciting potential as clinically relevant biomarkers.

While the role of miRNAs in cancer has been well described, much less is known about miRNAs in CTCs. In order to further investigate the role of miRNAs in tumour progression and determine additional clinically relevant correlations, next-generation miRNA-sequencing technologies must be applied to liquid biopsy research. Advances in this direction have recently been made by Faridani *et al.*, who published a protocol for single-cell small-RNA sequencing (154), although there remained significant challenges in library construction efficiency. Thus, single-cell miRNA sequencing represents an untapped area of CTC research that may lead to exciting biomarker discoveries and/or clinical applications.

1.3.4 Summary

Over the past decade, the field of CTC liquid biopsy research has experienced sustained growth by consistently taking advantage of state-of-the-art analysis techniques. What began with enumeration and basic immunofluorescence has now become one of the most high-potential applications of single-cell sequencing. By using this wide variety of analysis techniques, researchers have already developed several exciting potential clinical utilities for CTCs.

Enumeration has been cleared by the FDA for prognostic uses in metastatic prostate cancer patients (67,102). Immunofluorescence has shown promise as a method for monitoring cellular localization of the androgen receptor, which appears to have clinical implications with respect to taxane therapy outcome-predictions (27). Detecting the presence of the *AR-V7* splice variant using RT-PCR has shown immense potential for predicting responses to anti-androgen therapies (28,29). Finally, single-cell sequencing—whether it be genomic or transcriptomic—is being used to investigate potential novel biomarkers which may one day be used in the clinic (31–33,140). What becomes clear when reviewing these exciting findings is that the field of CTC research must continue to operate at the forefront of molecular analysis. As new and improved methods for single-cell analysis arise, such as single-cell miRNA sequencing, researchers must implement these tools into CTC research. In doing so, it is possible that CTC liquid biopsies eventually become a standard clinical practice for obtaining early diagnosis, determining prognosis, monitoring tumour burden, predicting treatment outcomes, and guiding therapies.

1.4 Research Statement

The goal of this thesis is to develop a novel, integrated method for single-cell miRNA sequencing of CTCs in prostate cancer patients. This is intended to exhibit feasibility and utility for the clinical setting, and help progress the field of liquid biopsy research by demonstrating a novel analysis method.

The goals of this project are:

1. Develop an integrated CTC enrichment/detection method by combining negative selection, high-throughput fluorescent imaging, and micropipette-based micromanipulation from an open microwell format.

2. Modify an existing single-cell miRNA library prep protocol for compatibility with the open microwell format.

3. Generate sequencing data, and use bioinformatic analysis techniques to search for correlations with patient data.

Chapter 2: CTC Enrichment

The first technical challenge that my project had to overcome was devising a way to enrich CTCs from whole-blood with high efficiency. Our general plan was to combine a negative selection-based pre-enrichment step with high-throughput fluorescent imaging and subsequent micromanipulation. To integrate the various aspects of our protocol, we used a semi-automated robotic platform that had been previously designed by Marijn van Loenhout, called the PReMiSe (Pipette Recovery and Microscopy for Sequencing) platform. For negative selection, we planned to use the RosetteSep™ kit from STEMCELL™ Technologies to remove all red blood cells (RBCs) and other unwanted hematopoietic cells from the sample. The resulting sample would be treated with anti-EpCAM and anti-CD45 antibodies and loaded onto a microwell chip, which would be scanned via high-throughput fluorescent microscopy to detect CTCs based on EpCAM/CD45 expression signatures. Following CTC detection, the micromanipulation functionality of the PReMiSe platform would be used to individually isolate these cells in a separate microwell chip for subsequent analysis (Figure 2.1). Designing this workflow required precise optimization at nearly every step, which this chapter will describe in detail.

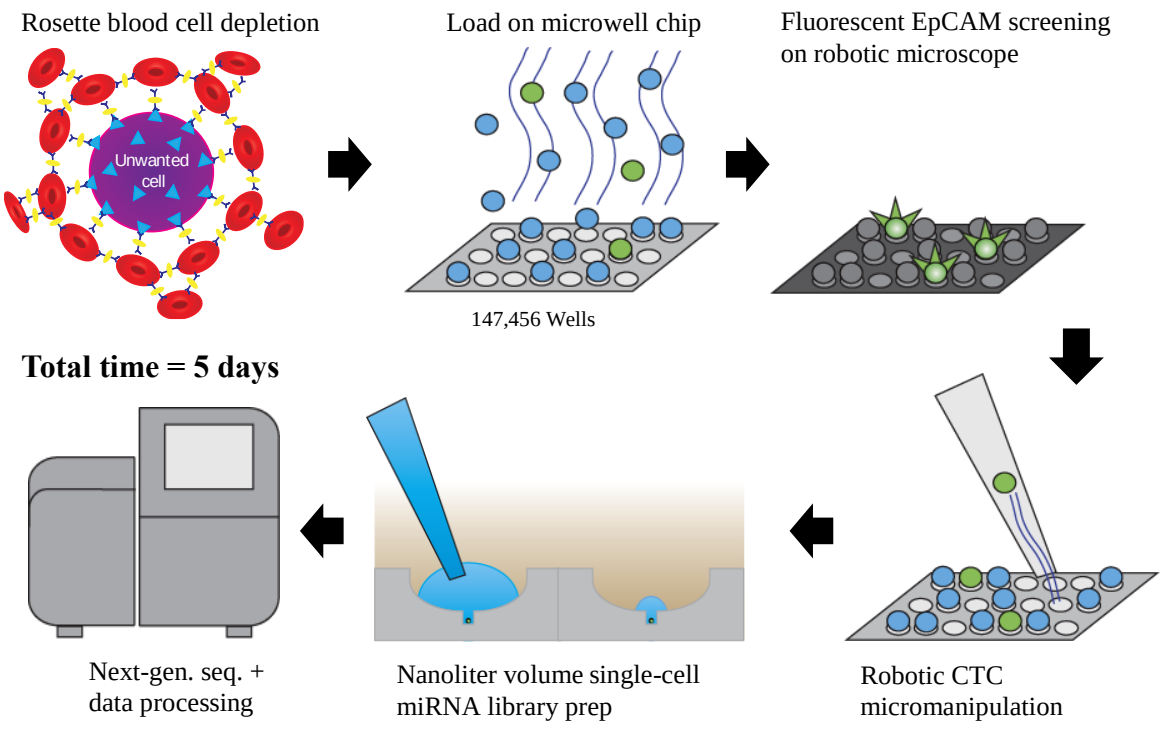

Figure 2.1 Overview of the protocol workflow. The entire protocol can be broken down into distinct steps that required design, optimization, and verification. These steps included pre-enrichment negative selection, cell loading, fluorescent screening, robotic micromanipulation, library prep, and sequencing.

2.1 Materials

2.1.1 The PReMiSe Platform

As mentioned above, in order to integrate the different steps of our protocol, we used a semi-automated robotic system, the PReMiSe platform. PReMiSe combines high-throughput microscopy with micromanipulation and reagent dispensing capabilities. Its microscopy functionality allows for the visual tracking of rare cells and high-throughput fluorescent detection of CTCs. Additionally, it has a microfluidic flow-controlled robotic micropipette that can gently micromanipulate cells; this capability is required for efficient single-cell isolation. Lastly, the same micropipette can be used for nanolitre volume reagent dispensing steps required for single-cell library preparation protocols (Figure 2.2).

While the PReMiSe platform was largely in place before the start of this research project, it needed to be optimized for our experiments. To do so, LabView scripts were written to implement our protocol. This included programs for single-cell aspiration, single-cell dispensing, reagent dispensing, and micropipette washing. Furthermore, settings for high-throughput microscopy were tested and optimized to discriminate between CTCs and PBMCs based on immunofluorescence.

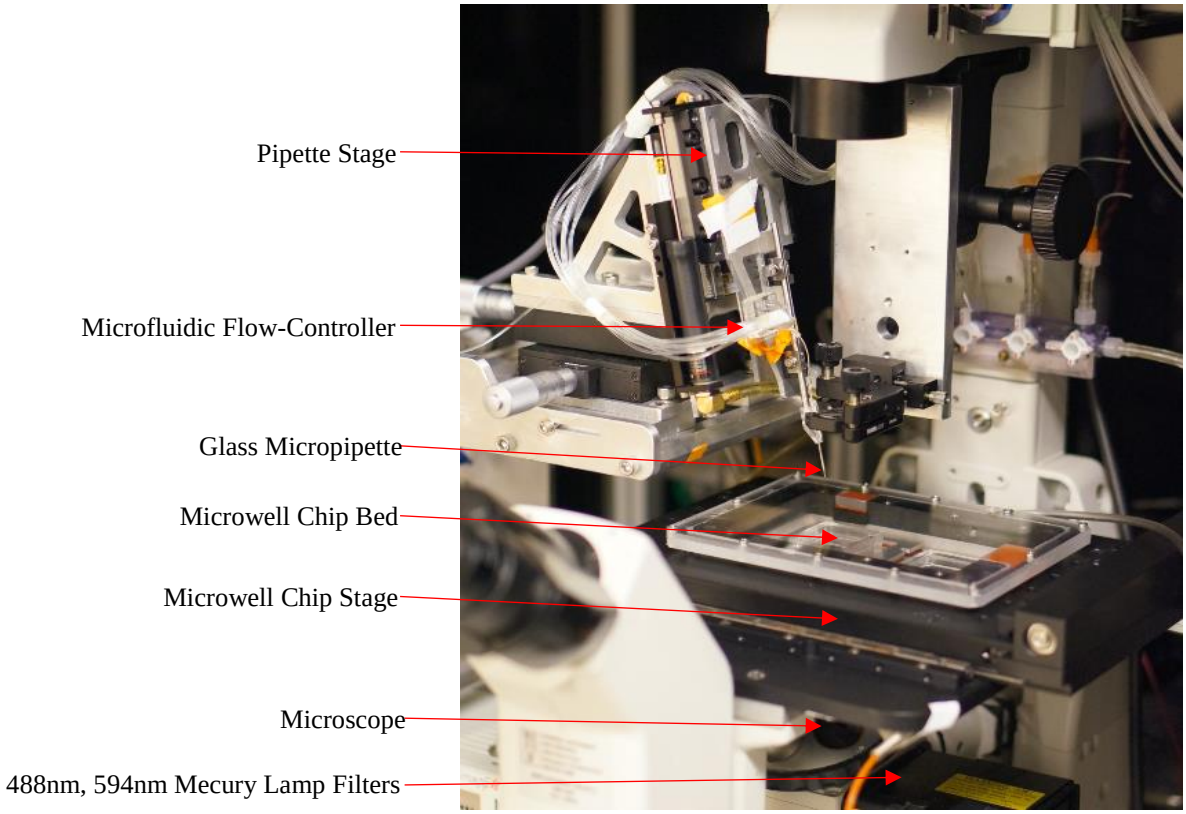

Figure 2.2 The PReMiSe Platform. The PReMiSe (Pipette Recovery and Microscopy for Sequencing) Platform is a semi-automated robotic device that allows for the visual tracking of rare cells, immunofluorescence, micromanipulation, and reagent dispensing. The pipette stage and microwell chip stage allow precise control of the glass micropipette along the vertical axis and the horizontal plane, respectively. The microfluidic flow-controller allows for gentle micromanipulation and precise reagent dispensing at nanolitre volumes. The microwell chip bed holds the microwell chip in place throughout analysis. The microscope enables the visual tracking of rare cells, while the mercury lamp filters can be used for immunofluorescence-based CTC detection.

2.1.2 Detection Chip Design and Optimization

To support CTC isolation, we designed and optimized a microwell detection chip. The chip was designed to allow cells to naturally settle into individual microwells where they could be rapidly analyzed by the PReMiSe platform's high-throughput fluorescent scanning functionality. Our chips were designed using polydimethylsiloxane (PDMS) coated over a glass slide; the transparency of these materials allowed for immunofluorescence experiments once the cells had settled in the wells. Our initial design contained 147,456 square microwells, separated into 12 × 12 arrays with dimensions of 600 μm × 600 μm (1024 total arrays, aligned 32 × 32 on the chip). The dimensions of each microwell was 30 μm × 30 μm with a depth of 45 μm. The microwells were separated by ~22 μm in each direction within the array; arrays were separated by ~60 μm in each direction. Surrounding the entire chip was a square PDMS barrier, designed to allow for the adding of ~4 mL of media or wash solution to the chips (Figure 2.3).

We tested the original design by observing how K562 cells—a human *BCR/ABL*-positive cell line derived from a patient with chronic myeloid leukemia in blast crisis (155)—settled into the wells. Initial trials resulted in a large proportion of cells settling on the chip surface between wells. For this reason, we added a "wiggle" function to the PReMiSe platform, which gently shook the microwell chip stage to help cells fall into microwells. A separate issue that was revealed from these initial tests was that a significant proportion of cells ended up settling outside the total array of wells. To fix this problem, we designed a thin piece of PDMS to surround the well array that functioned to contain cells within the array as they settled (Figure 2.3). Upon settling, ~4 mL of media or wash solution could be added to, or removed from, the chip without disrupting the cells.

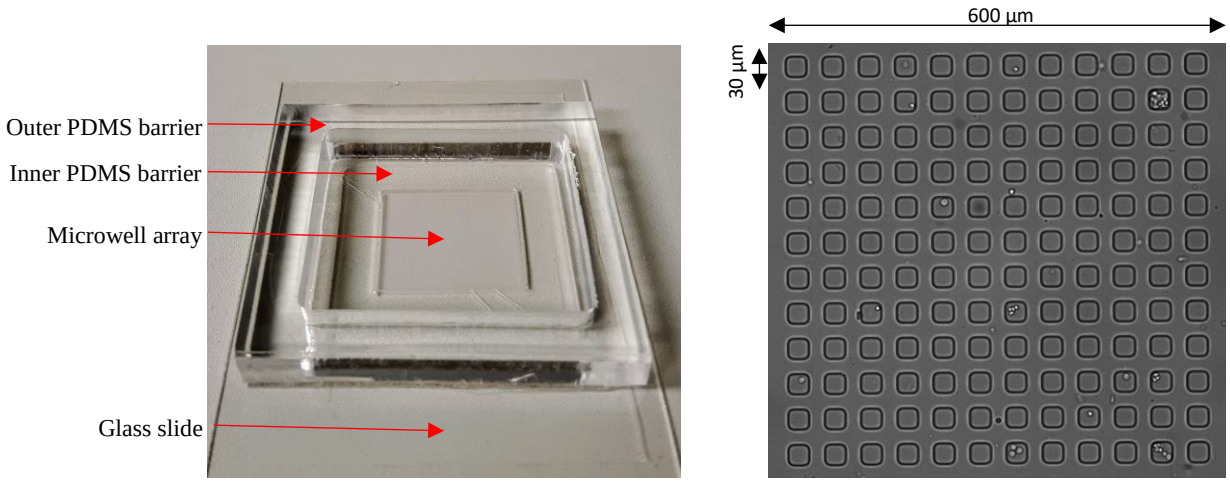

Figure 2.3 Detection chip design. The detection microwell chip consisted of 147,456 microwells designed to allow single cells to settle into individual wells. The inner PDMS barrier (see left) was designed to contain cells within in the microwell array while they settled. The outer PDMS barrier (see left) allowed for ~4 mL of buffer and/or washing solution to be added to the chip. The microwell array consisted of a 32 × 32 array of subarrays, each of which were composed of 12 × 12 microwells (see right). The dimensions of each individual microwell were 30 µm × 30 µm × 30 µm.

2.2 Methods

Once we established cell manipulation capabilities on the PReMiSe platform functionalities, we proceeded to the optimization of the CTC isolation and analysis protocol. As mentioned above, our CTC enrichment protocol could be broken down into three key stages: negative selection, high-throughput microscopy, and micromanipulation.

2.2.1 Negative Selection

To develop our enrichment protocol, the first step was to optimize RosetteSep™ negative selection for our specific workflow, and generate rough estimates of cell recovery rates. For our first trials, we spiked K562 cells and 1000 LNCaP—a cell line established from a metastatic lesion of human prostate adenocarcinoma (156)—cells into Dulbecco's phosphate buffered saline (DPBS) containing 2% fetal bovine serum (FBS) and 4 mM EDTA. The resulting mixture was layered on top of Lymphoprep™ density gradient medium, and centrifuged at 1200 g for 20

minutes. Following centrifugation, the solution lying just above the Lymphoprep™ layer was collected, transferred into a 1.5 mL Eppendorf tube, washed twice with DPBS, and then treated with anti-EpCAM and anti-CD45 antibodies for subsequent immunofluorescence-based counting. The resulting solution was transferred onto a detection microwell chip, allowed to settle, and was then loaded onto the PReMiSe platform for immunofluorescence-based cell counting. Epithelial-derived cancer cells (ie. LNCaP cells) were counted using a semi-automated algorithm to detect cells exhibiting EpCAM+/CD45- expression patterns.

During initial experiments using this protocol, we calculated a recovery rate of 64 ± 5% (an average of ~642/1000 LNCaP cells recovered). However, our actual recovery rate was likely higher, because LNCaP cells formed large aggregations during centrifugation which led to cell-counting problems. Also, it appeared that depletion of non-epithelial cells (ie. K562 cells) was functioning well. In order to improve negative selection recovery rates, we tested recovery from different layers above the Lymphoprep™. We also optimized the volume of liquid to collect, eliminated unneeded wash steps, and altered the protocol to allow all wash steps to take place in the same 15 mL Falcon tube.

2.2.2 High-Throughput Microscopy

We then focused on fine-tuning the high-throughput microscopy parameters for this specific experiment. The overall experimental goal for this section was to rapidly scan the well arrays of the detection microwell chip using PReMiSe's segmentation algorithms, and automatically determine which cells were CTCs and PBMCs, respectively. This would be done by rapidly taking three images for each well array: one bright-field image, one image with 488 nm light, and one image with 594 nm light. The bright-field image would allow us to manually

inspect basic characteristics of the cell, and determine whether it was a contaminant or a true cell. The 488 nm and 594 nm images would be used to stimulate immunofluorescent CD45 and EpCAM antibodies, respectively, in order to determine the antigen-expression patterns of each cell. After scanning the detection chip in this fashion, the image-processing algorithms of PReMiSe would segment images to display individual microwells and then measure the fluorescence occurring in each microwell at the two wavelengths. Using this plot, we would be able to select only the wells containing cells that expressed EpCAM+/CD45- patterns, and return to these cells for further inspection and subsequent micromanipulation (Figure 2.4)

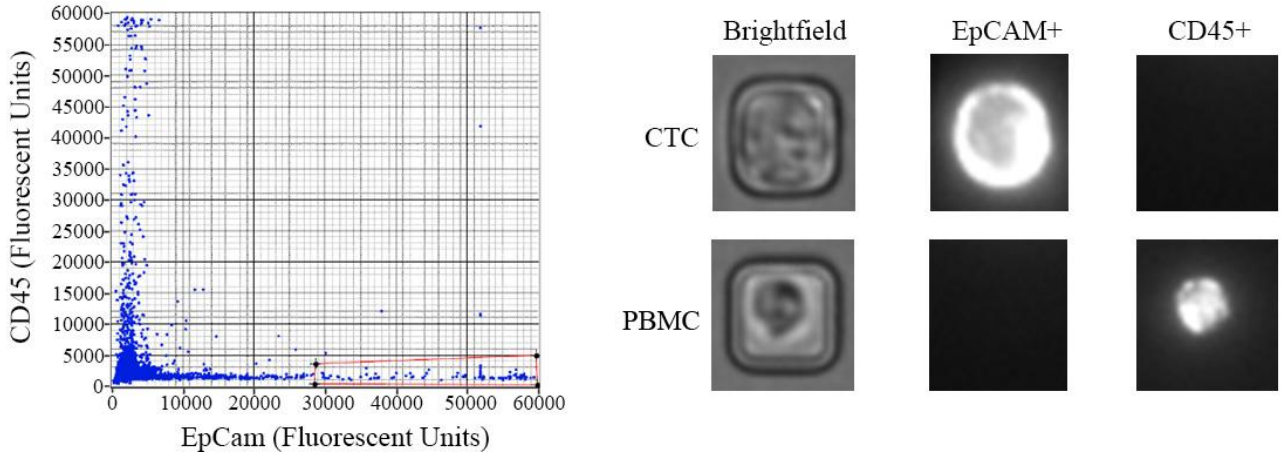

Figure 2.4 High-throughput microscopy. CTC detection using PReMiSe's cell-detection algorithms. Cells expressing EpCAM+/CD45- patterns could be selected for subsequent analysis (see left). PReMiSe would return to these wells for manual verification of bright-field image. CTCs and PBMCs were detected based on antigen expression patterns (see right).

Early high-throughput microscopy trials using K562 and LNCaP cells revealed several areas requiring further optimization. First, excess unbound fluorescent antibodies caused far too much background fluorescence after loading the negatively-selected samples onto the detection chip, thereby preventing PReMiSe's algorithms from accurately predicting cell-type. To address this issue, we added two 10 mL wash steps following antibody staining—this drastically reduced background fluorescence and allowed the detection algorithms to function better. Additionally,

we noticed there was a significant amount of cross-staining occurring, as K562 cells fluoresced slightly in 594 nm light even though they do not express EpCAM. This problem was solved by incubating negatively-selected cell samples with 5 μL of Human TruStain FcX™ (Fc Receptor Blocking Solution) for 10 minutes prior to antibody staining. Other factors that required optimization were the exposure time, gain, and focal plane during high-throughput microscopy; each of these variables were fine-tuned for each wavelength independently in order to most accurately predict antigen expression patterns.

2.2.3 Micromanipulation

After successfully fine-tuning high-throughput imaging, we optimized the subsequent micromanipulation steps that would be necessary for cell isolation. We used the micropipette-based micromanipulation functionality of the PReMiSe platform to gently aspirate cells from a given microwell, transport the cells to a separate chip, and dispense them in individual microwells. The main challenge that arose during early micromanipulation trials was due to cell adhesion. Once the cells settled into the wells of the detection microwell chip, they often adhered to the PDMS surface of the chip, rendering them extremely difficult to aspirate. To fix this problem, we began soaking the chips in ~500 μL of 1% Pluronic® F-127 for ~20 minutes to passivate the chip surface prior to the addition of cells. Pluronics are PEO-based triblock polymers that have been shown to prevent protein adsorption and cell attachment to PDMS (157–159); they are commonly used in biotechnological applications due to their extremely low toxicity and immunogenic response (159). This passivation step ensured that cells could be easily aspirated using the micropipette of the PReMiSe platform.

Another micromanipulation issue arose after cells had been successfully aspirated into the micropipette. Occasionally, cells would lyse in the micropipette, likely due to osmotic forces pulling water into the cells as they became surrounded by decreased solute concentrations. Additionally, cells would often adhere to the inner surface of the micropipette and prevent them from being dispensed properly. In order to address these issues, we added 0.05% Pluronic® F-68—another Pluronic polymer with similar functionality to Pluronic F-127, but with higher solubility (160)—to the detection chip media and aspirated this media into the micropipette for approximately 30 seconds immediately prior to micromanipulation. This step allowed micropipette solute concentrations to be similar to the on-chip media—thereby preventing cell lysis—while simultaneously passivating the inner surface of the micropipette to prevent cell adhesion during micromanipulation.

2.3 Results

Using our optimized CTC enrichment pipeline, we performed several experiments in order to measure the efficacy of our methods. These included healthy blood spike-in experiments, CTC enrichment trials with metastatic patient blood samples, and direct comparisons to CellSearch® count values. Performing these experiments exposed additional unforeseen problems that helped us further refine our protocol.

2.3.1 Spike-In Experiments

To estimate recovery rates when dealing with blood samples, we collected blood from healthy individuals in 2 BD Vacutainer® K2 EDTA (K2E) Plus Blood Collection Tubes, ~5mL per tube, and spiked in 1000 DU145 cells; this prostate cancer cell line exhibited decreased cell-

cell adhesion, and thus, we expected more accurate recovery rate calculations than when dealing with LNCaP. The samples were run through the standard RosetteSep™ enrichment protocol, where blood is treated with the RosetteSep™ CTC Enrichment Cocktail Containing Anti-CD36 from STEMCELL™ Technologies; this reagent consists of tetrameric antibodies that crosslink all unwanted cells together, thereby causing them to pellet out in subsequent steps. After crosslinking, samples were run through the same pipeline as described above. Using our optimized enrichment protocol, we calculated an average recovery rate of 77 ± 8% (an average of ~773/1000 DU145 cells recovered). These results indicated that our protocol was working well and we were ready to collect patient blood samples.

2.3.2 Enriching/Detecting CTCs from Metastatic Prostate Cancer Patients

Upon completion of spike-in experiments, we began collecting late-stage metastatic prostate cancer patient blood samples from the BC Cancer Agency. Samples were processed using the protocol described above in order to enrich and detect for prostate cancer CTCs; this took approximately 4 hours, from negative selection to high-throughput scanning. In our first set of experimental trials, we collected blood samples from 16 metastatic prostate cancer patients and were able to detect and isolate CTCs from 12 of these samples (Figure 2.5). The remaining 4 samples failed due to a common issue following centrifugation, where the layer above the LymphoPrep™ density gradient appeared to be significantly contaminated with RBCs. After further investigation, we determined this contamination was the result of fragments of RBCs that had lysed during centrifugation. This negatively impacted high-throughput CTC detection efficacy and rendered subsequent micromanipulation attempts extremely difficult. In order to address this issue, we decreased the acceleration and deceleration of the centrifuge, thereby

decreasing sheer forces acting upon the RBCs. This alteration was successful, as it prevented this observed behaviour from ever occurring again in patient samples.

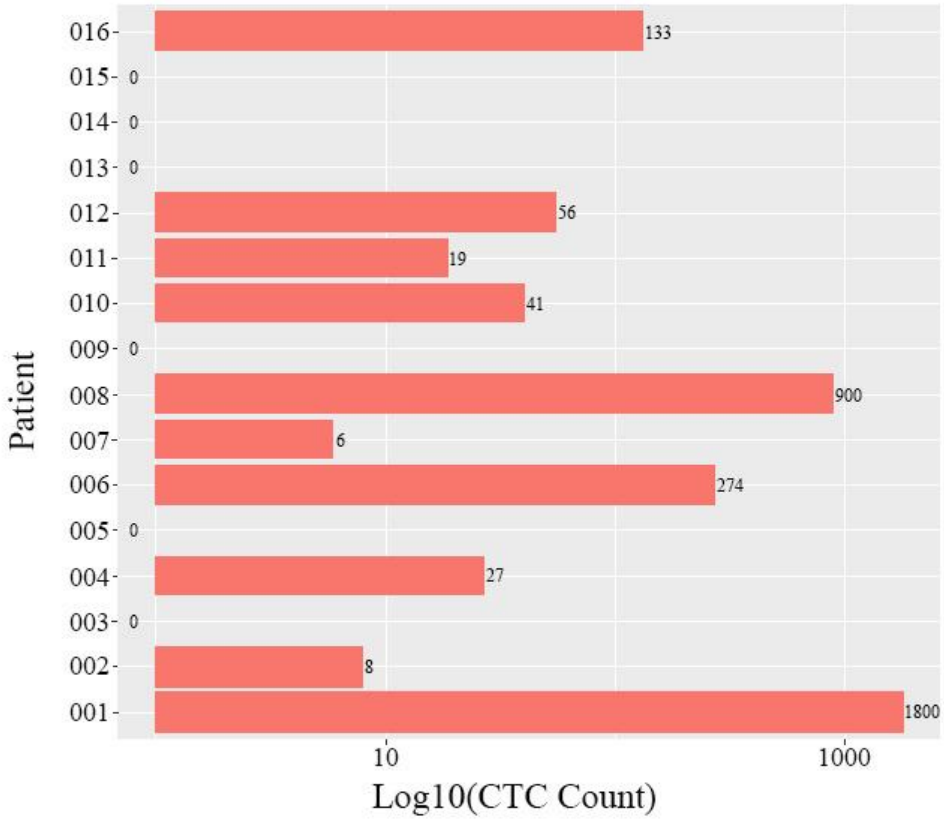

Figure 2.5 CTC Counts from initial metastatic prostate cancer patient experiments. CTC counts from 16 late-stage metastatic patients shows significant heterogeneity between patients. A quarter (4/16) of samples either had no detectable CTCs or were the result of failed runs.

Another issue that arose during these initial patient samples was that samples were often collected late in the afternoon, which led to several late nights processing samples in the lab. The fatigue associated with these late-night experiments often resulted in errors, which lead to longer processing times and occasionally affected processing-efficacy. In order to address this problem, we began exchanging media on the detection microwell chip with Cell*Cover* solution (Anacyte Laboratories) after the cells had been loaded onto the slide and settled into the wells. This solution is designed to stabilize cellular RNA for up to 48 hours, and has been used in many

scRNA-seq experiments (161). By using Cell*Cover* to stabilize cellular miRNA, we were able to place the loaded detection microwell chips in a 4 °C fridge overnight and continue with high-throughput imaging and the remainder of the protocol the following day. This alteration allowed for higher performance during CTC detection/micromanipulation on the second day of sample processing by reducing the number of human errors due to fatigue.

To evaluate the efficacy of our protocol, we began performing CellSearch® measurements in parallel with our protocol to compare our CTC count values with those of a clinically used method. These experiments showed that our protocol was highly effective and outperformed the CellSearch® system in most cases (Figure 2.6). Over the course of 6 of these parallel patient experiments, our protocol detected equal or greater CTC counts than CellSearch® approximately 67% of the time (4/6). Furthermore, in patients with <50 CTCs per 10 mL of blood, our method outperformed CellSearch® in 75% of patients (3/4). One of the patients had >2000 CTCs per 10 mL of blood, and we were able to achieve a CTC count that was 94% of the CellSearch® value (2174/2311). Taken together, it appears that our negative selection-based protocol results in improved CTC detection in patients exhibiting low-CTC counts when compared with CellSearch®'s positive selection methodology, likely by enabling the detection of additional CTC subpopulations.

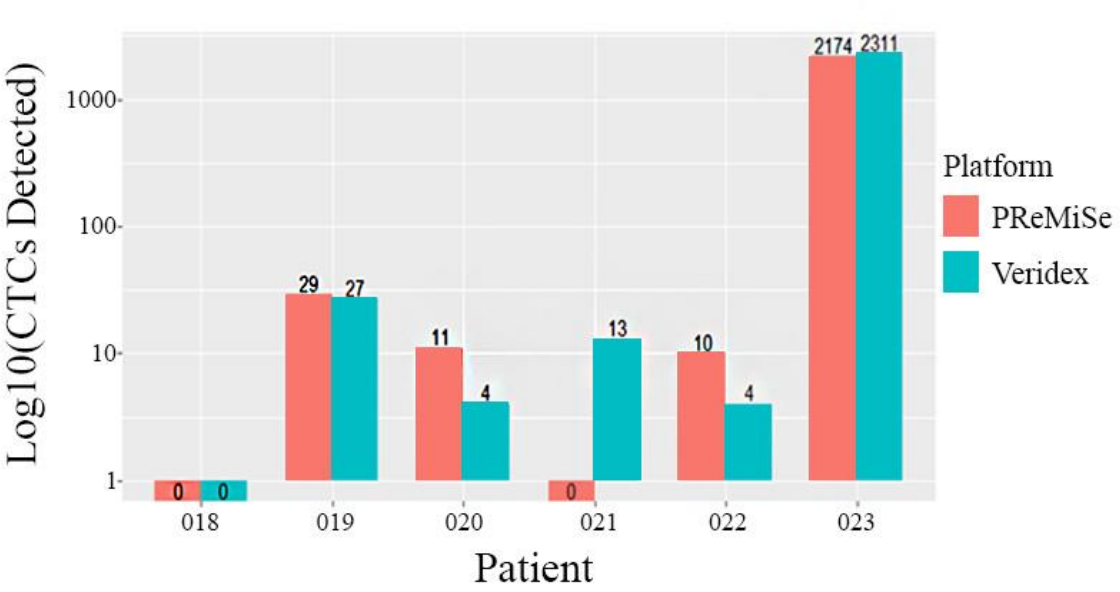

Figure 2.6 PReMiSe CTC counts compared with CellSearch®. The PReMiSe platform detects higher CTC counts than Veridex CellSearch® 75% of the time on patients with <50 CTCs per 7.5mL of blood. For Patient VCC CTC-023, which had very high CTC counts (2311 CTCs), the PReMiSe platform detected 94% of the CellSearch® value.

However, we identified a significant technician bias in our protocol that became evident after beginning to process samples following a lengthy hiatus. After approximately 2 months of not performing our protocol, we were unable to detect CTCs from 3 patient samples in a row (VCC-CTC-025, -026, -027). We attributed this to a lack of practice in the removal of the liquid layer containing CTCs above the LymphoPrep™. This step requires considerable dexterity and experience in order to determine exactly where the layer lies, and to collect it. Other potential sources of technician bias are the various washing steps; if one is not careful, there is a high risk of losing CTCs throughout this process. As mentioned above, we performed all washes and antibody-staining steps in one tube to reduce loss during these steps. Following this decrease in CTC counts, these values returned to where they were during peak performance due to increased practice.

In total, we were able to detect over 6000 CTCs from 40 late-stage metastatic prostate cancer patients. Out of the 40 patients, we were able to detect CTCs in ~68% (27/40) of patients. Of the patients where CTCs were detected, we observed a mean number of CTCs per patient of ~226 ± 538.

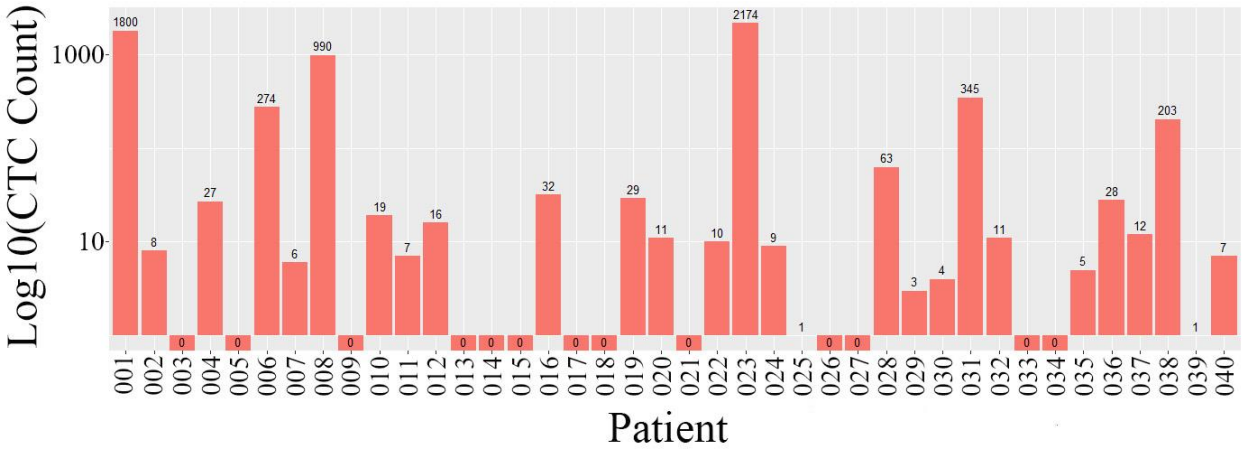

Figure 2.7 Distribution of CTCs detected from late-stage prostate cancer patients.

2.4 Discussions

We successfully designed a protocol for high-efficiency enrichment, detection, and isolation of CTCs from metastatic prostate cancer patients. Our method combined a negative selection-based pre-enrichment step with high-throughput imaging in order to detect a wide variety of CTCs in an antigen-independent manner. In doing so, we obtained blood samples from 40 late-stage metastatic prostate cancer patients and were able to detect ~6000 CTCs. When functioning at peak levels, this represented a marked improvement when compared to the CellSearch® platform. Furthermore, our protocol used micropipette-based micromanipulation to successfully isolate 310 CTCs and 56 PBMCs from 16 late-stage metastatic patients for single-cell miRNA sequencing library preparation. In all, our negative selection/high-throughput

imaging/micromanipulation protocol presents a highly efficient way to enrich, detect, and isolate CTCs, and is compatible with numerous downstream single-cell analysis techniques.

Chapter 3: Single-cell Sequencing Protocol and Analysis

In parallel with designing a successful CTC enrichment protocol, we devised a novel method for single-cell miRNA sequencing of CTCs. Our approach was based on a single-cell miRNA library preparation protocol previously designed and optimized by Michael VanInsberghe in the Hansen lab; recently, a related protocol was published by Faridani *et al.* in Nature Biotechnology (154). After library prep completion, libraries were run on the Agilent Bioanalyzer as a quality control step, size-selected using polyacrylamide gel electrophoresis (PAGE), quantified using a fluorometer or qPCR device, and finally, sequenced on an Illumina MiSeq (Figure 3.1). While many aspects of VanInsberghe's protocol remained the same, we were required to optimize many different facets of the methodology in order to render it compatible with our CTC experiments.

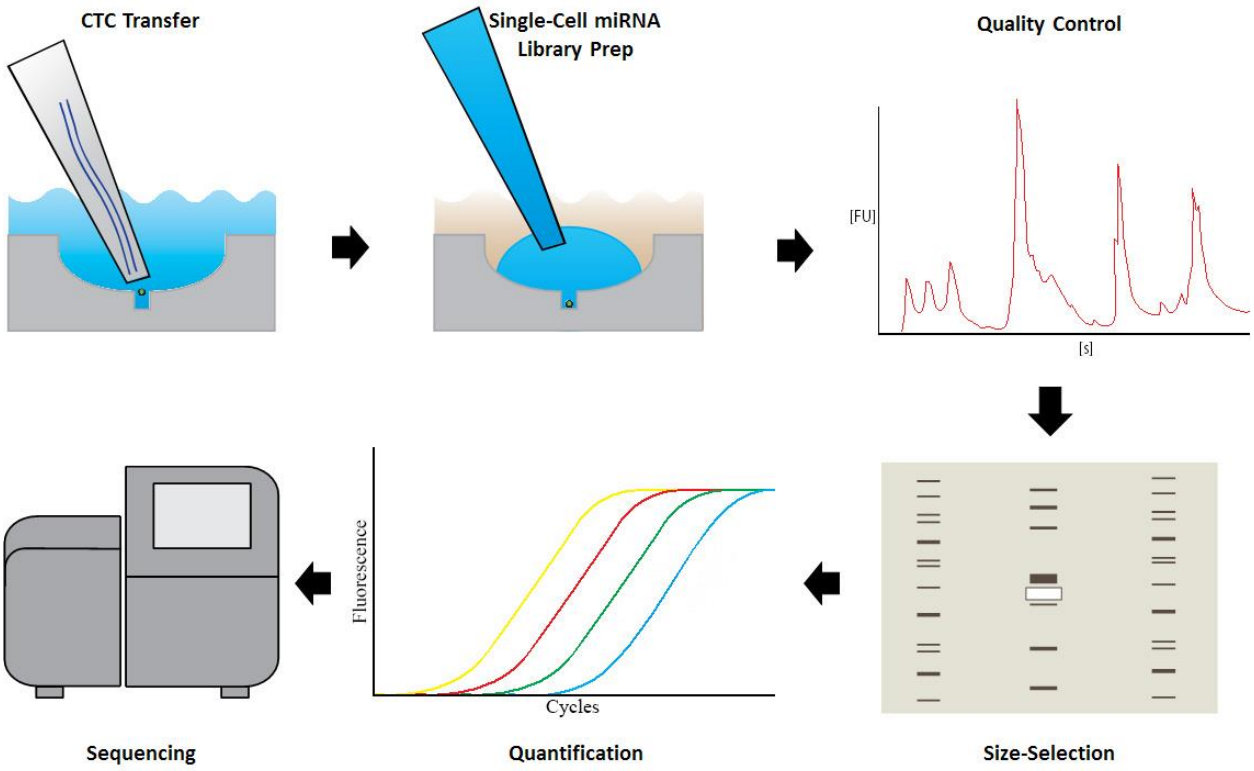

Figure 3.1 Overview of the CTC analysis workflow. The CTC analysis protocol can be broken down into distinct steps that required design, optimization, and verification. These steps included CTC transfer using the PReMiSe platform, library prep using dispensing functionality of PReMiSe, quality control using the Agilent Bioanalyzer, PAGE size-selection, qPCR library quantification, and sequencing.

3.1 Materials

3.1.1 Microwell Library Prep Chip Design and Optimization

In order to implement our single-cell miRNA sequencing protocol, we were first required to design a PDMS microwell chip that would be compatible with the PReMiSe platform and our proposed under-oil droplet-based microwell method. Our original library prep chips contained 140 microwells, organized in a 14 × 10 array, each with a well diameter of 100 µm and a well depth of 150 µm. Surrounding the array of wells, we used plasma oxidation to attach a PDMS barrier that allowed for the addition of up to ~4 mL of wash media or mineral oil (Figure 3.2). We hoped to isolate single cells within this chip's microwells through micromanipulation, and

then replace the media with mineral oil to create isolated reaction droplets to which reagents could be added for subsequent single-cell miRNA library prep. All of this would be performed using the micropipette functionality of the PReMiSe platform (Figure 3.3).

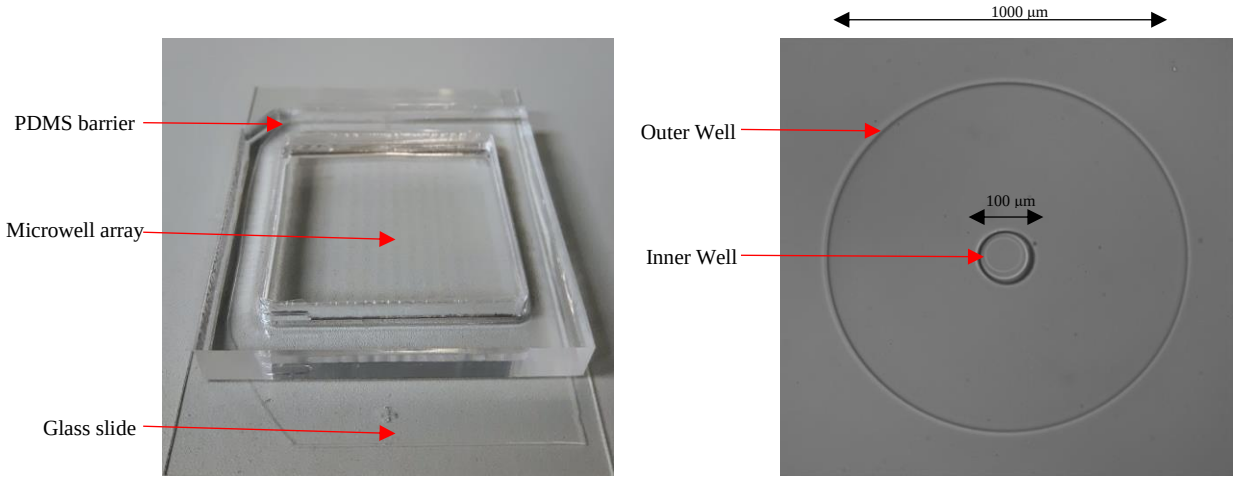

Figure 3.2 Library prep chip design. The library prep microwell chip consisted of 140 microwells designed to hold individual CTCs and anchor reaction droplets. The PDMS barrier (see left) allowed for ~4 mL of washing solution or mineral oil to be added to the chip. The microwell array consisted of a 14x10 array of wells, each of which were composed of an inner and outer well (see right). The inner well (diameter = 100 µm) was designed to hold individual CTCs and a starting volume of ~2 nL of PBS. The outer well (diameter = 1000 µm) was designed to anchor large reaction droplets to the chip surface while also protecting them from side-flow.

Initial experiments using this chip exposed several different issues with our initial design. One of the first major issues we discovered was that this design caused under-oil droplets to be significantly exposed to side-flow forces from moving liquid; this often resulted in larger droplets detaching from their microwell anchors. To fix this issue, we designed an outer well to surround the microwell, thereby protecting it from side-flow forces as droplet volume increased (Figure 3.2). While this design solved the original problem, it led to the outer wells retaining liquid after we removed media to prepare for under-oil reagent dispensing; this was a significant problem as the required starting volume for single-cell miRNA library prep was the volume of the inner microwell alone. To address this issue, we began preparing chips for reagent dispensing

by blotting off the outer droplets using a porous glass disk, leaving only the inner droplet (Figure 3.3).

In a similar vein, early experiments with our library prep chip exposed the importance of PDMS hydrophobicity for droplet stability. Droplets would easily detach from the microwell anchor if the PDMS was too hydrophobic, while they would spread along the chip surface if the PDMS was too hydrophilic. Ideally, we sought to promote nice, round reaction droplets in order to decrease droplet radii and increase reagent mixing efficiency. For this reason, optimizing the hydrophobicity of our library prep chip was crucial for our protocol. To do so, we tested several parameters and determined that plasma oxidizing the PDMS chips for 12 seconds followed by baking them for 2 hours at 80 °C resulted in the desired chip hydrophobicity. Plasma oxidizing was used as it has been shown to render hydrophobic PDMS surfaces more hydrophilic by introducing polar functional groups (162). Occasionally, baking times were slightly altered based on the PDMS batch.

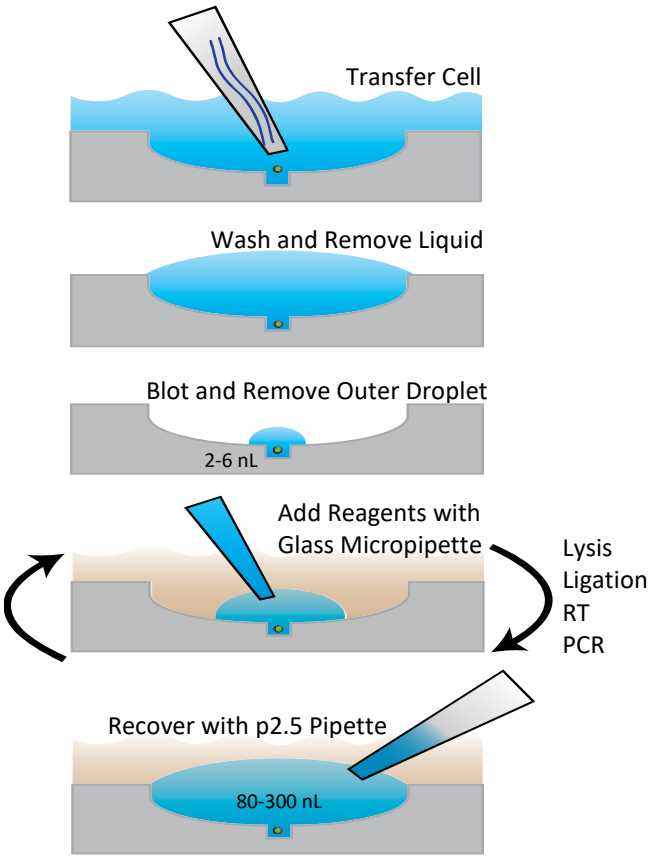

Figure 3.3 PReMiSe single-cell miRNA library prep workflow. The diverse functionality of the PReMiSe platform allowed us to use this device for CTC isolation via micropipette-based micromanipulation, and precise reagent dispensing of nanolitre volumes.

3.1.2 Reagent-Dispensing Micropipette

An additional issue presented itself during early attempts at under-oil reagent dispensing using the PReMiSe platform's micropipette. Due to the hydrophilicity of the glass micropipette, under-oil reaction droplets would occasionally attach to the micropipette following reagent dispensing. This not only caused the obvious problem of detaching reaction droplets, but it also led to concern of potential well-to-well contamination via the micropipette. In order to fix this issue, we began designing micropipettes with hydrophobic outer surfaces by pre-soaking them in trichloro (1H,1H,2H,2H-perfluoro-octyl) silane (Sigma Aldrich).

3.2 Methods

Once we believed we had all the requisite PReMiSe functionalities, an optimized chip design, and a functional reagent-dispensing micropipette, we began developing our single-cell miRNA sequencing protocol for CTCs. This protocol can be segmented into several key steps: single-cell miRNA library prep, quality control, size-selection, quantification, and sequencing. This subsection will provide an overview of the methods which remained the same as described by VanInsberghe; an in-depth description of changes we made to the single-cell miRNA library prep protocol will be provided in the following subsection.

3.2.1 Single-Cell miRNA Library Prep

As mentioned above, we based our method off a single-cell miRNA library preparation protocol that had been previously designed by Michael VanInsberghe in the Hansen Lab. VanInsberghe's protocol was optimized for use in microfluidic chips and tubes, which are not ideal for dealing with rare, precious cells. For this reason, we were required to alter the protocol to render it compatible with the PReMiSe platform and a droplet-based methodology. However, the general library prep reactions initially remained the same. First, single cells are lysed using a chaotropic lysis buffer containing a consistent quantity of spike-in miRNAs. The spike-in miRNAs are 10 different random 22-basepair RNA sequences that do not align with either the human or mouse reference genomes of miRBase, and are used to monitor batch effects and library quality (163). The final amount of each spike-in is 5000, 500, 5, 0.5, 1000, 100, 10, 1, 0.1 molecules/reaction, respectively. Following cell lysis, adenylated adapters are used to target the free hydroxyl group on the 3' end of miRNAs, and are ligated using a truncated RNA ligase 2. This enzyme has been truncated so that it cannot use ATP for ligation, and instead requires pre-

adenylated substrates; this modification prevents the formation of side products (164). Furthermore, this enzyme harbours a K227Q mutation that reduces enzyme lysyl adenylation, thereby further reducing side product formation (165). Additional adapters are then ligated to the 5' ends of miRNA using an RNA ligase 1, which targets the 5' phosphate moiety. The resulting adapter-ligated miRNAs are then reverse-transcribed into cDNA, in the presence of an LNA-modified "block" nucleotide designed to prevent reverse transcription of adapter-dimers (166),and amplified via 16 PCR cycles (Figure 3.8). To render this protocol compatible with our under-oil droplet mechanism, we were required to increase the volume of all reagents by 3 fold in order to accommodate the dispensing technique and microwell volume, which is limited by the construction strategy.

3.2.2 Quality Control

Upon completion of single-cell miRNA library prep, we performed a quality control step prior to subsequent processing. This measure was designed as a checkpoint for library prep success, and prevented low-quality libraries from being processed further, saving both time and money. Our quality control was to qualitatively measure library prep success using the Agilent Bioanalyzer; 1 uL of pooled libraries were analyzed using the High Sensitivity DNA kit. Trials were deemed successful based on the presence of a miRNA peak ~22 bases longer than the adapter-dimer peak; additional markers of success were the presence of heavier peaks which likely arose from small, nucleolar RNA (snoRNA) species based on size (Figure 3.4).

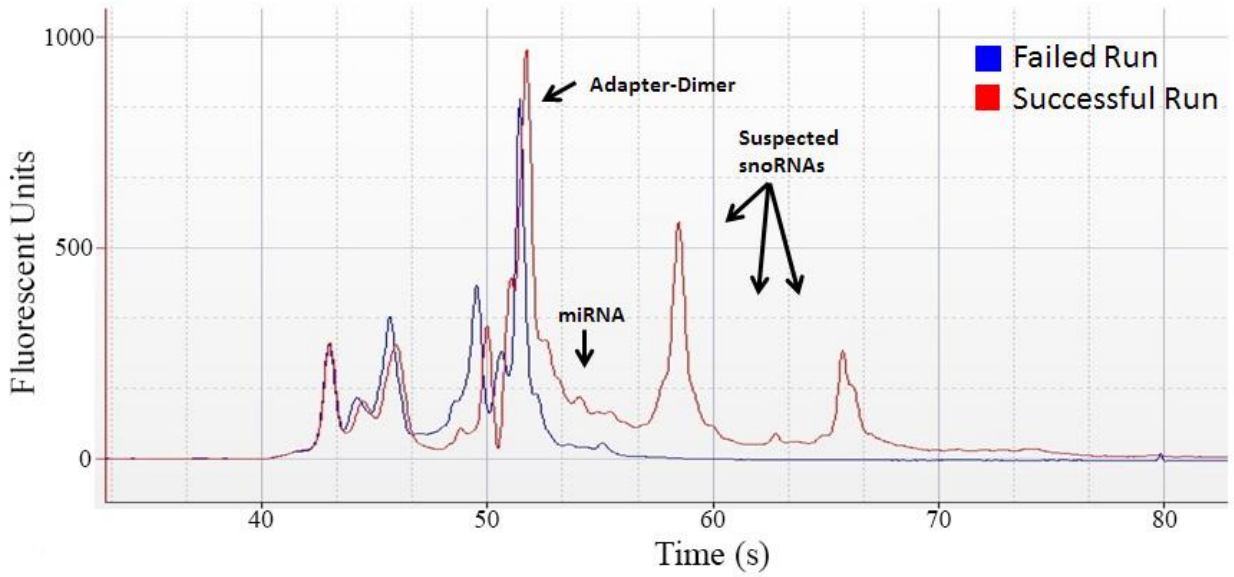

Figure 3.4 Quality control using the Agilent Bioanalzyer. Completed libraries were run on the Agilent Bioanalyzer as a method of quality control. High quality samples exhibited relatively narrow peaks with three distinct patterns. The adapter dimer peak indicated successful PCR amplification; the miRNA peak on the shoulder of the adapter dimer peak indicated successful library prep; the snoRNA provided a measure of lysis success as well as library quality.

3.2.3 Size-Selection

In order to efficiently sequence our miRNA libraries, we isolated sequences of the desired length (~22 bases longer than adapter-dimers = 114 base-pairs) via PAGE size selection. To do so, we followed the Michael Smith Genome Sciences Centre protocol for miRNA Library Construction. This involved pooling our single-cell libraries (up to 96 indexes), running them for 6 hours on a 12% polyacrylamide gel, cutting out the desired cDNA band, eluting it from the gel, and performing ethanol precipitation/purification.

3.2.4 Library Quantification

Following size-selection of our pooled single-cell miRNA libraries, we quantified libraries in order to accurately load the desired concentration onto the sequencer. This was achieved in two ways. For early experiments, we used the Invitrogen QuBit—a fluorometric

DNA quantification device. After the accuracy of this device was called into question based on cluster densities of sequencing runs, we began quantifying libraries using qPCR via the KAPA Library Quantification Kit (Kapa Biosystems®). Sequencing cluster densities showed that this was a much more accurate quantification method, as we were able to achieve cluster densities closer to the calculated theoretical maximum. For both methods, 1 uL of pooled, size-selected library would be used for quantification.

3.2.5 Sequencing

After quantification, libraries were diluted to 4 nM and run through Illumina's Standard Normalization Method for diluting and denaturing libraries. This was performed using the MiSeq Reagent Kit v2; libraries were loaded onto the Illumina MiSeq at 12.5 pM and run for 50 cycles.

3.2.6 Data Processing

Raw sequencing was processed by following a previous pipeline developed by Chu *et al.* to profile miRNAs for The Cancer Genome Atlas. This protocol involves demultiplexing pools, trimming 3' adapters, aligning reads to the miRBase reference genome, and annotating reads with genomic features (167,168). Alterations to this protocol were made by Michael VanInsberghe, which allowed for the identification of -5p and -3p miRNA isoforms (163). Following the application of this pipeline, the sequencing data was collected in a read matrix for each single-cell.

3.3 Results

After successfully integrating the various aspects of our method, we performed experiments to test the efficacy of our single-cell miRNA sequencing protocol. These included bulk cell-line experiments, single-cell cell-line experiments, and, lastly, metastatic prostate cancer patient CTC experiments. Performing these experiments exposed some key methodological flaws, which were addressed by significant alterations to the protocol; these will be described in detail below.

3.3.1 Cell-Line Experiments

The initial trials to test the efficacy of our protocol were bulk cell-line experiments. Since our protocol required 3 times the volume of the original method, we tested the effect of this alteration by performing bulk miRNA library prep experiments on ~1000 K562 cells in tubes. Based on quality control measures, it appeared that our protocol worked well for the initial bulk cell-line experiments.

To further validate our protocol, we ran trials at the single cell level using K562 and LNCaP cell-lines. To do so, we loaded 48 single cells—24 of each cell-line—into 48 microwells of a library prep chip and performed our under oil droplet-based miRNA library prep protocol on the PReMiSe platform. Quality control showed that the resulting libraries were of good quality, so we proceeded with the requisite size-selection, quantification, sequencing, and data analysis steps. Upon analyzing the sequencing data, we found that there was an average of 320,776 total reads—62% of which were aligned to miRNA using miRBase (167)—and 218 unique detected miRNA species per cell; these results indicated that our protocol was generating robust miRNA

data from single cells. Furthermore, exploratory analysis using this preliminary dataset exhibited the cell-classification capabilities of miRNA expression signatures (Figure 3.5).

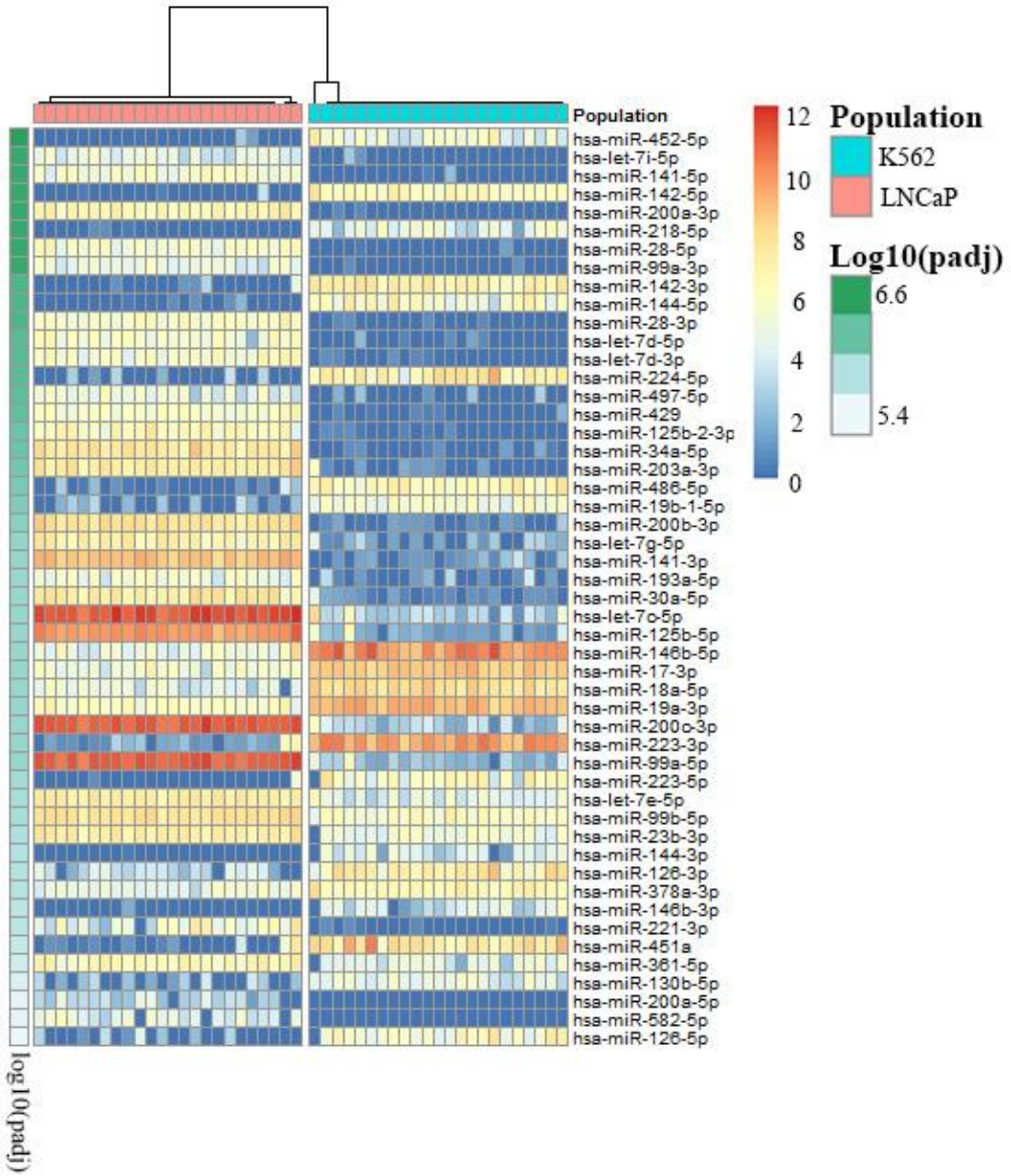

Figure 3.5 Differentially expressed genes of LNCaP and K562 cell lines. Exploratory analysis on initial single-cell miRNA sequencing library using PReMiSe protocol. Differential gene expression analysis shows that miRNA signatures can act as classifiers of cell type. Analysis was performed using SC3, which combines multiple clustering solutions, including Euclidean, Pearson, Spearmen and k-means, into a consensus approach (169).

Following this initial single-cell experiment, we ran another cell-line trial where we sequenced 96 single cells from 4 different prostate cancer cell lines (24 LNCaP, 24 PC3, 24 DU-145, and 24 LN95). As part of this experiment we also tested for bias associated with the use of Cell*Cover* for overnight storage of isolated CTCs, comparing overnight incubation with processing of fresh samples. The results of this experiment demonstrated the classification ability of miRNA signatures, as each cell line formed nice clusters when run through the t-Distributed Stochastic Neighbor Embedding (t-SNE) algorithm, which is a nonlinear dimensionality reduction technique that is commonly used with next-generation sequencing data (170). Furthermore, separate t-SNE clustering analyses using only the treated/untreated LNCaP cells showed that Cell*Cover* exhibits no discernable effect on miRNA expression patterns, thereby allowing us to continue to use this reagent as a means of extending our enrichment/detection/isolation protocol over 2 days (Figure 3.6).

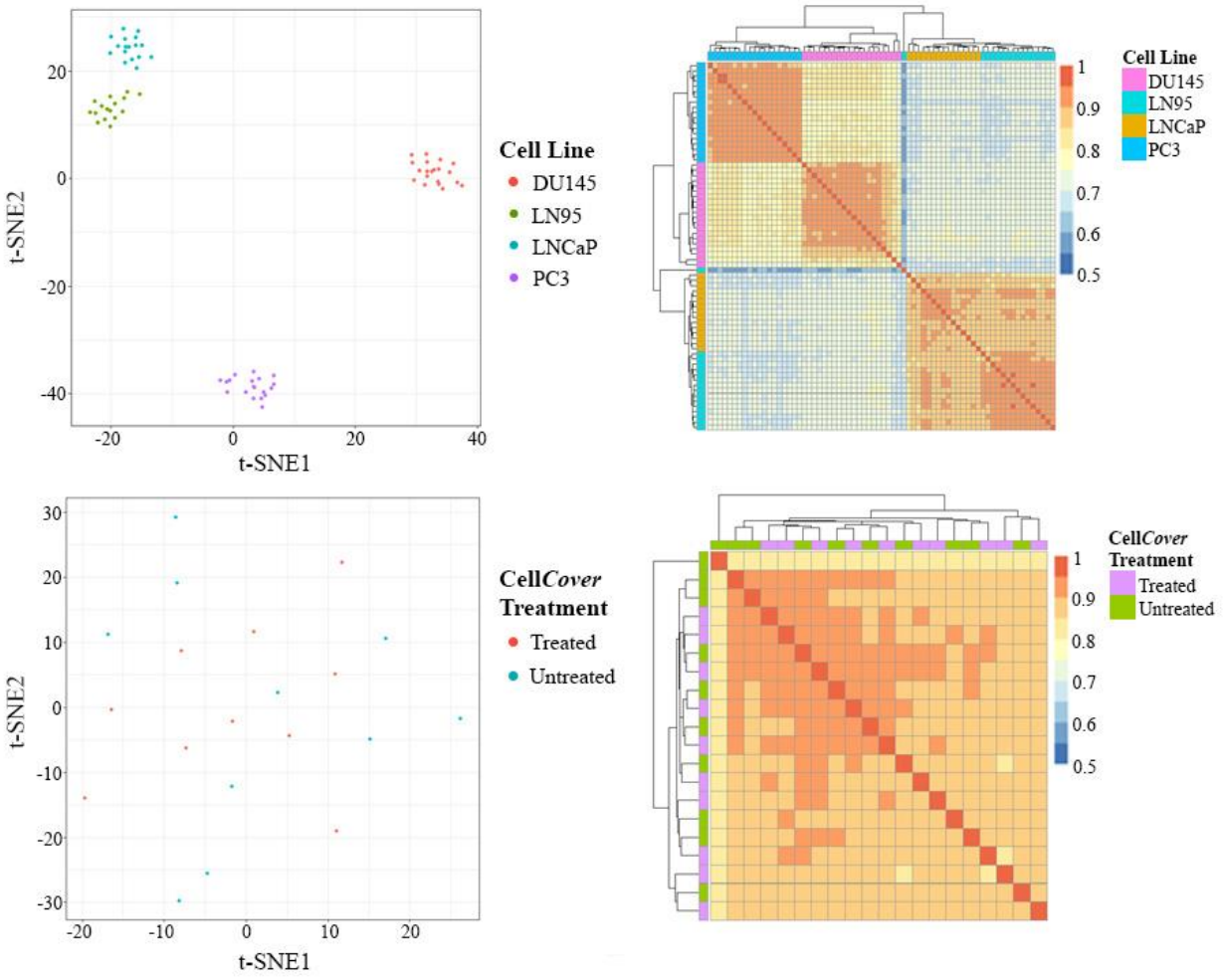

Figure 3.6 Prostate cancer cell line single-cell miRNA sequencing exploratory analysis. Single-cell miRNA sequencing run on four different prostate cell lines demonstrates the classification power of miRNA expression patterns. t-SNE clustering analysis shows that each cell line forms a distinct cluster (top left), and calculating the Pearson correlation of all cell pairs verifies this observation (top right). t-SNE clustering analysis shows that Cell*Cover* reagent does not have a noticeable effect on miRNA expression patterns (bottom left), and this was verified by Pearson correlation calculations (bottom right). Clustering distances for heat maps are Euclidean.

3.3.2 Alterations to Library Prep Protocol

Following the success of our cell-line single-cell sequencing experiments, we began collecting CTCs from metastatic prostate cancer patients and running them through our complete protocol—from enrichment to single-cell sequencing. To start, we successfully sequenced miRNA in the CTCs of 4 patients. However, subsequent bioinformatic analyses of these early

trials exposed two major issues with our library prep protocol: RNA degradation and adapter dimers.

RNA degradation is a serious issue since degradation products can act as targets for the adapter ligation steps of our miRNA library prep method. This presents a significant problem, as it can lead to a subset of ligated degradation products contaminating completed sequencing libraries, thereby reducing the achievable proportion of sequenced miRNA reads. A major issue with RNA degradation is that it cannot be accurately assessed using our quality control method prior to sequencing; Bioanalyzer plots of samples with high degrees of degradation show slightly wider peaks, however the difference is subtle and difficult to quantify (Figure 3.7). By analyzing sequencing data from our early trials, we determined that the proportion of RNA degradation products was consistently over 20%, which led to drastically reduced miRNA reads. This analysis was done by aligning non-miRNA reads to common RNA degradation products, such as ribosomal RNA segments. We postulated that this was due to RNase contamination of our library prep reagents, so we tested each reagent using the Ambion® RNaseAlert™ Lab Test kit (Thermo Fisher Scientific). Using this assay, we were able to detect which reagents were subjected to RNase contamination; these reagents were split into single-use aliquots to reduce the effect of RNA degradation going forward. After addressing this issue, sequenced reads from RNA degradation products decreased by ~66 ± 38% ($P < 1 \times 10^{-15}$; Welch's *t*-test) (Figure 3.7).

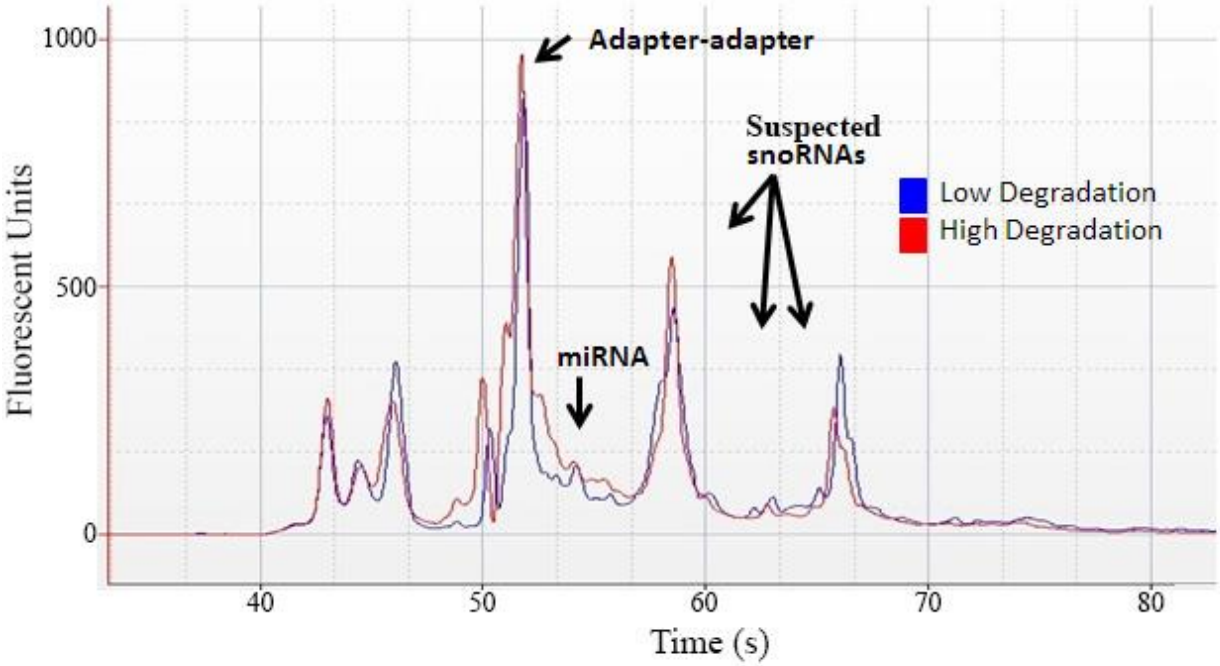

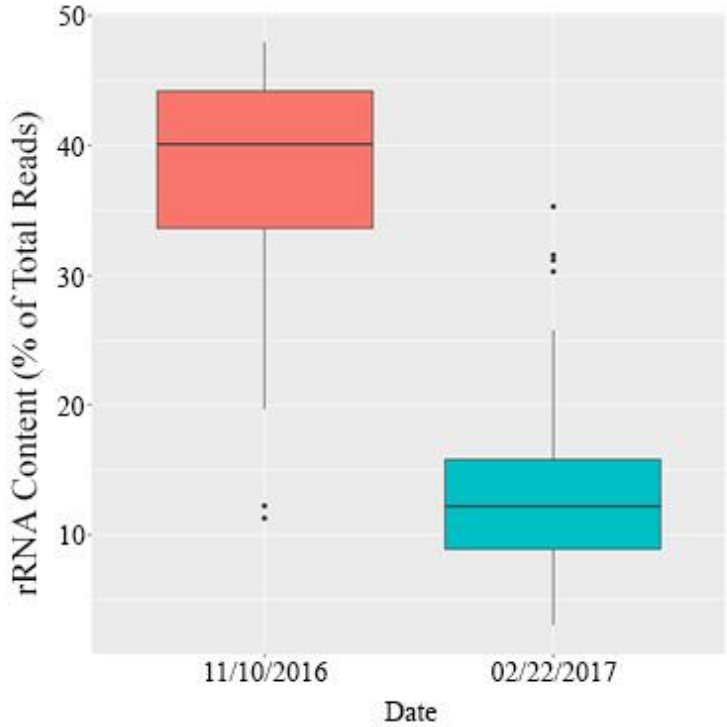

Figure 3.7 Solving RNA degradation problem. RNA degradation is a serious issue because it is not clearly observable during quality control (see top). RNA degradation was diminished by aliquoting all reagents and improving RNase awareness. These changes dropped the RNA degradation products percentage from 38 ± 8% to 13 ± 7%, $P < 1 \times 10^{-15}$ (see bottom).

The other major issue that was exposed after analysis of our early patient trials was the presence of high levels of adapter dimer contamination. Adapter dimers form when the 3'- and 5'-adapter molecules are ligated directly to each other. VanInsberghe's single-cell miRNA library prep protocol used a "block" oligo designed to limit reverse transcription of adapter dimers, thereby preventing them from being amplified during subsequent PCR cycles. However, a significant proportion of dimers nonetheless were able to become reverse transcribed and amplified during initial patient trials. This was likely due to our 3-fold increase in reaction volume, as increased excess reagents naturally lead to increased side-product formation. Adapter dimers presented a major issue because large amounts of these species would contaminate the miRNA band during gel-based size selection, thereby reducing the achievable proportion of sequenced miRNA reads. In fact, early CTC trials showed that adapter dimer content in some patients was as high as 60%. To address this problem, we altered the miRNA library prep protocol by adding a RT-primer anneal step in between 3' and 5' adapter ligation (171). Since the RT-primer was designed to hybridize with the 3' adapter, excess 3' adapter was sequestered by RT-primers, rendering the pair double-stranded. The T4 RNA ligase 1 enzyme used for subsequent 5' adapter ligation can only act on single-stranded oligos and therefore, this alteration acted as a means of preventing adapter dimer ligation (Figure 3.8).

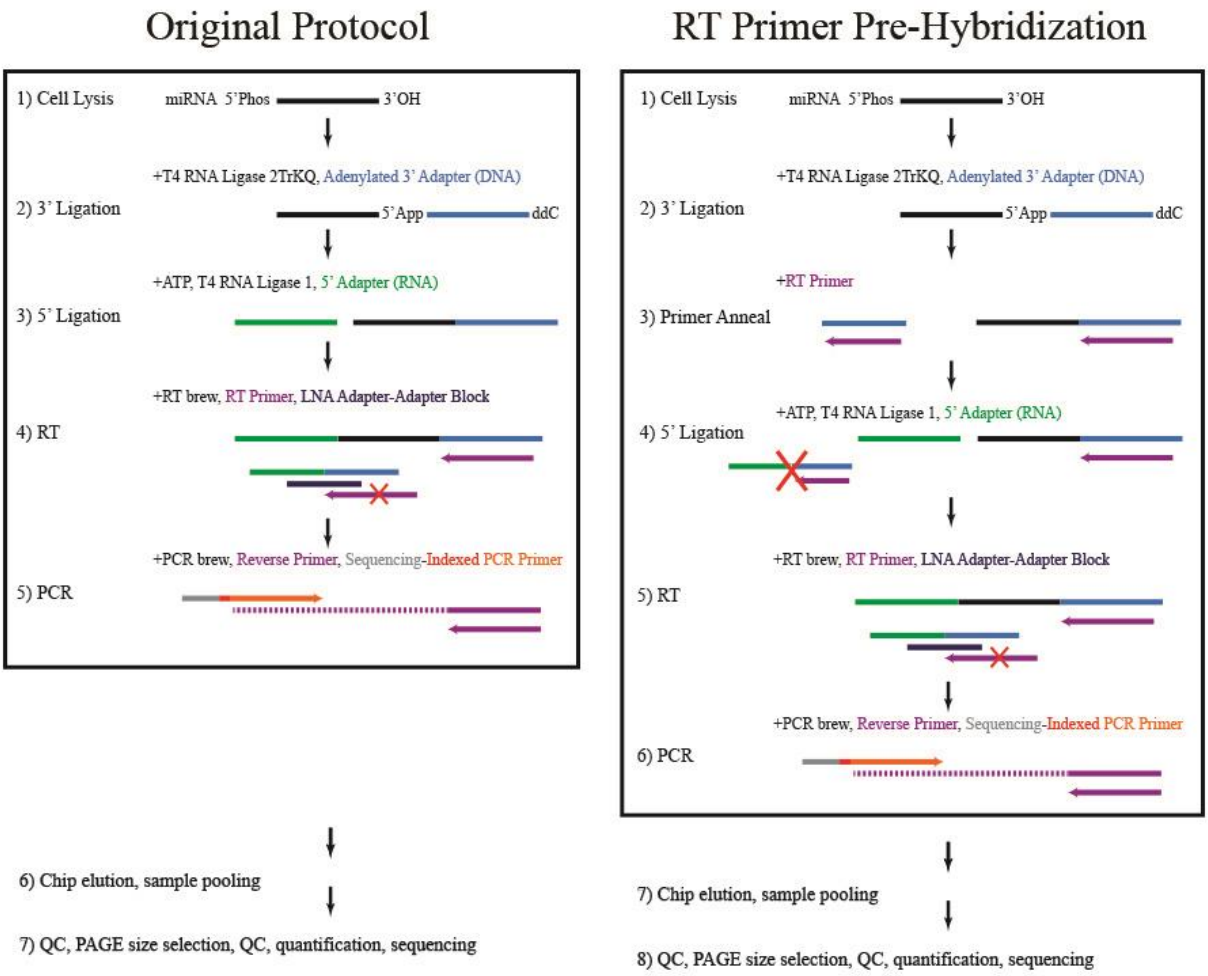

Figure 3.8 Alterations to miRNA library prep protocol. The altered protocol uses an RT primer pre-hybridization step as a second method of preventing adapter dimer formation (see right).

To test the efficacy of our altered library prep method, we sequenced single K562 cells using each protocol and compared adapter dimer percentages between the two. The results of this experiment showed that our new protocol successfully reduced adapter dimers down to an average of 8 ± 2% of aligned reads ($P < 10^{-13}$; Welch's *t*-test) (Figure 3.9). Furthermore, this alteration increased total reads by approximately 39 ± 20% ($P < 0.001$; Welch's *t*-test), did not have a significant effect on miRNA reads percentage ($P > 0.1$; Welch's *t*-test), and increased the number of miRNA species detected by approximately 15 ± 3% ($P < 0.001$; Welch's *t*-test).

Therefore, this experiment showed that the RT primer pre-anneal protocol would be the best option for subsequent experiments.

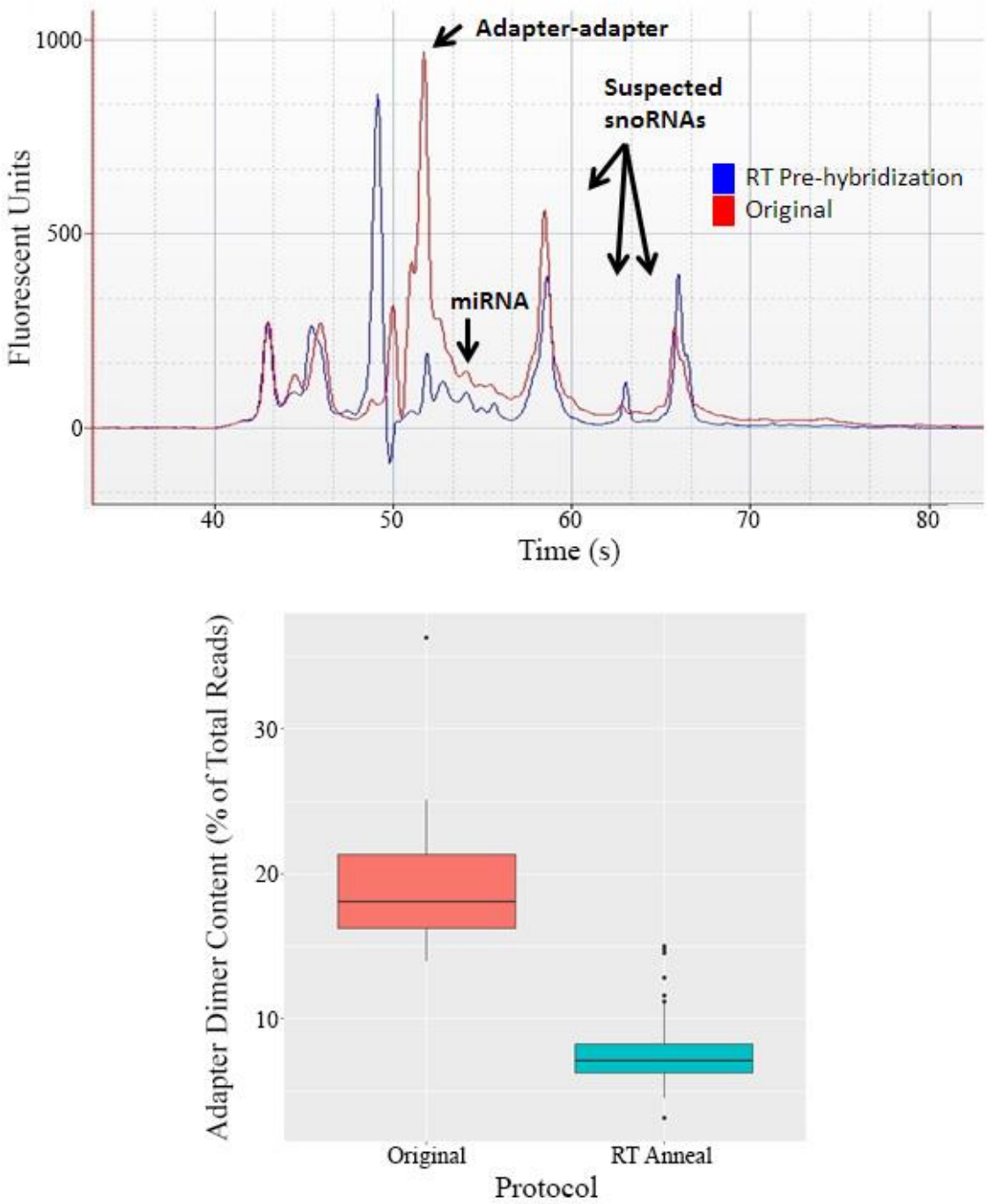

Figure 3.9 Solving adapter dimer problem. Adapter dimers are a significant problem because they bleed into the miRNA peak and contaminate libraries following size selection (see top). Adapter dimer content was diminished by altering the single-cell miRNA library prep protocol. These changes dropped the adapter dimer percentage from 19 ± 5% to 8 ± 2% (N = 26, N = 39, respectively; $P < 1 \times 10^{-13}$; Welch's t-test) (see bottom).

While altering our miRNA library prep protocol helped prevent adapter dimer contamination, it also caused concern for potentially serious batch effects going forward. By analyzing miRNA expression patterns of K562 cells between the two protocols, it appeared that while most miRNA were highly correlated (Pearson's Correlation = 0.91), there was a subset of miRNAs that suffered from selection bias (see Figure 3.10). We postulated that this difference in selection might be caused by differing capabilities of dealing with the secondary structures of miRNA. Regardless of cause, we remained cognizant of this batch effect when performing subsequent analyses that compared patient data that had been analyzed using the different library prep protocols.

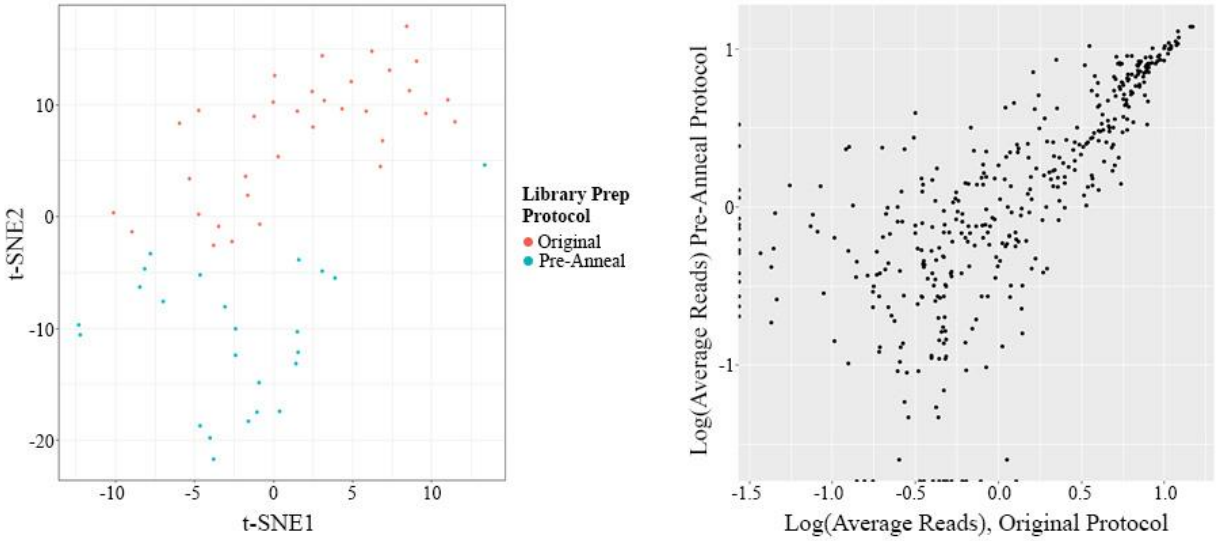

Figure 3.10 Batch effects due to alterations of protocol. Altering protocol caused noticeable batch effect. t-SNE clustering analysis showed distinct clusters for K562 cells processed with original and pre-anneal protocols, respectively (see left). Although most miRNA were highly correlated between protocols (Pearson's Correlation = 0.91), 30 miRNA species were highly expressed in one protocol and not expressed in the other (see right). These miRNA species can be observed along the axes.

3.3.3 Single-Cell miRNA Sequencing of Prostate CTCs

In order to demonstrate the potential impact of our complete method, we collected CTCs from metastatic prostate cancer patients and ran them through our sequencing protocol. In total, we were able to sequence 258 CTCs and 49 PBMCs from 14 metastatic prostate cancer patients (Figure 3.11). As a positive control, we also sequenced 63 K562 cells along with the patient cells. For the CTC libraries, the mean total miRNA reads per cell was 27,423—accounting for 39% of aligned reads—while the mean detected miRNA species per cell was 155; these values indicate successful sequencing libraries. These experiments represented the first time single-cell miRNA sequencing has ever been performed on CTCs; to investigate this novel data set we performed additional bioinformatics analyses.

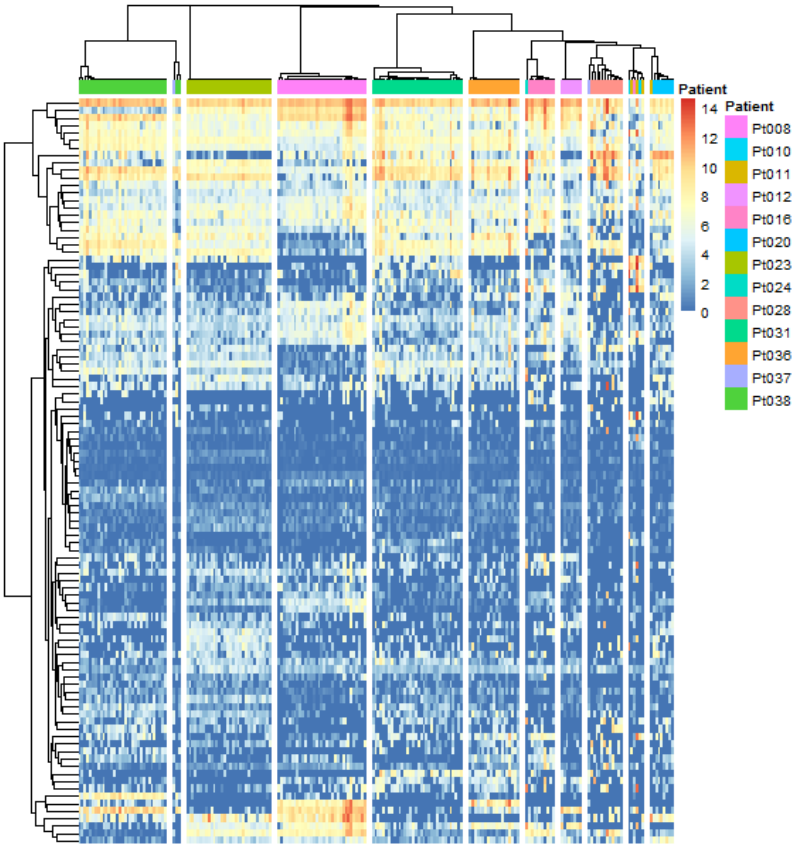

Figure 3.11 MiRNA heatmap of patient CTCs. Patient CTCs displayed differential miRNA expression patterns. Provides initial evidence of interpatient heterogeneity. Analysis was performed using SC3, which combines multiple clustering solutions, including Euclidean, Pearson, Spearmen and k-means, into a consensus approach (105).

3.3.3.1 Normalization

Our data were normalized using the single-cell RNA-seq normalization pipeline described by Lun *et al.* in 2016 (172). This pipeline was directly applicable to our analysis, because it addresses the same problems inherent to single-cell miRNA datasets—namely, dealing low-quality cells and zero-read counts. Low-quality cells, which were detected based on library size and number of expressed features, were removed from the dataset. Additionally, cells were filtered out based on proportions of spike-in reads, as low quality cells naturally have higher relative amounts of spike reads. These filtering steps resulted in the removal of 48 CTCs from our final dataset. The relatively large number of low-quality cells is not entirely surprising given the short half-life of CTCs in the circulation. Furthermore, a proportion of these low-quality cells are likely due to technical problems involving issues with the microwell chip or reagent dispensing. Using this normalization pipeline, low-abundance miRNAs—that is, miRNA which had an average expression across all cells of less than 1—were also filtered out, as zero-count values are problematic for downstream analyses. After this filtering step, our dataset was left with 355 miRNA species.

3.3.3.2 Heterogeneity Analysis

As an exploratory analysis, we performed t-SNE clustering on our normalized data set. We found that nearly every patient's CTCs clustered independently from each other, providing initial evidence of high interpatient heterogeneity of CTC miRNA expression patterns (Figure 3.12). However, the clusters of patient CTCs were relatively spread out when compared to cell line clusters; this observation indicated that intrapatient heterogeneity was potentially significant as well. This was not a very surprising result, as it was expected that there would be several

subpopulations of CTCs within a given patient's blood. To quantify inter-/intrapatient heterogeneity values, we calculated means of Pearson's correlation coefficients and jackknife estimates. These calculations showed that for all but one patient, interpatient heterogeneity was significantly higher than intrapatient heterogeneity. Furthermore, interpatient heterogeneity was similar to heterogeneity between different prostate cancer cell lines (Figure 3.12). These results highlight the cell classification capabilities of miRNA expression signatures.

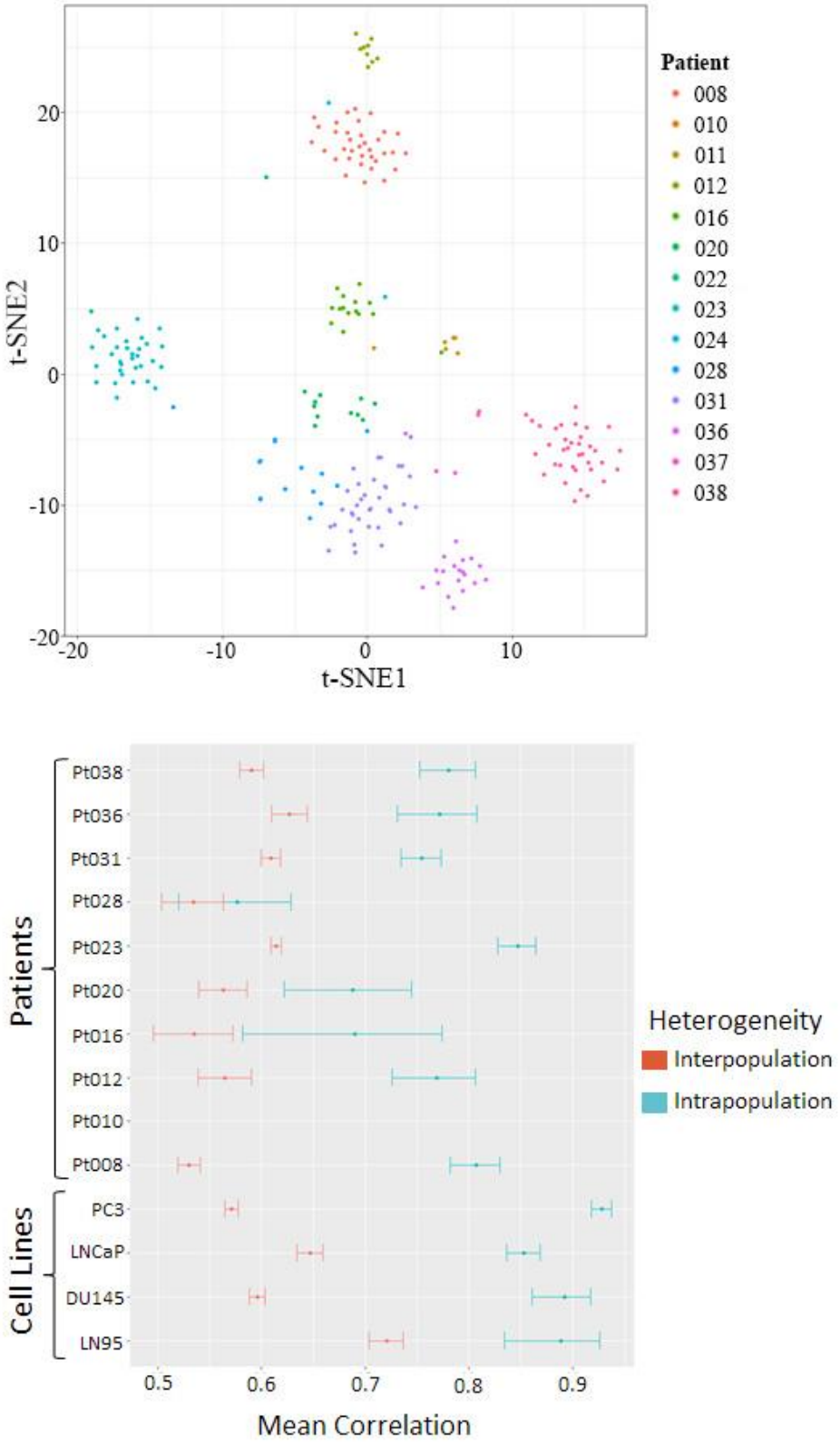

Figure 3.12 miRNA heterogeneity analysis of CTCs. t-SNE plot shows the majority of patient CTCs form distinct clusters, indicating interpatient heterogeneity (see top). Inter- and intrapopulation heterogeneity for patients with 3 or more CTCs, and cell lines, were calculated using mean correlation coefficient.

To ensure that this observed heterogeneity was not due to batch effects, we performed t-SNE clustering analysis on the entire dataset, including the K562 cells which were sequenced in parallel with the patients. This analysis showed that batch effects only had a marginal effect on differential expression, as the K562 cluster containing cells sequenced from each batch exhibited similar dispersion to a given patient CTC cluster (Figure 3.13). Therefore, we were confident that the observed interpatient heterogeneity was a result from real biological effects, and not batch effects.

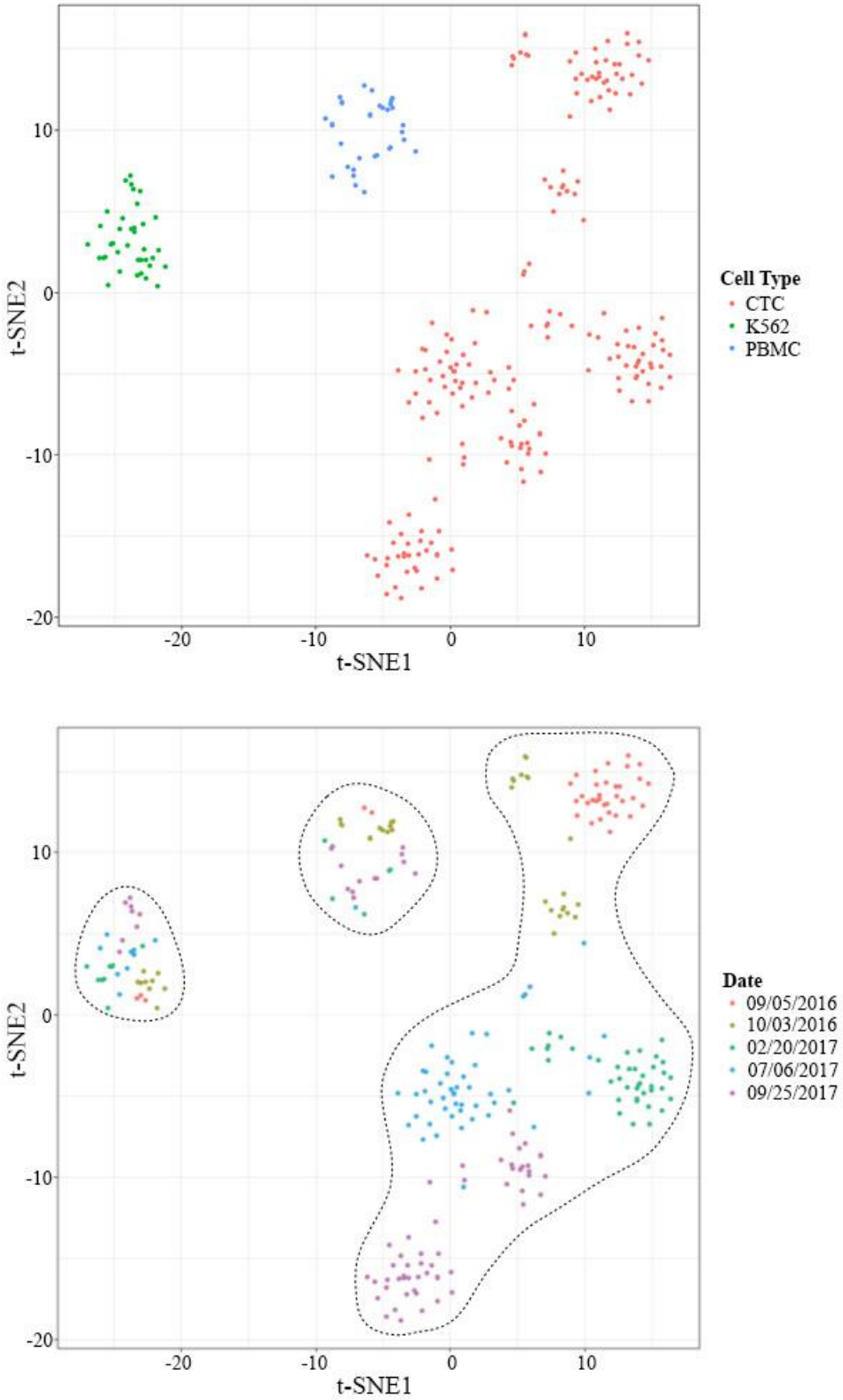

Figure 3.13 Monitoring batch effect. Using t-SNE analysis to reveal contributions of batch effects.

3.3.3.3 Differential Expression Analysis

In order to determine any potentially clinically relevant information from our dataset, we collected additional patient history data (Table 3.1) and performed differential expression analysis (DEA). Patients were divided into two groups, based on whether their disease progressed within 10 months of first-line anti-androgen therapy or not (Table 3.1). Patients whose disease progressed within 10 months of first-line anti-androgen therapy were classified with "aggressive" tumour phenotypes, while the remaining patients were classified with "standard" tumour phenotypes. Using this classifier, there were 6 patients in the aggressive phenotype group and 6 patients in the standard phenotype group. One patient (VCC CTC-028) was removed from the analysis due to the fact that anti-androgen therapy was not used as first-line treatment; instead, OGX-427—a Hsp27 inhibitor (173)—was used. DEA of these patient groups was performed using the Model-based Analysis of Single-cell Transcriptomics (MAST) pipeline (174). The fold-change threshold was set at 10, to ensure that only the strongest biological signals would be observed. The false discovery rate (FDR) threshold was set at 0.05. Results of this analysis showed that two miRNAs, miR-200b-3p and miR-200a-3p, were significantly under-expressed in aggressive phenotype patients ($P < 10^{-15}$ and $P < 10^{-15}$, respectively; Welch's *t*-test) (Figure 3.14). To ensure that this observation was not the result of our library prep batch effect, CTCs were broken into "original" and "RT pre-anneal" groups and MAST DEA was performed. This analysis returned 12 miRNA which were differentially expressed between the two processing methods. Since none of these hit miRNA were miR-200b or miR-200a, we were confident that our observations were not a result of technical artifacts.

Patient	Therapy	>10 Months Anti-Androgen Therapy?	Phenotype
VCC CTC-008	Enzalutamide	Yes	Standard
VCC CTC-011	Enzalutamide	Yes	Standard
VCC CTC-012	Abiraterone	No	Aggressive
VCC CTC-016	Enzalutamide	Yes	Standard
VCC CTC-020	Nilutamide	No	Aggressive
VCC CTC-022	Enzalutamide	No	Aggressive
VCC CTC-023	Enzalutamide, Abiraterone, Radium 223	Yes	Standard
VCC CTC-024	Enzalutamide, Abiraterone	Yes	Standard
VCC CTC-028	oGX427	N/A	N/A
VCC CTC-031	Enzalutamide	No	Aggressive
VCC CTC-036	Abiraterone	No	Aggressive
VCC CTC-037	Enzalutamide	Yes	Standard
VCC CTC-038	Enzalutamide	No	Aggressive

Table 3.1 Patient treatment history. The majority of patients were treated with an anti-androgen drug (ie. Enzalutamide, Abiraterone, Nilutamide) following castration-resistance diagnosis of tumour. Patient VCC CTC-028 was treated with a different class of drug, oGX427, and thus was not included in subsequent differential expression analysis. Tumors of patients treated with anti-androgen drugs were classified as Standard or Aggressive based on the time that the therapy was effective (<10 months classified as Aggressive, >10 months classified as Standard).

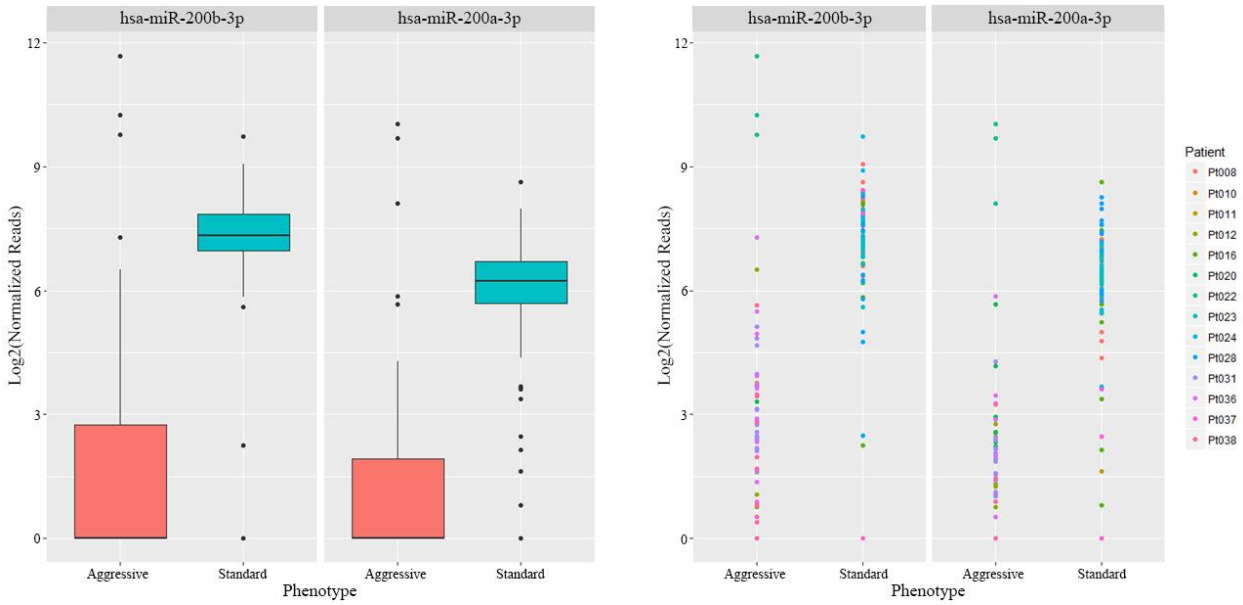

Figure 3.14 Differential gene expression analysis. Differential expression analysis between Aggressive and Standard phenotype patients shows that expression of both miR-200b-3p ($P < 1 \times 10^{-15}$) and miR-200a-3p ($P < 1 \times 10^{-15}$) are negatively correlated with aggressive phenotypes.

3.3.3.4 Analysis of Differentially Expressed miRNA

To determine the biological significance of differential miR-200b and miR-200a expression, these miRNA were queried in the miRTarBase database (175) to determine their mRNA targets. Upon obtaining this list, it was evident that several key proteins involved in tumourigenic processes—including TP53, PTEN, MAPK, and ETS1—were associated with these miRNA (Table 3.2; Figure 3.15). Using this list of mRNA targets, STRING analysis (176) was used to determine which biological pathways these target proteins were enriched for. Results of this analysis showed that the strongest enrichment for biological process GO terms were largely associated with metabolic processes, developmental processes, differentiation pathways, and cellular responses to stimuli (Table 3.2). Molecular function GO terms that the target proteins were strongly enriched for largely involved DNA binding at transcription regulatory regions (Table 3.2). These results indicate that miR-200b and miR-200a are involved in potentially tumourigenic processes.

In order to gain a deeper understanding of miR-200a and miR-200b function in the cell, we reviewed the relevant literature. Recent studies have demonstrated that miR-200a suppresses EMT in liver cancer stem cells and pancreatic cancer stem cells (177,178), and miR-200b has been shown to inhibit EMT, growth and metastasis in prostate cancer (179). These studies indicate that miR-200a and miR-200b function as tumour suppressors in the cell, which is consistent with our finding that their under-expression may be associated with more aggressive tumour phenotypes. Furthermore, miR-200a has been previously established as a potential biomarker in colorectal cancer patients, as low miR-200a expression is correlated with poor survival ($P < 0.05$) (180). Therefore, the under-expression of miR-200a and miR-200b appear to have clinical potential as biomarkers of aggressive metastatic prostate cancer tumours.

miRNA	Target Genes	Enriched GO Terms (FDR)
hsa-miR-200b-3p	BAP1, BCL2, BMI1, BTC, CCNE2, CDKN1B, CREB1, DDX53, DLC1, DNMT1, DNMT3A, DNMT3B, E2F3, ELMO2, ERBB2IP, ETS1, EZH2, FERMT2, FLT1, FN1, GATA4, HFE, HNRNPA3, HOXB5, KDR, KLF11, KLHL20, LOX, MATR3, MSN, MYB, NOTCH1, OXR1, PHLPP1, PIN1, PTPN12, PTPRD, QRSL1, RAB18, RAB21, RAB23, RAB3B, RASSF2, RERE, RIN2, RND3, RNF2, ROCK2, SEC23A, SEPT7, SHC1, SMAD2, SP1, SUZ12, TCF7L1, VAC14, VEGFA, WASF3, WDR37, WNT1, XIAP, ZEB1, ZEB2, ZFPM2	Biological Process (GO) • Positive regulation of macromolecule metabolic process (3.65e-08) • Embryo development (4.78e-08) • Positive regulation of cellular metabolic process (4.78e-08) • Tube development (4.78e-08) • Enzyme linked receptor protein signaling pathway (2.06e-07) Molecular Function (GO) • Chromatin binding (5.04e-07) • Macromolecular complex binding (2.63e-06) • Sequence-specific DNA binding (3.32-06) • Transcription regulatory region DNA binding (3.06e-05) • Protein binding (3.36e-05)
hsa-miR-200a-3p	AREG, ATRX, BAP1, CCNE2, CDK6, CTNNB1, DLC1, DLX5, DNMT1, ELMO2, ERBB2IP, EZH2, GDAP1, GRB2, HFE, HOXB5, KEAP1, KLF11, KLHL20, MAPK14, MYB, PTEN, PTPRD, RASSF2, RIN2, SEPT7, SHC1, SIP1, SMAD2, SMAD3, SRF, TCF7L1, TFAM, TP53, TRAPPC2P1, UBASH3B, VAC14, WASF3, WDR37, YAP1, ZEB1, ZEB2, ZFPM2	Biological Process (GO) • Positive regulation of gene expression (3.04e-09) • Positive regulation of metabolic process (6.01e-09) • Positive regulation of macromolecule process (7.45e-09) • Positive regulation of cellular metabolic process (2.27e-08) • Positive regulation of biological process (2.5e-08) Molecular Function (GO) • Chromatin binding (8.75e-10) • Macromolecular complex binding (1.03e-08) • Transcription regulatory region DNA binding (1.31e-07) • RNA polymerase II transcription factory activity, sequence specific DNA binding (6.77e-05) • Sequence-specific DNA binding (2.73e-04)

Table 3.2 Analysis of differentially expressed miRNA. List of miRNA target genes found by querying the miRTarBase database, and selecting target genes backed by strong experimental evidence (Functional MTI). STRING analysis was used to determine list of enriched gene ontology (GO) terms; the terms with the top five false discovery rates (values listed in parentheses) for biological process and molecular function are listed.

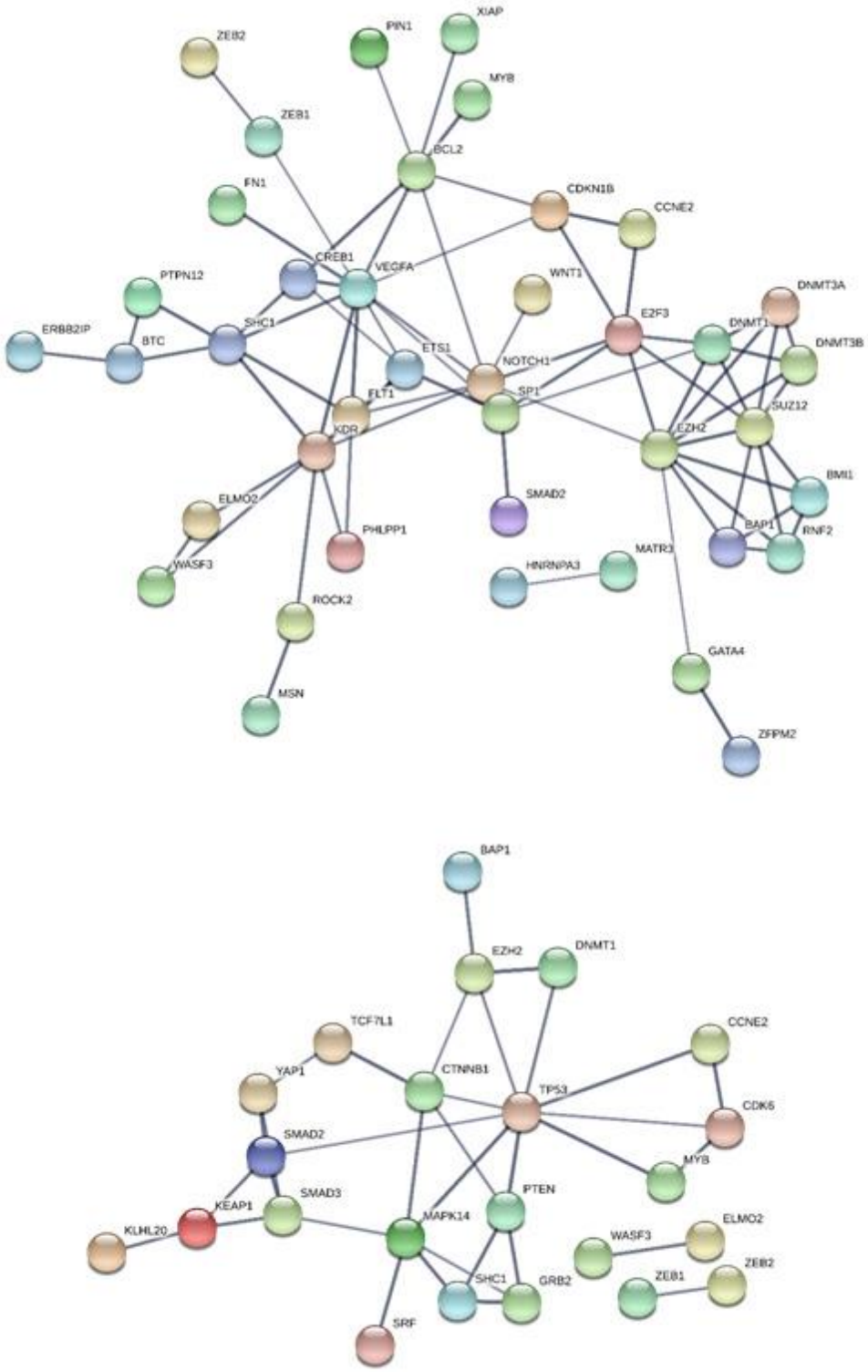

Figure 3.15 STRING interaction network of differentially expressed miRNA target proteins. Top: network of miRNA-200b target proteins. Bottom: network of miRNA-200a target proteins. Unconnected proteins omitted from figure.

Chapter 4: Conclusions and Future Steps

In this work, I have presented an integrated method for the enrichment, isolation, and single-cell analysis of CTCs. Our enrichment/detection protocol achieved recovery rates of 77%, and was able to detect over 6000 metastatic prostate cancer CTCs from patient samples. In a direct comparison with the only FDA-approved CTC enumeration device, CellSearch®, our protocol was able to detect more CTCs in 67% of metastatic prostate cancer patients. To demonstrate the functionality and feasibility of our integrated protocol, we successfully captured and isolated 310 CTCs from 16 late-stage metastatic prostate cancer patients. Of these captured cells, we were able to generate single-cell miRNA profiles of 258 CTCs from 14 patients (mean 18 per patient). This was the first documented example of such an analysis ever being performed on CTCs. The mean total miRNA reads per cell was 27,423—accounting for 39% of aligned reads—while the mean detected miRNA species per cell was 155; these values indicate successful sequencing libraries. Single CTCs from each patient displayed significant interpatient heterogeneity, while intrapatient heterogeneity was rather low. Due to this observed low intrapatient heterogeneity, it is conceivable that future experiments would be able to pool cells from patients together as a means of performing deep miRNA sequencing, while still maintaining single-cell observations. To demonstrate the potential clinical utility of single-cell miRNA sequencing on CTCs, we performed a retrospective analysis of these profiles, which provided preliminary evidence that miR-200a and miR-200b expression is negatively correlated with aggressive tumour phenotypes. Although additional studies must be done to confirm this finding, it has potential clinical utility for the monitoring and managing of castration-resistant

prostate cancer patients. In conclusion, this study demonstrates the feasibility and potential utility of single-cell miRNA sequencing CTCs in the clinical setting.

This study measured single-cell miRNA expression in CTCs because this represented a novel CTC analysis technique, however, our protocol could also be applied to a wide variety of different research problems. For example, the front-end of the protocol could be used to enrich for other rare cell types, such as circulating fetal cells, or immune cells, thereby allowing for downstream single-cell molecular analyses of these cells. Additionally, the back-end of the protocol is capable of being used for a wide variety of molecular analysis protocols, including single-cell RNA sequencing, whole-genome sequencing, and more. Therefore, the technical aspects of this study are widely applicable and represent a potent method for enriching rare cells and performing single-cell molecular analyses.

4.1 Comparisons to Published CTC Enrichment Methods

As previously described in detail, our CTC enrichment protocol combined a negative selection pre-enrichment step with high-throughput fluorescent imaging. The published CTC enrichment technique which most closely resembles our protocol is the Accucyte CyteFinder® from Rarecyte®, Inc (Seattle, WA, USA) (84–87).

Both protocols begin with a density-based pre-enrichment method. Our protocol cross-linked unwanted cells together using tetrameric antibodies via the RosetteSep™ kit (STEMCELL™ Technologies, Vancouver, BC, Canada), and centrifuged samples through Lymphoprep™ (STEMCELL™ Technologies, Vancouver, BC, Canada) density gradient to remove the majority of unwanted cells (80). In contrast, the Accucyte CyteFinder® centrifuges whole-blood samples through a density gradient along with a “float” intended to mark the

nucleated cell layer (84). This allows the Accucyte® protocol to be standardized, and helps reduce a major source of technician bias, thereby improving reproducibility. Furthermore, performing this pre-enrichment as a one-pot system without any washing steps reduces a potential source of CTC loss. Following pre-enrichment, both protocols perform high-throughput imaging followed by micropipette-based micromanipulation to detect and isolate single CTCs for downstream analyses (85,87). It should be noted that at the beginning of my research project, the Accucyte CyteFinder® was not commercially available.

4.2 Comparisons to Published Single-Cell miRNA Sequencing Protocol

As mentioned above, a similar single-cell miRNA sequencing protocol had previously been developed by Faridani *et al.* (154). This method used slightly different reagent concentrations, and performed the reactions in tubes, rather than with microfluidics. For example, our method resulted in a final volume of ~300 nL while their method resulted in a final volume of ~50 μL (154). By not taking a microfluidic approach, Faridani *et al.* were required to add several different mechanisms to reduce side product formation, such as rRNA masking oligonucleotides to remove degradation products and Lambda exonuclease to remove free adapters (154). By performing our protocol at nanolitre volumes, the libraries we generated were of significantly higher quality. Our libraries contained an average of 40 ± 14 % miRNA reads per library, while theirs contained only 2.0 ± 1.1 % (163). To overcome this deficiency, Faridani *et al.* were required to sequence their library libraries much deeper—$4.4 \times 10^6 \pm 3.5 \times 10^6$ reads per cell, compared with $6.3 \times 10^5 \pm 3.9 \times 10^5$ reads per cell for our method (163). Based on this observation, it appears that our microfluidic library prep method is much more efficient and cost-effective, thereby making it the more feasible technique for future research.

4.3 Suggestions for Further Protocol Improvements

This study has demonstrated the clinical feasibility of single-cell miRNA sequencing CTCs. However, there are areas of the protocol that require additional work in order to reduce the variability and increase the reproducibility of this CTC enrichment/detection/analysis method. Such improvements are necessary in order for this protocol to exert its full experimental and clinical potential.

4.3.1 Eliminating Technician Bias During Negative Selection

Issues with technician bias during the negative-selection steps of CTC enrichment resulted in variable CTC counts, thereby limiting the number of patients we were able to analyze. A likely source of this bias arises when removing the liquid layer containing CTCs above the LymphoPrep™ following centrifugation. This step requires practice to perform accurately, as the layer is often not clearly visible, and therefore is subject to human error. For this study, we used this negative selection method due to it's simplicity, cost-effectiveness, and availability; however, other methods would be able to avoid its flaws. To ameliorate this issue, a marker additive with the approximate density of an individual cell could be added to the blood sample prior to centrifugation; this would allow the CTC-containing layer to be visible, thereby eliminating the need for judgement calls during this step. Similarly, centrifuging blood samples through density gradients could help this issue. If the approximate area where CTCs equilibrate within the density gradient is known, technicians would be able to standardize negative selection by eluting cells from a consistent section of density gradient for each patient. Lastly, using a micropost-based microfluidic chip for negative selection would also eliminate technician bias and human error.

4.3.2 Improving CTC Detection

Although negative selection methods allow for the collection of more heterogeneous CTC populations, detecting multiple subpopulations of CTCs remains an issue. For our protocol, we detected CTCs based on EpCAM/CD45 expression patterns, due to consistency with previous CTC detection methods, cost-effectiveness, and simplicity. This method likely results in selection bias towards epithelial-like CTCs, and may cause other subpopulations to be underrepresented in subsequent analyses; such bias reduces CTC detection reproducibility. In order to eliminate this issue, additional work must be done to develop a standard CTC antibody cocktail in conjunction with a detailed algorithm that is capable of detecting a wide variety of CTC subpopulations. In doing so, the variability of CTC count measurements and molecular analyses will be reduced, thereby allowing for replication studies from independent researchers to solidify findings.

4.4 Suggested Future Experiments

This study provided preliminary evidence that miR-200b and miR-200a expression is negatively correlated with aggressive tumour phenotypes. However, due to the nature of the dataset, providing a clear interpretation of the potential role miR-200b and miR-200a play in prostate tumour progression is quite difficult, as there are several possible explanations. One explanation is that certain patients under-express miR-200b and miR-200a prior to treatment, and this manifests itself as an aggressive tumour phenotype upon commencement of anti-androgen therapy. However, we have not presented enough data to accurately postulate such an association, and additional experiments must be performed in order to do so.

4.4.1 *in vitro* Assays

One way in which to provide further evidence describing the role of miR-200b and miR-200a expression in prostate tumour progression would be to perform *in vitro* experiments. Expression of these miRNA could be knocked-down in prostate cancer cell lines using CRISPR, siRNA, or some other method, and various tumourigenic characteristics could be measured in comparison with a control. Furthermore, the response of knock-down cells to anti-androgen drugs could be compared with a control. In doing so, the role of miR-200b and miR-200a expression in prostate tumour progression may become better understood.

4.4.2 Longitudinal Prostate Cancer Patient Studies

To demonstrate the potential prognostic value of miR-200b and miR-200a expression, longitudinal studies that analyze single-cell miRNA sequencing profiles of castration-resistant prostate cancer patient CTCs prior to, and following, anti-androgen therapy must be performed. Solidifying such an association may provide clinicians with an additional prognostic biomarker, and a way in which to predict anti-androgen treatment responses in patients. Furthermore, such studies would be well suited to discover additional associations between CTC miRNA expression patterns, prognosis and/or treatment response; this is necessary for single-cell miRNA sequencing of CTCs to become common clinical practice in the management of cancer.

Bibliography

1. Bertram JS. The molecular biology of cancer. Mol Aspects Med. 2000;21:167–223.
2. McGranahan N, Swanton C. Clonal Heterogeneity and Tumor Evolution: Past, Present, and the Future. Vol. 168, Cell. 2017. p. 613–28.
3. Tabassum DP, Polyak K. Tumorigenesis: It takes a village. Vol. 15, Nature Reviews Cancer. 2015. p. 473–83.
4. Khalil DN, Smith EL, Brentjens RJ, Wolchok JD. The future of cancer treatment: Immunomodulation, CARs and combination immunotherapy. Vol. 13, Nature Reviews Clinical Oncology. 2016. p. 273–90.
5. Robert C, Long G V., Brady B, Dutriaux C, Maio M, Mortier L, et al. Nivolumab in previously untreated melanoma without BRAF mutation. N Engl J Med [Internet]. 2015;372(4):320–30. Available from: http://www.nejm.org/doi/abs/10.1056/NEJMoa1412082%5Cnhttp://www.ncbi.nlm.nih.gov/pubmed/25399552
6. Robert C, Schachter J, Long G V., Arance A, Grob JJ, Mortier L, et al. Pembrolizumab versus Ipilimumab in Advanced Melanoma. N Engl J Med [Internet]. 2015;372(26):2521–32. Available from: http://www.nejm.org/doi/10.1056/NEJMoa1503093
7. Bartkowiak T, Curran MA. 4-1BB Agonists: Multi-Potent Potentiators of Tumor Immunity. Front Oncol [Internet]. 2015;5. Available from: http://journal.frontiersin.org/Article/10.3389/fonc.2015.00117/abstract
8. Schaer DA, Cohen AD, Wolchok JD. Anti-GITR antibodies--potential clinical applications for tumor immunotherapy. Curr Opin Investig Drugs [Internet]. 2010;11(12):1378–86. Available from: http://www.ncbi.nlm.nih.gov/pubmed/21154120
9. Gross G, Waks T, Eshhar Z. Expression of immunoglobulin-T-cell receptor chimeric molecules as functional receptors with antibody-type specificity. Proc Natl Acad Sci [Internet]. 1989;86(24):10024–8. Available from: http://www.pnas.org/cgi/doi/10.1073/pnas.86.24.10024
10. Brentjens RJ, Latouche JB, Santos E, Marti F, Gong MC, Lyddane C, et al. Eradication of systemic B-cell tumors by genetically targeted human T lymphocytes co-stimulated by CD80 and interleukin-15. Nat Med. 2003;9(3):279–86.
11. Brentjens RJ, Santos E, Nikhamin Y, Yeh R, Matsushita M, La Perle K, et al. Genetically targeted T cells eradicate systemic acute lymphoblastic leukemia xenografts. Clin Cancer Res. 2007;13(18):5426–35.
12. Davila ML, Riviere I, Wang X, Bartido S, Park J, Curran K, et al. Efficacy and toxicity management of 19-28z CAR T cell therapy in B cell acute lymphoblastic leukemia. Sci Transl Med. 2014;6(224).

13. Imai C, Mihara K, Andreansky M, Nicholson IC, Pui CH, Geiger TL, et al. Chimeric receptors with 4-1BB signaling capacity provoke potent cytotoxicity against acute lymphoblastic leukemia. Leukemia. 2004;18(4):676–84.

14. Maude SL, Frey N, Shaw PA, Aplenc R, Barrett DM, Bunin NJ, et al. Chimeric Antigen Receptor T Cells for Sustained Remissions in Leukemia. N Engl J Med [Internet]. 2014;371(16):1507–17. Available from: http://www.nejm.org/doi/10.1056/NEJMoa1407222

15. Siravegna G, Marsoni S, Siena S, Bardelli A. Integrating liquid biopsies into the management of cancer. Nat Rev Clin Oncol [Internet]. 2017;14(9):531–48. Available from: http://www.nature.com/doifinder/10.1038/nrclinonc.2017.14

16. Fisher R, Pusztai L, Swanton C. Cancer heterogeneity: Implications for targeted therapeutics. Vol. 509, Nature. 2014. p. 479–85.

17. Merlo LMF, Pepper JW, Reid BJ, Maley CC. Cancer as an evolutionary and ecological process. Vol. 6, Nature Reviews Cancer. 2006. p. 924–35.

18. Wan JCM, Massie C, Garcia-Corbacho J, Mouliere F, Brenton JD, Caldas C, et al. Liquid biopsies come of age: towards implementation of circulating tumour DNA. Nat Rev Cancer [Internet]. 2017;17(4):223–38. Available from: http://www.nature.com/doifinder/10.1038/nrc.2017.7

19. Silberstein JL, Pal SK, Lewis B, Sartor O. Current clinical challenges in prostate cancer. Transl Androl Urol [Internet]. 2013;2(3):122–36. Available from: http://www.pubmedcentral.nih.gov/articlerender.fcgi?artid=4708189&tool=pmcentrez&rendertype=abstract

20. Wallace TJ, Torre T, Grob M, Yu J, Avital I, Brücher B, et al. Current Approaches, Challenges and Future Directions for Monitoring Treatment Response in Prostate Cancer. J Cancer [Internet]. 2014;5(1):3–24. Available from: http://www.ncbi.nlm.nih.gov/pmc/articles/PMC3881217/%5Cnhttp://www.ncbi.nlm.nih.gov/pmc/articles/PMC3881217/pdf/jcav05p0003.pdf

21. De Bono JS, Oudard S, Ozguroglu M, Hansen S, MacHiels JP, Kocak I, et al. Prednisone plus cabazitaxel or mitoxantrone for metastatic castration-resistant prostate cancer progressing after docetaxel treatment: A randomised open-label trial. Lancet [Internet]. 2010;376(9747):1147–54. Available from: http://dx.doi.org/10.1016/S0140-6736(10)61389-X

22. Miyamoto DT, Sequist L V., Lee RJ. Circulating tumour cells—monitoring treatment response in prostate cancer. Nat Rev Clin Oncol [Internet]. 2014;11(7):401–12. Available from: http://www.nature.com/doifinder/10.1038/nrclinonc.2014.82

23. Schilling D, Todenhöfer T, Hennenlotter J, Schwentner C, Fehm T, Stenzl A. Isolated, disseminated and circulating tumour cells in prostate cancer. Nat Rev Urol [Internet]. 2012;9(8):448–63. Available from: http://www.nature.com/doifinder/10.1038/nrurol.2012.136

24. Ankeny JS, Court CM, Hou S, Li Q, Song M, Wu D, et al. Circulating tumour cells as a

biomarker for diagnosis and staging in pancreatic cancer. Br J Cancer. 2016;114(12):1367–75.

25. Heitzer E, Perakis S, Geigl JB, Speicher MR. The potential of liquid biopsies for the early detection of cancer. npj Precis Oncol [Internet]. 2017;1(1):36. Available from: http://www.nature.com/articles/s41698-017-0039-5

26. Li Y, Gong J, Zhang Q, Lu Z, Gao J, Li Y, et al. Dynamic monitoring of circulating tumour cells to evaluate therapeutic efficacy in advanced gastric cancer. Br J Cancer. 2016;114(2):138–45.

27. Miyamoto DT, Lee RJ, Stott SL, Miyamoto DT, Lee RJ, Stott SL, et al. Androgen Receptor Signaling in Circulating Tumor Cells as a Marker of Hormonally Responsive Prostate Cancer Androgen Receptor Signaling in Circulating Tumor Cells as a Marker of Hormonally Responsive Prostate Cancer. 2012;2(11):995–1003.

28. Antonarakis ES, Lu C, Wang H, Luber B, Nakazawa M, Roeser JC, et al. AR-V7 and Resistance to Enzalutamide and Abiraterone in Prostate Cancer. N Engl J Med [Internet]. 2014;371(11):1028–38. Available from: http://www.nejm.org/doi/10.1056/NEJMoa1315815

29. Antonarakis ES, Lu C, Luber B, Wang H, Chen Y, Zhu Y, et al. Clinical Significance of Androgen Receptor Splice Variant-7 mRNA Detection in Circulating Tumor Cells of Men With Metastatic Castration-Resistant Prostate Cancer Treated With First- and Second-Line Abiraterone and Enzalutamide. J Clin Oncol [Internet]. 2017;35(19):2149–56. Available from: http://ascopubs.org/doi/10.1200/JCO.2016.70.1961

30. Darshan MS, Loftus MS, Thadani-Mulero M, Levy BP, Escuin D, Zhou XK, et al. Taxane-induced blockade to nuclear accumulation of the androgen receptor predicts clinical responses in metastatic prostate cancer. Cancer Res. 2011;71(18):6019–29.

31. Lohr JG, Adalsteinsson VA, Cibulskis K, Choudhury AD, Rosenberg M, Cruz-Gordillo P, et al. Whole-exome sequencing of circulating tumor cells provides a window into metastatic prostate cancer. Nat Biotechnol [Internet]. 2014;32(5):479–84. Available from: http://www.nature.com/doifinder/10.1038/nbt.2892

32. Jiang R, Lu Y-T, Ho H, Li B, Chen J-F, Lin M, et al. A comparison of isolated circulating tumor cells and tissue biopsies using whole-genome sequencing in prostate cancer. Oncotarget [Internet]. 2015;6(42):44781–93. Available from: http://www.oncotarget.com/fulltext/6330

33. Yu M, Ting DT, Stott SL, Wittner BS, Ozsolak F, Ciciliano JC, et al. RNA sequencing of pancreatic tumour cells implicates WNT signaling in metastasis. Nature. 2013;487(7408):510–3.

34. Mandel P, Metais P. Les acides nucleiques du plasma sanguin chez l'homme. C R Seances Soc Biol Fil [Internet]. 1948;142(3–4):241–3. Available from: http://www.ncbi.nlm.nih.gov/pubmed/7119438%5Cnhttp://www.ncbi.nlm.nih.gov/pubmed/18875018

35. Leon SA, Shapiro B, Sklaroff DM, Leon SA, Shapiro B, Sklaroff DM, et al. Free DNA in

the Serum of Cancer Patients and the Effect of Therapy Free DNA in the Serum of Cancer Patients and the Effect of Therapy. Cancer Res. 1977;37(March):646–50.

36. Stroun M, Anker P, Maurice P, Lyautey J, Lederrey C, Beljanski M. Neoplastic Characteristics of the DNA Found in the Plasma of Cancer Patients. Oncology [Internet]. 1989;46(5):318–22. Available from: http://www.karger.com/?doi=10.1159/000226740

37. Sorenson GD, Pribish DM, Valone FH, Memoli V a, Bzik DJ, Yao SL. Soluble Normal and Mutated Dna-Sequences From Single-Copy Genes in Human Blood. Cancer Epidemiol Biomarkers Prev. 1994;3(February):67–71.

38. Wyatt AW, Annala M, Aggarwal R, Beja K, Feng F, Youngren J, et al. Concordance of Circulating Tumor DNA and Matched Metastatic Tissue Biopsy in Prostate Cancer. JNCI J Natl Cancer Inst [Internet]. 2017;109(12):1–9. Available from: https://academic.oup.com/jnci/article-lookup/doi/10.1093/jnci/djx118

39. Gonzales JC, Fink LM, Goodman OB, Symanowski JT, Vogelzang NJ, Ward DC. Comparison of circulating MicroRNA 141 to circulating tumor cells, lactate dehydrogenase, and prostate-specific antigen for determining treatment response in patients with metastatic prostate cancer. Clin Genitourin Cancer [Internet]. 2011;9(1):39–45. Available from: http://dx.doi.org/10.1016/j.clgc.2011.05.008

40. De Souza MF, Kuasne H, Barros-Filho MDC, Cilião HL, Marchi FA, Fuganti PE, et al. Circulating mRNAs and miRNAs as candidate markers for the diagnosis and prognosis of prostate cancer. PLoS One. 2017;12(9):1–16.

41. Mitchell PS, Parkin RK, Kroh EM, Fritz BR, Wyman SK, Pogosova-Agadjanyan EL, et al. Circulating microRNAs as stable blood-based markers for cancer detection. Proc Natl Acad Sci [Internet]. 2008;105(30):10513–8. Available from: http://www.pnas.org/cgi/doi/10.1073/pnas.0804549105

42. Zhang HL, Yang LF, Zhu Y, Yao XD, Zhang SL, Dai B, et al. Serum miRNA-21: Elevated levels in patients with metastatic hormone-refractory prostate cancer and potential predictive factor for the efficacy of docetaxel-based chemotherapy. Prostate. 2011;71(3):326–31.

43. Bryant RJ, Pawlowski T, Catto JWF, Marsden G, Vessella RL, Rhees B, et al. Changes in circulating microRNA levels associated with prostate cancer. Br J Cancer [Internet]. 2012;106(4):768–74. Available from: http://dx.doi.org/10.1038/bjc.2011.595

44. El Messaoudi S, Rolet F, Mouliere F, Thierry AR. Circulating cell free DNA: Preanalytical considerations. Vol. 424, Clinica Chimica Acta. 2013. p. 222–30.

45. Heitzer E, Ulz P, Belic J, Gutschi S, Quehenberger F, Fischereder K, et al. Tumor-associated copy number changes in the circulation of patients with prostate cancer identified through whole-genome sequencing. Genome Med [Internet]. 2013;5(4):30. Available from: http://www.ncbi.nlm.nih.gov/pubmed/23561577

46. Leary RJ, Kinde I, Diehl F, Schmidt K, Clouser C, Duncan C, et al. Development of personalized tumor biomarkers using massively parallel sequencing. Sci Transl Med. 2010;2(20).

47. Kinde I, Papadopoulos N, Kinzler KW, Vogelstein B. FAST-SeqS: A Simple and Efficient Method for the Detection of Aneuploidy by Massively Parallel Sequencing. PLoS One. 2012;7(7):18.

48. Belic J, Koch M, Ulz P, Auer M, Gerhalter T, Mohan S, et al. Rapid identification of plasma DNA samples with increased ctDNA levels by a modified FAST-SeqS approach. Clin Chem. 2015;61(6):838–49.

49. Ono S, Lam S, Nagahara M, Hoon D. Circulating microRNA Biomarkers as Liquid Biopsy for Cancer Patients: Pros and Cons of Current Assays. J Clin Med [Internet]. 2015;4(10):1890–907. Available from: http://www.mdpi.com/2077-0383/4/10/1890/

50. Schwarzenbach H, Nishida N, Calin GA, Pantel K. Clinical relevance of circulating cell-free microRNAs in cancer. Nat Rev Clin Oncol. 2014;11(3):145–56.

51. Ashworth TR. A case of cancer in which cells similar to those in the tumors were seen in the blood after death. Aust Med J. 1869;14:146–9.

52. Krebs MG, Metcalf RL, Carter L, Brady G, Blackhall FH, Dive C. Molecular analysis of circulating tumour cells—biology and biomarkers. Nat Rev Clin Oncol [Internet]. 2014;11(3):129–44. Available from: http://www.nature.com/doifinder/10.1038/nrclinonc.2013.253

53. Gravdal K, Halvorsen OJ, Haukaas SA, Akslen LA. A switch from E-cadherin to N-cadherin expression indicates epithelial to mesenchymal transition and is of strong and independent importance for the progress of prostate cancer. Clin Cancer Res. 2007;13(23):7003–11.

54. Mol AJM, Geldof AA, Meijer GA, Van Der Poel HG, Van Moorselaar RJA. New experimental markers for early detection of high-risk prostate cancer: Role of cell-cell adhesion and cell migration. J Cancer Res Clin Oncol. 2007;133(10):687–95.

55. Cooper CR, Mclean L, Walsh M, Taylor J, Hayasaka S, Bhatia J, et al. Preferential Adhesion of Prostate Cancer Cells to Bone Is Mediated by Binding to Bone Marrow Endothelial Cells as Compared to Extracellular Matrix Components in Vitro Preferential Adhesion of Prostate Cancer Cells to Bone Is Mediated by Binding to Bone Ma. 2000;6(December):4839–47.

56. Saha B, Arase A, Imam SS, Tsao-Wei D, Naritoku WY, Groshen S, et al. Overexpression of E-cadherin and beta-catenin proteins in metastatic prostate cancer cells in bone. Prostate [Internet]. 2008;68(1):78–84. Available from: http://www.ncbi.nlm.nih.gov/pubmed/18008331

57. Litvinov S V., Velders MP, Bakker HAM, Fleuren GJ, Warnaar SO. Ep-CAM: A human epithelial antigen is a homophilic cell-cell adhesion molecule. J Cell Biol. 1994;125(2):437–46.

58. Trzpis M, McLaughlin PMJ, de Leij LMFH, Harmsen MC. Epithelial Cell Adhesion Molecule. Am J Pathol [Internet]. 2007;171(2):386–95. Available from: http://linkinghub.elsevier.com/retrieve/pii/S0002944010619724

59. Hyun K-A, Goo K-B, Han H, Sohn J, Choi W, Kim S-I, et al. Epithelial-to-mesenchymal transition leads to loss of EpCAM and different physical properties in circulating tumor cells from metastatic breast cancer. Oncotarget. 2016;7(17):24677–87.

60. Bitting RL, Boominathan R, Rao C, Kemeny G, Foulk B, Garcia-Blanco MA, et al. Development of a method to isolate circulating tumor cells using mesenchymal-based capture. Methods. 2013;64(2):129–36.

61. Allard WJ, Matera J, Miller MC, Repollet M, Connelly MC, Rao C, et al. Tumor Cells Circulate in the Peripheral Blood of All Major Carcinomas but not in Healthy Subjects or Patients With Nonmalignant Diseases Tumor Cells Circulate in the Peripheral Blood of All Major Carcinomas but not in Healthy Subjects or Patients With Non. Clin Cancer Res. 2005;10(October):6897–904.

62. Swennenhuis JF, van Dalum G, Zeune LL, Terstappen LWMM. Improving the CellSearch® system. Expert Rev Mol Diagn [Internet]. 2016;16(12):1291–305. Available from: http://dx.doi.org/10.1080/14737159.2016.1255144

63. Kraan J, Sleijfer S, Strijbos MH, Ignatiadis M, Peeters D, Pierga JY, et al. External quality assurance of circulating tumor cell enumeration using the CellSearch® system: A feasibility study. Cytom Part B - Clin Cytom. 2011;80 B(2):112–8.

64. Ligthart ST, Coumans FAW, Attard G, Cassidy A, de Bono JS, Terstappen LWMM. Unbiased and automated identification of a circulating tumour cell definition that associates with overall survival. PLoS One. 2011;6(11).

65. Ligthart ST, Coumans FA, Bidard FC, Simkens LH, Punt CJ, de Groot MR, et al. Circulating Tumor Cells Count and Morphological Features in Breast, Colorectal and Prostate Cancer. PLoS One [Internet]. 2013;8(6):e67148. Available from: http://www.ncbi.nlm.nih.gov/pubmed/23826219%0Ahttps://www.ncbi.nlm.nih.gov/pmc/articles/PMC3695007/pdf/pone.0067148.pdf

66. Todenhöfer T, Hennenlotter J, Feyerabend S, Aufderklamm S, Mischinger J, Kühs U, et al. Preliminary experience on the use of the adnatest® system for detection of circulating tumor cells in prostate cancer patients. Anticancer Res. 2012;32(8):3507–13.

67. De Bono JS, Scher HI, Montgomery RB, Parker C, Miller MC, Tissing H, et al. Circulating tumor cells predict survival benefit from treatment in metastatic castration-resistant prostate cancer. Clin Cancer Res. 2008;14(19):6302–9.

68. Talasaz AH, Powell AA, Huber DE, Berbee JG, Roh K-H, Yu W, et al. Isolating highly enriched populations of circulating epithelial cells and other rare cells from blood using a magnetic sweeper device. Proc Natl Acad Sci [Internet]. 2009;106(10):3970–5. Available from: http://www.pnas.org/cgi/doi/10.1073/pnas.0813188106

69. Cann GM, Gulzar ZG, Cooper S, Li R, Luo S, Tat M, et al. mRNA-Seq of Single Prostate Cancer Circulating Tumor Cells Reveals Recapitulation of Gene Expression and Pathways Found in Prostate Cancer. PLoS One. 2012;7(11):1–10.

70. Saucedo-Zeni N, Mewes S, Niestroj R, Gasiorowski L, Murawa D, Nowaczyk P, et al. A novel method for the in vivo isolation of circulating tumor cells from peripheral blood of

cancer patients using a functionalized and structured medical wire. Int J Oncol. 2012;41(4):1241–50.

71. Gorges TM, Penkalla N, Schalk T, Joosse SA, Riethdorf S, Tucholski J, et al. Enumeration and Molecular Characterization of Tumor Cells in Lung Cancer Patients Using a Novel In Vivo Device for Capturing Circulating Tumor Cells. Clin Cancer Res. 2016;22(9):2197–206.

72. Nagrath S, Sequist L V., Maheswaran S, Bell DW, Irimia D, Ulkus L, et al. Isolation of rare circulating tumour cells in cancer patients by microchip technology. Nature [Internet]. 2007;450(7173):1235–9. Available from: http://www.nature.com/doifinder/10.1038/nature06385

73. Kirby BJ, Jodari M, Loftus MS, Gakhar G, Pratt ED, Chanel-Vos C, et al. Functional characterization of circulating tumor cells with a prostate-cancer-specific microfluidic device. PLoS One. 2012;7(4):1–10.

74. Gleghorn JP, Pratt ED, Denning D, Liu H, Bander NH, Scott T, et al. Capture of circulating tumor cells from whole blood of prostate cancer patients using geometrically enhanced differential immunocapture (GEDI) and a prostate-specific antibody. Lab Chip. 2011;10(1):27–9.

75. Stott SL, Hsu C-HC-H, Tsukrov DI, Yu M, Miyamoto DT, Waltman B a., et al. Isolation of circulating tumor cells using a microvortex-generating herringbone-chip. October [Internet]. 2010;107(35):18392–7. Available from: http://www.pnas.org/cgi/doi/10.1073/pnas.1012539107%5Cnhttp://www.pubmedcentral.nih.gov/articlerender.fcgi?artid=2972993&tool=pmcentrez&rendertype=abstract

76. Wang S, Wang H, Jiao J, Chen K, Owens GE, Kamei K, et al. NIH Public Access. 2010;48(47):8970–3.

77. Wang S et al. Highly Efficient Capture of Circulating Tumor Cells Using Nanostructured Silicon Substrates with Integrated Chaotic Micromixers. Angew Chem Int Ed Engl. 2011;10 (2)(1):116–25.

78. Lu YT, Zhao L, Shen Q, Garcia MA, Wu D, Hou S, et al. NanoVelcro chip for CTC enumeration in prostate cancer patients. Methods [Internet]. 2013;64(2):144–52. Available from: http://dx.doi.org/10.1016/j.ymeth.2013.06.019

79. Ozkumur E, Shah AM, Ciciliano JC, Emmink BL, Miyamoto DT, Brachtel E, et al. Inertial Focusing for Tumor Antigen-Dependent and -Independent Sorting of Rare Circulating Tumor Cells. Sci Transl Med [Internet]. 2013;5(179):179ra47-179ra47. Available from: http://stm.sciencemag.org/cgi/doi/10.1126/scitranslmed.3005616

80. Lansdorp PM, Thomas TE. Purification and analysis of bispecific tetrameric antibody complexes. Mol Immunol. 1990;27(7):659–66.

81. Werner SL, Graf RP, Landers M, Valenta DT, Schroeder M, Greene SB, et al. Analytical Validation and Capabilities of the Epic CTC Platform: Enrichment-Free Circulating Tumour Cell Detection and Characterization. J Circ Biomarkers [Internet]. 2015;1. Available from: http://cbx.sagepub.com/lookup/doi/10.5772/60725

82. Lu D, Graf RP, Harvey M, Madan RA, Heery C, Marte J, et al. Detection and Characterization of Circulating Tumour Cells from Frozen Peripheral Blood Mononuclear Cells. J Circ Biomarkers [Internet]. 2015;1. Available from: http://www.intechopen.com/books/journal-of-circulating-biomarkers/detection-and-characterization-of-circulating-tumour-cells-from-frozen-peripheral-blood-mononuclear-

83. Marrinucci D, Bethel K, Kolatkar A, Luttgen M, Malchiodi M, Baehring F, et al. Fluid biopsy in patients with metastatic prostate, pancreatic, and breast cancers. Phys Biol. 2012;9(1):1–19.

84. Ramirez AB, U'Ren L, Campton DE, Stewart D, Nordberg JJ, Stilwell JL, et al. Rarecyte® CTC Analysis Step 1: AccuCyte® Sample Preparation for the Comprehensive Recovery of Nucleated Cells from Whole Blood. In: Methods in Molecular Biology. 2017. p. 163–72.

85. Werbin JL, Nordberg JJ, Tzucker J, Varshavskaya P, Stilwell JL, Kaldjian EP. RareCyte® CTC analysis step 2: Detection of circulating tumor cells by cytefinder® automated scanning and semiautomated image analysis. In: Methods in Molecular Biology. 2017. p. 173–80.

86. Campton DE, Ramirez AB, Nordberg JJ, Drovetto N, Clein AC, Varshavskaya P, et al. High-recovery visual identification and single-cell retrieval of circulating tumor cells for genomic analysis using a dual-technology platform integrated with automated immunofluorescence staining. BMC Cancer [Internet]. 2015;15(1):360. Available from: http://bmccancer.biomedcentral.com/articles/10.1186/s12885-015-1383-x

87. Stilwell JL, Varshavskaya P, Werbin JL, Nordberg JJ, Ramirez AB, Quarre S, et al. RareCyte® CTC analysis step 3: Using the CytePicker® module for individual cell retrieval and subsequent whole genome amplification of circulating tumor cells for genomic analysis. In: Methods in Molecular Biology. 2017. p. 181–92.

88. Alix-Panabières C, Rebillard X, Brouillet J-P, Barbotte E, Iborra F, Segui B, et al. Detection of Circulating Prostate-Specific Antigen-Secreting Cells in Prostate Cancer Patients. Clin Chem. 2005;51(8):1538–41.

89. Hayes DF, Smerage JB. Circulating Tumor Cells. Vol. 95, Molecular Biology of Cancer: Translation to the Clinic. 2010. 95-112 p.

90. Paris PL, Kobayashi Y, Zhao Q, Zeng W, Sridharan S, Fan T, et al. Functional phenotyping and genotyping of circulating tumor cells from patients with castration resistant prostate cancer. Cancer Lett [Internet]. 2009;277(2):164–73. Available from: http://dx.doi.org/10.1016/j.canlet.2008.12.007

91. Vona G, Sabile A, Louha M, Sitruk V, Romana S, Schütze K, et al. Isolation by Size of Epithelial Tumor Cells. Am J Pathol [Internet]. 2000;156(1):57–63. Available from: http://linkinghub.elsevier.com/retrieve/pii/S0002944010647062

92. Lin HK, Zheng S, Williams AJ, Balic M, Groshen S, Scher HI, et al. Portable Filter-Based Microdevice for Detection and Characterization of Circulating Tumor Cells. 2011;16(20):5011–8.

93. Park S, Ang RR, Duffy SP, Bazov J, Chi KN, Black PC, et al. Morphological differences between circulating tumor cells from prostate cancer patients and cultured prostate cancer cells. PLoS One. 2014;9(1).

94. Lee HJ, Oh JH, Oh JM, Park JM, Lee JG, Kim MS, et al. Efficient isolation and accurate in situ analysis of circulating tumor cells using detachable beads and a high-pore-density filter. Angew Chemie - Int Ed. 2013;52(32):8337–40.

95. Gascoyne PRC, Noshari J, Anderson TJ, Becker FF. Isolation of rare cells from cell mixtures by dielectrophoresis. Electrophoresis. 2009;30(8):1388–98.

96. Shim S, Gascoyne P, Noshari J, Stemke Hale K. Dynamic physical properties of dissociated tumor cells revealed by dielectrophoretic field-flow fractionation. Integr Biol. 2011;3(8):115–25.

97. Pethig R. Review Article—Dielectrophoresis: Status of the theory, technology, and applications. Biomicrofluidics [Internet]. 2010;4(2):22811. Available from: http://aip.scitation.org/doi/10.1063/1.3456626

98. Gascoyne PRC, Noshari J, Anderson TJ, Becker FF. Isolation of Rare Cells from Cell Mixtures by Dielectrophoresis. Electrophoresis. 2009;30(8)(1):1388–98.

99. Gupta V, Jafferji I, Garza M, Melnikova VO, Hasegawa DK, Pethig R, et al. ApoStream, a new dielectrophoretic device for antibody independent isolation and recovery of viable cancer cells from blood. Biomicrofluidics. 2012;6(2):850–64.

100. Balasubramanian P, Kinders RJ, Kummar S, Gupta V, Hasegawa D, Menachery A, et al. Antibody-independent capture of circulating tumor cells of non-epithelial origin with the ApoStream® system. PLoS One. 2017;12(4):1–15.

101. Navin NE. Cancer genomics: one cell at a time. Genome Biol [Internet]. 2014;15(8):452. Available from: http://genomebiology.biomedcentral.com/articles/10.1186/s13059-014-0452-9

102. Scher HI, Jia X, de Bono JS, Fleisher M, Pienta KJ, Raghavan D, et al. Circulating tumour cells as prognostic markers in progressive, castration-resistant prostate cancer: a reanalysis of IMMC38 trial data. Lancet Oncol [Internet]. 2009;10(3):233–9. Available from: http://dx.doi.org/10.1016/S1470-2045(08)70340-1

103. Lonergan PE, Tindall DJ. Androgen receptor signaling in prostate cancer development and progression. J Carcinog [Internet]. 2011;10(1):20. Available from: http://www.ncbi.nlm.nih.gov/pubmed/21886458%5Cnhttp://www.pubmedcentral.nih.gov/articlerender.fcgi?artid=PMC3162670

104. Wyatt AW, Gleave ME. Targeting the adaptive molecular landscape of castration-resistant prostate cancer. EMBO Mol Med [Internet]. 2015;7(7):878–94. Available from: http://embomm.embopress.org/content/early/2015/04/20/emmm.201303701.abstract%5Cnhttp://www.ncbi.nlm.nih.gov/pubmed/25896606%5Cnhttp://www.pubmedcentral.nih.gov/articlerender.fcgi?artid=PMC4520654

105. Chandrasekar T, Yang JC, Gao AC, Evans CP. Mechanisms of resistance in castration-

resistant prostate cancer (CRPC). Transl Androl Urol [Internet]. 2015;4(3):365–80. Available from: http://www.pubmedcentral.nih.gov/articlerender.fcgi?artid=4708226&tool=pmcentrez&rendertype=abstract

106. Swiger R, Tucker J. Fluorescence in situ hybridization: a brief review. Environ Mol Mutagen [Internet]. 1996;27(1996):245–54. Available from: http://onlinelibrary.wiley.com/doi/10.1002/(SICI)1098-2280(1996)27:4%3C245::AID-EM1%3E3.0.CO;2-C/full

107. Shah S, Lubeck E, Schwarzkopf M, He T-F, Greenbaum A, Sohn CH, et al. Single-molecule RNA detection at depth by hybridization chain reaction and tissue hydrogel embedding and clearing. Development [Internet]. 2016;143(15):2862–7. Available from: http://dev.biologists.org/lookup/doi/10.1242/dev.138560

108. Kwon S. Single-molecule fluorescence in situ hybridization: Quantitative imaging of single RNA molecules. Vol. 46, BMB Reports. 2013. p. 65–72.

109. Shaffer DR, Leversha MA, Danila DC, Lin O, Gonzalez-Espinoza R, Gu B, et al. Circulating tumor cell analysis in patients with progressive castration-resistant prostate cancer. Clin Cancer Res. 2007;13(7):2023–9.

110. Leversha MA, Han J, Asgari Z, Danila DC, Lin O, Gonzalez-Espinoza R, et al. Fluorescence in situ hybridization analysis of circulating tumor cells in metastatic prostate cancer. Clin Cancer Res. 2009;15(6):2091–7.

111. Attard G, Swennenhuis JF, Olmos D, Reid AHM, Vickers E, A'Hern R, et al. Characterization of ERG, AR and PTEN Gene Status in Circulating Tumor Cells from Patients with Castration-Resistant Prostate Cancer. Cancer Res [Internet]. 2009;69(7):2912–8. Available from: http://cancerres.aacrjournals.org/cgi/doi/10.1158/0008-5472.CAN-08-3667

112. Jiang Y, Palma JF, Agus DB, Wang Y, Gross ME. Detection of Androgen Receptor Mutations in Circulating Tumor Cells in Castration-Resistant Prostate Cancer. Clin Chem. 2010;56(9):1492–5.

113. Punnoose EA, Ferraldeschi R, Szafer-Glusman E, Tucker EK, Mohan S, Flohr P, et al. PTEN loss in circulating tumour cells correlates with PTEN loss in fresh tumour tissue from castration-resistant prostate cancer patients. Br J Cancer [Internet]. 2015;113(8):1225–33. Available from: http://www.nature.com/doifinder/10.1038/bjc.2015.332

114. Lin H-K, Hu Y-C, Lee DK, Chang C. Regulation of androgen receptor signaling by PTEN (phosphatase and tensin homolog deleted on chromosome 10) tumor suppressor through distinct mechanisms in prostate cancer cells. Mol Endocrinol. 2004;18(10):2409–23.

115. Kim J, Coetzee GA. Prostate specific antigen gene regulation by androgen receptor. J Cell Biochem. 2004;93(2):233–41.

116. Yin L, Rao P, Elson P, Wang J, Ittmann M, Heston WDW. Role of TMPRSS2-ERG gene fusion in negative regulation of PSMA expression. PLoS One. 2011;6(6):1–7.

117. Zhu ML, Horbinski CM, Garzotto M, Qian DZ, Beer TM, Kyprianou N. Tubulin-targeting chemotherapy impairs androgen receptor activity in prostate cancer. Cancer Res. 2010;70(20):7992–8002.

118. Stott SL, Stott SL, Lee RJ, Nagrath S, Yu M, Miyamoto DT, et al. Isolation and Characterization of Circulating Tumor Cells from Patients with Localized and Metastatic Prostate Cancer. 2010;23(25).

119. Danila DC, Anand A, Sung CC, Heller G, Leversha MA, Cao L, et al. TMPRSS2-ERG Status in Circulating Tumor Cells as a Predictive Biomarker of Sensitivity in Castration-Resistant Prostate Cancer Patients Treated with Abiraterone Acetate. Eur Urol. 2011;60(5):897–904.

120. Hu R, Dunn T a, Wei S, Isharwal S, Veltri RW, Han M, et al. Ligand-independent Androgen Receptor Variants. 2010;69(1):16–22.

121. Dehm SM, Schmidt LJ, Heemers H V, Vessella RL, Tindall DJ. Splicing of a novel AR exon generates a constitutively active androgen receptor that mediates prostate cancer therapy resistance. Cancer Res. 2009;68(13):612–26.

122. Gawad C, Koh W, Quake SR. Single-cell genome sequencing: current state of the science. Nat Rev Genet [Internet]. 2016;17(3):175–88. Available from: http://www.nature.com/doifinder/10.1038/nrg.2015.16

123. Telenius H, Carter NP, Bebb CE, Nordenskjöld M, Ponder BAJ, Tunnacliffe A. Degenerate oligonucleotide-primed PCR: General amplification of target DNA by a single degenerate primer. Genomics. 1992;13(3):718–25.

124. Zhang L, Cui X, Schmitt K, Hubert R, Navidi W, Arnheim N. Whole genome amplification from a single cell: implications for genetic analysis. Proc Natl Acad Sci U S A [Internet]. 1992;89(13):5847–51. Available from: http://www.pubmedcentral.nih.gov/articlerender.fcgi?artid=49394&tool=pmcentrez&rendertype=abstract

125. Deleye L, Tilleman L, Van Der Plaetsen AS, Cornelis S, Deforce D, Van Nieuwerburgh F. Performance of four modern whole genome amplification methods for copy number variant detection in single cells. Sci Rep. 2017;7(1).

126. De Bourcy CFA, De Vlaminck I, Kanbar JN, Wang J, Gawad C, Quake SR. A quantitative comparison of single-cell whole genome amplification methods. PLoS One. 2014;9(8).

127. Dean FB, Nelson JR, Giesler TL, Lasken RS. Rapid amplification of plasmid and phage DNA using Phi29 DNA polymerase and multiply-primed rolling circle amplification. Genome Res. 2001;11(6):1095–9.

128. Langmore JP. Rubicon Genomics, Inc. Pharmacogenomics [Internet]. 2002;3(4):557–60. Available from: http://www.ncbi.nlm.nih.gov/pubmed/12164778

129. Zong C, Lu S, Chapman A, Xie XS. Genome-wide detection of single-nucleotide and copy number variations of a single human cell. Science (80-). 2012;338(6114):1622–6.

130. Hou Y, Wu K, Shi X, Li F, Song L, Wu H, et al. Comparison of variations detection between whole-genome amplification methods used in single-cell resequencing. Gigascience [Internet]. 2015;4(1):37. Available from: https://academic.oup.com/gigascience/article-lookup/doi/10.1186/s13742-015-0068-3

131. Wilhelm BT, Landry JR. RNA-Seq-quantitative measurement of expression through massively parallel RNA-sequencing. Methods [Internet]. 2009;48(3):249–57. Available from: http://dx.doi.org/10.1016/j.ymeth.2009.03.016

132. Sasagawa Y, Nikaido I, Hayashi T, Danno H, Uno KD, Imai T, et al. Quartz-Seq: a highly reproducible and sensitive single-cell RNA sequencing method, reveals non-genetic gene-expression heterogeneity. Genome Biol [Internet]. 2013;14(4):3097. Available from: http://genomebiology.biomedcentral.com/articles/10.1186/gb-2013-14-4-r31

133. Picelli S, Faridani OR, Björklund ÅK, Winberg G, Sagasser S, Sandberg R. Full-length RNA-seq from single cells using Smart-seq2. Nat Protoc [Internet]. 2014;9(1):171–81. Available from: http://www.nature.com/doifinder/10.1038/nprot.2014.006

134. Picelli S, Björklund ÅK, Faridani OR, Sagasser S, Winberg G, Sandberg R. Smart-seq2 for sensitive full-length transcriptome profiling in single cells. Nat Methods [Internet]. 2013;10(11):1096–8. Available from: http://www.nature.com/doifinder/10.1038/nmeth.2639

135. Ramsköld D, Luo S, Wang Y-C, Li R, Deng Q, Faridani OR, et al. Full-length mRNA-Seq from single-cell levels of RNA and individual circulating tumor cells. Nat Biotechnol [Internet]. 2012;30(8):777–82. Available from: http://www.nature.com/doifinder/10.1038/nbt.2282

136. Islam S, Kjällquist U, Moliner A, Zajac P, Fan JB, Lönnerberg P, et al. Characterization of the single-cell transcriptional landscape by highly multiplex RNA-seq. Genome Res. 2011;21(7):1160–7.

137. Islam S, Zeisel A, Joost S, La Manno G, Zajac P, Kasper M, et al. Quantitative single-cell RNA-seq with unique molecular identifiers. Nat Methods [Internet]. 2013;11(2):163–6. Available from: http://www.nature.com/doifinder/10.1038/nmeth.2772

138. Zhang XHF, Jin X, Malladi S, Zou Y, Wen YH, Brogi E, et al. Selection of bone metastasis seeds by mesenchymal signals in the primary tumor stroma. Cell. 2013;154(5):1060–73.

139. Ting DT, Wittner BS, Ligorio M, Jordan NV, Ajay M, Miyamoto DT, et al. Single-Cell RNA Sequencing Identifies Extracellular Matrix Gene Expression by Pancreatic Circulating Tumor Cells. Cell Rep. 2015;8(6):1905–18.

140. Miyamoto DT, Zheng Y, Wittner BS, Lee RJ, Zhu H, Broderick KT, et al. RNA-Seq of single prostate CTCs implicates noncanonical Wnt signaling in antiandrogen resistance. Science (80-) [Internet]. 2015;349(6254):1351–6. Available from: http://www.sciencemag.org/cgi/doi/10.1126/science.aab0917

141. Chalfie M, Horvitz HR, Sulston JE. Mutations that lead to reiterations in the cell lineages of C. elegans. Cell. 1981;24:59–69.

142. Wightman B, Ha I, Ruvkun G. Posttranscriptional regulation of the heterochronic gene lin-14 by lin-4 mediates temporal pattern formation in C. elegans. Cell. 1993;75(5):855–62.

143. Lee RC, Feinbaum RL, Ambros V. the C. elegans heterochronic gene lin-4 encodes small RNAs with antisense complementarity to lin-14. Cell. 1993;75:843–54.

144. Li T, Li RS, Li YH, Zhong S, Chen YY, Zhang CM, et al. MiR-21 as an independent biochemical recurrence predictor and potential therapeutic target for prostate cancer. J Urol. 2012;187(4):1466–72.

145. Ribas J, Ni X, Haffner M, Wentzel E a, Hassanzadeh A, Chowdhury WH, et al. miR-21: An androgen receptor regulated microRNA which promotes hormone dependent and independent prostate cancer growth. Cancer Res. 2010;69(18):7165–9.

146. Shi X-B, Xue L, Yang J, Ma A-H, Zhao J, Xu M, et al. An androgen-regulated miRNA suppresses Bak1 expression and induces androgen-independent growth of prostate cancer cells. Proc Natl Acad Sci [Internet]. 2007;104(50):19983–8. Available from: http://www.pnas.org/cgi/doi/10.1073/pnas.0706641104

147. Prueitt RL, Yi M, Hudson RS, Wallace TA, Howe TM, Yfantis G, et al. Expression of microRNAs and protein-coding genes associated with perineural invasion in prostate cancer. Prostate, The. 2009;68(11):1152–64.

148. Amir S, Ma AH, Shi XB, Xue L, Kung HJ, deVere White RW. Oncomir miR-125b Suppresses p14ARF to Modulate p53-Dependent and p53-Independent Apoptosis in Prostate Cancer. PLoS One. 2013;8(4).

149. Shi X-B, Xue L, Ma A-H, Tepper CG, Kung H-J, White RW deVere. miR-125b promotes growth of prostate cancer xenograft tumor through targeting pro-apoptotic genes. Prostate [Internet]. 2011;71(5):538–49. Available from: http://www.pubmedcentral.nih.gov/articlerender.fcgi?artid=3017658&tool=pmcentrez&rendertype=abstract

150. Sachdeva M, Zhu S, Wu F, Wu H, Walia V, Kumar S, et al. p53 represses c-Myc through induction of the tumor suppressor miR-145. Proc Natl Acad Sci [Internet]. 2009;106(9):3207–12. Available from: http://www.pnas.org/cgi/doi/10.1073/pnas.0808042106

151. Avgeris M, Stravodimos K, Fragoulis EG, Scorilas A. The loss of the tumour-suppressor miR-145 results in the shorter disease-free survival of prostate cancer patients. Br J Cancer [Internet]. 2013;108(12):2573–81. Available from: http://dx.doi.org/10.1038/bjc.2013.250

152. Goto Y, Nishikawa R, Kojima S, Chiyomaru T, Enokida H, Inoguchi S, et al. Tumour-suppressive microRNA-224 inhibits cancer cell migration and invasion via targeting oncogenic TPD52 in prostate cancer. FEBS Lett [Internet]. 2014;588(10):1973–82. Available from: http://dx.doi.org/10.1016/j.febslet.2014.04.020

153. Mavridis K, Stravodimos K, Scorilas A. Downregulation and prognostic performance of microRNA 224 expression in prostate cancer. Clin Chem. 2013;59(1):261–9.

154. Faridani OR, Abdullayev I, Hagemann-Jensen M, Schell JP, Lanner F, Sandberg R. Single-cell sequencing of the small-RNA transcriptome. Nat Biotechnol [Internet]. 2016;34(12):18–22. Available from: http://www.nature.com/doifinder/10.1038/nbt.3701

155. Lozzio C, Lozzio B. Human With Chronic Positive. Blood. 1975;45(3):321–34.

156. Horoszewicz JS, Leong SS, Kawinski E, Karr JP, Rosenthal H, Chu TM, et al. LNCaP Model of Human Prostatic Carcinoma LNCaP Model of Human Prostatic Carcinoma1. Cancer Res ICANCER Res [Internet]. 1983;43(43):1809–18. Available from: http://cancerres.aacrjournals.org/content/43/4/1809%5Cnhttp://cancerres.aacrjournals.org/content/43/4/1809#related-urls

157. Liu VA, Jastromb WE, Bhatia SN. Engineering protein and cell adhesivity using PEO-terminated triblock polymers. J Biomed Mater Res. 2002;60(1):126–34.

158. Li Y, Keefe AJ, Giarmarco M, Brault ND, Jiang S. Simple and robust approach for passivating and functionalizing surfaces for use in complex media. Langmuir. 2012;28(25):9707–13.

159. Wu Z, Hjort K. Surface modification of PDMS by gradient-induced migration of embedded Pluronic. Lab Chip [Internet]. 2009;9(11):1500. Available from: http://xlink.rsc.org/?DOI=b901651a

160. Tharmalingam T, Goudar CT. Evaluating the impact of high Pluronic® F68 concentrations on antibody producing CHO cell lines. Biotechnol Bioeng. 2015;112(4):832–7.

161. Gierahn TM, Wadsworth MH, Hughes TK, Bryson BD, Butler A, Satija R, et al. Seq-Well: portable, low-cost RNA sequencing of single cells at high throughput. Nat Methods [Internet]. 2017;14(4):395–8. Available from: http://www.nature.com/doifinder/10.1038/nmeth.4179

162. Tan SH, Nguyen NT, Chua YC, Kang TG. Oxygen plasma treatment for reducing hydrophobicity of a sealed polydimethylsiloxane microchannel. Biomicrofluidics. 2010;4(3).

163. VanInsberghe M. The development of single-cell microfluidic technologies for the analysis of microRNA expression. University of British Columbia; 2018.

164. Viollet S, Fuchs RT, Munafo DB, Zhuang F, Robb GB. T4 RNA Ligase 2 truncated active site mutants: Improved tools for RNA analysis. BMC Biotechnol. 2011;11.

165. Hafner M, Renwick N, Brown M, Mihailovic A, Holoch D, Lin C, et al. RNA-ligase-dependent biases in miRNA representation in deep-sequenced small RNA cDNA libraries. RNA [Internet]. 2011;17(9):1697–712. Available from: http://rnajournal.cshlp.org/cgi/doi/10.1261/rna.2799511

166. Koshkin AA, Nielsen P, Meldgaard M, Rajwanshi VK, Singh SK, Wengel J. LNA (locked nucleic acid): An RNA mimic forming exceedingly stable LNA:LNA duplexes [3]. J Am Chem Soc. 1998;120(50):13252–3.

167. Kozomara A, Griffiths-Jones S. MiRBase: Annotating high confidence microRNAs using

deep sequencing data. Nucleic Acids Res. 2014;42(D1).

168. Chu A, Robertson G, Brooks D, Mungall AJ, Birol I, Coope R, et al. Large-scale profiling of microRNAs for the Cancer Genome Atlas. Nucleic Acids Res. 2016;44(1):e3.

169. Kiselev VY, Kirschner K, Schaub MT, Andrews T, Yiu A, Chandra T, et al. SC3: Consensus clustering of single-cell RNA-seq data. Nat Methods. 2017;14(5):483–6.

170. Van Der Maaten LJP, Hinton GE. Visualizing high-dimensional data using t-sne. J Mach Learn Res [Internet]. 2008;9:2579–605. Available from: https://lvdmaaten.github.io/publications/papers/JMLR_2008.pdf%0Ahttp://www.ncbi.nlm.nih.gov/entrez/query.fcgi?db=pubmed&cmd=Retrieve&dopt=AbstractPlus&list_uids=79114314791487345 48related:VOiAgwMNy20J

171. Huang X, Yuan T, Tschannen M, Sun Z, Jacob H, Du M, et al. Characterization of human plasma-derived exosomal RNAs by deep sequencing. BMC Genomics. 2013;14(1):1–14.

172. Lun ATL, McCarthy DJ, Marioni JC. A step-by-step workflow for low-level analysis of single-cell RNA-seq data with Bioconductor. F1000Research [Internet]. 2016;5:2122. Available from: https://f1000research.com/articles/5-2122/v2

173. Lamoureux F, Thomas C, Yin MJ, Fazli L, Zoubeidi A, Gleave ME. Suppression of heat shock protein 27 using OGX-427 induces endoplasmic reticulum stress and potentiates heat shock protein 90 inhibitors to delay castrate-resistant prostate cancer. Eur Urol. 2014;66(1):145–55.

174. Finak G, McDavid A, Yajima M, Deng J, Gersuk V, Shalek AK, et al. MAST: A flexible statistical framework for assessing transcriptional changes and characterizing heterogeneity in single-cell RNA sequencing data. Genome Biol [Internet]. 2015;16(1):1–13. Available from: http://dx.doi.org/10.1186/s13059-015-0844-5

175. Chou CH, Shrestha S, Yang CD, Chang NW, Lin YL, Liao KW, et al. MiRTarBase update 2018: A resource for experimentally validated microRNA-target interactions. Nucleic Acids Res. 2018;46(D1):D296–302.

176. Szklarczyk D, Morris JH, Cook H, Kuhn M, Wyder S, Simonovic M, et al. The STRING database in 2017: Quality-controlled protein-protein association networks, made broadly accessible. Nucleic Acids Res. 2017;45(D1):D362–8.

177. Lu Y, Lu J, Li X, Zhu H, Fan X, Zhu S, et al. MiR-200a inhibits epithelial-mesenchymal transition of pancreatic cancer stem cell. BMC Cancer [Internet]. 2014;14(1):1–9. Available from: BMC Cancer

178. Wang J, Yang X, Ruan B, Dai B, Gao Y, Duan J, et al. Overexpression of miR-200a suppresses epithelial-mesenchymal transition of liver cancer stem cells. Tumor Biol. 2015;36(4):2447–56.

179. Williams L V., Veliceasa D, Vinokour E, Volpert O V. MiR-200b inhibits prostate cancer EMT, growth and metastasis. PLoS One. 2013;8(12):1–10.

180. Pichler M, Ress AL, Winter E, Stiegelbauer V, Karbiener M, Schwarzenbacher D, et al. MiR-200a regulates epithelial to mesenchymal transition-related gene expression and

determines prognosis in colorectal cancer patients. Br J Cancer [Internet]. 2014;110(6):1614–21. Available from: http://dx.doi.org/10.1038/bjc.2014.51